Self- Propagating Metathesis Preparations of Inorganic Materials.

A thesis presented by
Andrew Lee Hector, B.Sc.(Hons.), A.R.C.S., C.Chem. M.R.S.C.
in partial fullfilment for the award of Ph.D.
University College London, Chemistry Department.
November 1995.

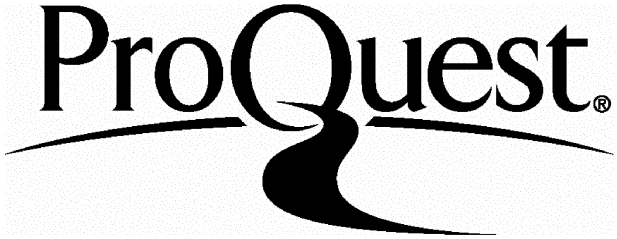

Abstract.

The potential of self- propagating reactions, with reagents such as lithium nitride, calcium nitride, sodium arsenide and magnesium silicide, in the production of inorganic materials has been investigated. Reactions were performed with anhydrous d- block and rare earth metal chlorides and can be described by the following generic equation where M is a Group 3- 12 metal, Alk is a Group 1 or 2 element and E is Si, N, P, As, Sb, Bi or O.

$$MCl_m + xAlk_nE \rightarrow yM_\alpha E + xAlkCl_\beta + zE_\gamma$$

Crude products were obtained normally as fused masses of material consisting of the products coated in the alkali chloride co- products. Grinding followed by washing with an appropriate solvent yielded the pure products with low levels of contamination from the other elements present in the reaction flux. The phases produced include rare earth and transition metal nitrides, metals and alloys, d- block phosphides, arsenides and antimonides, metal silicides and d- block oxides. The products were variously characterised by X- ray powder diffraction, scanning electron microscopy, energy dispersive X-ray analysis, magnetic susceptability, X- ray photoelectron spectroscopy, microanalysisand solid state (magic angle spinning) nuclear magnetic resonance spectroscopy.

Thermocouple experiments, differential scanning calorimetry, photography and constant pressure calculations were used to examine the thermal aspects and timescales of reactions. Dilution with inert solids was used to reduce voracity of reactions and to control crystallinity of products. Liquid chlorides ($TiCl_4$ and VCl_4) were successfully employed to make high quality ternary phases such as $Ti_{0.5}V_{0.5}E$ (E= N, P, As). Such reactions can progress *via* ionic or elemental mechanisms and evidence for either of these was gathered. Examples were found for both mechanisms which supported that the process was occurring. These conclusions were based on end- product analysis since the reaction conditions and timescales precluded the use of other techniques.

Acknowledgements.

Firstly, I would like to thank my boss, Ivan Parkin, for his help, ideas, comedy hairdo, enthusiasm, patience, etc. etc. Ade Rowley & Jon Fitzmaurice have been very influential in this work and their help is much appreciated. Also, thanks to the other members of the group: Jon Cotter, Qi Fang, Alexei Komarov, Graham Combe, Leigh Nixon, Graham Shaw & Mark Lavender.

Thanks to Tim Healy for inspiration.

Simon Drake & Tony Hill for originally suggesting me for the post. The Open University Research Council & University College London Provost Fund for providing the money to carry out this research.

At the OU, Little Robbie Thied, Jo Hood, Steve Robinson, Mick Boiler, Ade Parry, Hayley Jacobs, Graham Jeffs, Jim Gibbs, Alan Leslie, Pravin Patel, Graham Oates, Charlie Harding, Leslie Smart, David Roberts, David Johnson, Sally Eaton & Jenny Burridge.

Naomi Williams (OU Materials) for lots of time and help on the SEM.

At UCL, Laura Gellman, Ian Shannon, Elizabeth Maclean, Geoff Henshaw, Ken Harris, Steve Price, Andrea Sella, Dave Knapp, Joe Nolan, Peter Leighton, Alan Stones, Jill Maxwell, John Hill & John Cresswell

Kevin Reeves (Inst. of Archaeology) for assistance with the SEM. Marianne Odlyha (Birkbeck) for help with DSC/ TGA. Dr. Apperly of the EPSRC service at Durham for solid state NMR.

For their friendship, Jason, Catherine, Mark, Alison & David, Andy & Lucie, Patti & Ben, Sarah & Andy, Luke, Marte, Marcus, Dave, Anna, Paul, Shirley & Fletch.

My great gratitude to Mum & Dad for every kind of help and support. Thanks to the rest of my family, old and new, for being there. And most of all, thanks to Allison & Becky, my new wife & stepdaughter, for giving me great happiness and a focus for the future.

Contents. Page

Tables. Page

Figures. Page

Abbreviations.

SSM	solid state metathesis.
SHS	self- propagating high temperature synthesis.
CVD	chemical vapour deposition.
XRD	X- ray diffraction.
SEM	scanning electron microscopy.
EDXA	energy dispersive X- ray analysis.
FT-IR	fourier transform infrared.
MAS	magic angle spinning.
NMR	nuclear magnetic resonance.
GC	gas chromatography.
DSC	differential scanning calorimetry.
T_{ad}	adiabatic combustion temperature.
$T_{ad,s}$	T_{ad} for salt formation only.
C_p	constant pressure heat capacity.
EDTA	ethylene diamine tetraacetic acid.
PZT	lead zirconate titanate $PbZr_xTi_{1-x}O_3$.
THF	tetrahydrofuran.
Me	methyl.
Et	ethyl.
^{i}Pr	isopropyl.
M	metal.
E	non metal.
Pn	pnictogen (i.e. Group 15 element).
Ch	chalcogen (i.e. Group 16 element).
Ln	rare earth/ lanthanide
$\Rightarrow$	implies that.

1. Introduction.

The field of ceramics is often perceived by synthetic chemists to be one with few frontiers worth pursuing. However, the past few years have seen a renewal of interest stemming from a realisation that many emerging technologies will not be adequately served by current knowledge of ceramic science[1] and the subject area has moved ever closer to chemistry as new synthetic methods have emerged.[2] The multiplicity of unique physical and chemical properties exhibited by ceramics will provide solutions to many materials problems.[3] The development of new ceramics and novel routes to existing ones, to control the form in which they may be produced and discover more economical preparations, will provide the key to the realisation of this potential.

Ceramics are non- metal, inorganic, solid- state materials. Many exist in nature as minerals. Human usage of ceramic pottery dates from the time of ancient civilisations. The word ceramic is of Greek origin and it's translation (keramos) means potter's earth.[4] Traditional ceramics are those derived from naturally occurring substances, such as cements and the clay based materials used for crockery, bricks and pipes. Advanced ceramics are those which have been produced using chemical methods or those where the naturally occurring components have been highly refined.[4] Oxides in powdered form dominate this branch of science and the synthesis, processing and properties of these materials are highly developed. There are a large number of commercial and industrial applications. Less well developed is the understanding and utilisation of nonoxidic ceramics: beryllides, borides, carbides, chalcogenides, nitrides, phosphides and silicides.

This thesis is concerned with the development of a new method, *Solid State Metathesis (SSM)*, for the preparation of ceramics. A brief introduction to some of the conventional and new methods of ceramics synthesis will, therefore, be presented.

1.1 Synthetic Approaches.

A variety of methods have been used to produce ceramic materials. Binary oxides can often be made by heating metals or their chlorides in oxygen or air. Many are found as minerals and refined. Zircon sand ($ZrO_2 \cdot SiO_2$), for example, may be fused with sodium hydroxide and reacted in solution with hydrochloric acid to yield $ZrOCl_2$. Addition of a base causes precipitation of $Zr(OH)_4$ which is dried and calcined to ZrO_2.[4] Where more complex oxides are required, the classical methods most frequently used are the thermodynamically driven, high temperature *heat and beat* techniques. Starting materials, usually oxides or carbonates, are blended together then ground or milled. These mixtures are then calcined, sometimes in a compacted

form, and the firing sequence repeated several times with intermediate grinding stages. Thus, barium titanate may be produced from cofiring a mixture of $BaCO_3$ and TiO_2 at 1200°C.[5] One difficulty with such processing occurs when one component is volatile. For example in production of lead titanate the volatility of PbO can result in lead deficient compositions.[6]

Nonoxidic ceramics may sometimes be made by solid- state reactions such as those in Eqn. 1- 3.[1,7,8] Normally it is necessary to exclude oxygen or to employ a reductant. Synthesis is often, therefore, carried out under a stream of gas, Eqn. 4- 7.[1,7]

$$2W + C \rightarrow W_2C \text{ (arc furnace)} \qquad \text{-Eqn.1}$$

$$ZrO_2 + 3C \rightarrow ZrC + 2CO \text{ (>1700°C)} \qquad \text{-Eqn.2}$$

$$Ta + P \rightarrow TaP \text{ (1400°C)} \qquad \text{-Eqn.3}$$

$$2Ti + 2NH_3 \rightarrow 2TiN + 3H_2 \text{ (>1000°C)} \qquad \text{-Eqn.4}$$

$$Ta + 2CO \rightarrow TaC + CO_2 \text{ (>1600°C)} \qquad \text{-Eqn.5}$$

$$2TiO_2 + 4C + N_2 \rightarrow 2TiN + 4CO \text{ (1600°C)} \qquad \text{-Eqn.6}$$

$$VH_3 + NH_3 \rightarrow VN + 3H_2 \text{ (1000°C)} \qquad \text{-Eqn.7}$$

These methods are used reliably to produce ceramic powders and monoliths and by no means yield sub- standard materials. However, alternative routes are becoming increasingly of interest for a number of reasons:[4]

- Purity. High temperature mechanical properties of engineering ceramics and electrical properties of electroceramics may be adversely affected by contaminants. These may be introduced by the grinding process or be left over from the reagents, e.g. of oxide or carbide in Eqn. 6. Greater purity derived from novel syntheses can lead to improved physical properties.

- Product morphology. Uniform powder compositions are difficult to attain from conventional methods. Grinding or milling results in angular- shaped powders. Non- uniform compositions make reproducible component fabrication problematic because of chemical inhomogeneity and voids in the microstructure.

- Economy. Reductions in synthesis temperature and time may often be achieved.

- Many new methods are of interest purely for the academic challenge they present.

This section will briefly review some of the methods which show promise in improved ceramic synthesis. This work has been reviewed extensively and by no means will an attempt be made here to cover all the literature, but simply to give a general overview of some relevant and/ or interesting material. A great deal of effort has concentrated on thin films. These methods will largely be ignored as the work described here deals exclusively with synthesis of bulk powders.

1.2 Microwave Heating.

Microwave dielectric heating effects are well known in cooking and are gaining popularity in solution- based molecular chemistry.[9] Microwave plasma chemical vapour deposition has been used to produce films of, for example, diamond.[10] Many solids have been reported to reach quite impressive temperatures in short time periods, Table 1.[11,12]

The technique is of use in ceramic synthesis when either the dielectric loss properties of solvents may be utilised, for example in zeolite[9] and intercalation compound[13] formation, or for direct solid state synthesis when one or more component of a reaction mixture strongly absorbs microwave radiation. In this way a number of oxides have been produced, Table 2,[14,15] with improvements over conventional methods in time, energy, crystallinity and sample purity. The reagents were intimately mixed and compacted prior to heating in a crucible.

Bulk metals are inclined to undergo plasma discharges with microwave irradiation, so are not normally heated by this method. Metal powders, however, can often be efficiently coupled to microwave fields to produce temperatures of 1000°C and greater within a few seconds without noticeable electrical discharge. Thus, microwave heating has been used in the synthesis of binary and ternary chalcogenides from the elemental powders over extremely short time periods (e.g. 180 seconds for $CuInS_2$).[16,17]

Table 1. Effect of microwave heating on the temperatures of solids.[11,12]

Substance	Temperature (°C)	Time (Min.)
Al[a]	577	6
Ni[a]	384	1
Graphite[a]	1283	1
$MnCl_2$[a]	53	1.75
NaCl[a]	83	7
$SnCl_2$[a]	486	2
CaO[b]	83	30
TiO_2[b]	122	30
V_2O_5[b]	701	9
Fe_2O_3[b]	88	30
Fe_3O_4[b]	510	2
Co_2O_3[a]	1290	3

a. 25g samples in a 1kW oven (2.45 GHz) with a 1000ml vented water load.
b. 5- 6g samples in a 500W oven.

Heating of solids using microwaves may provide an alternative to conventional pyrolysis methods in precursor decomposition reactions. The advantage of rapid, even heating is that all the precursor should decompose at once. If a mixture of precursors is used, they could be heated throughout to above both decomposition temperatures very quickly, avoiding the possibility of nucleation of individual phases from each one. This could lead to greater product homogeneity and could be envisaged to make metastable phase formation more likely.

Table 2. Solid state synthesis of oxides.[14,15]

Product	Reagents	Synthesis time (Min. at 500W)	Conventional synthesis time (H)
KVO_3	K_2CO_3, V_2O_5	7	12
$CuFe_2O_4$	CuO, Fe_2O_3	30	23
$BaWO_4$	BaO, WO_3	30	2
$La_{1.85}Sr_{0.15}CuO_4$	La_2O_3, $SrCO_3$, CuO	35	12
$YBa_2Cu_3O_{7-x}$	Y_2O_3, $Ba(NO_3)_2$, CuO	70	24

Ceramic processing may be carried out using microwaves with several advantages over conventional heating:[18]

i) Reduced cracking and thermal stress. Heating occurs evenly throughout the sample rather than *via* absorption from the surrounding environment, so many of the problems of densification may be resolved.

ii) Economy. The oven itself is heated very little.

iii) Reduced contamination. Heating from the centre limits the extent of contamination from the walls of the containment vessel.

iv) Increased strength. Rapid heating decreases the extent of non- isothermal processes such as segregation of impurities to the grain boundaries. Decreasing the sintering time reduces the possibility for secondary crystallisation (exaggerated grain growth). Reduced segregation of impurities decreases grain size and increases the sintered density resulting in improvements in the mechanical strength of the ceramic.

1.3 The Sol- Gel Process.

This process was first reported in the mid- 19th century with Ebelman's studies of silica gels.[19,20] Hydrolysis of tetraethyl orthosilicate, $Si(OC_2H_5)_4$, under acidic conditions yielded SiO_2 as a "Glass- like material".[9] Fibres, monolithic lenses and composites could be formed[20] but drying times of the order of a year were required to prevent fracturing into a powder.[21] Gradual development culminating in a period of intensive research in the 1980's has resulted in the technology to produce spherical powders of controlled particle size and morphology, glass and polycrystalline ceramic fibres, coatings and films, abrasive grains and very low density to fully dense monoliths.[21]

The sol- gel process allows materials to be produced with high purity and excellent, well controlled homogeneity at lower process temperatures than traditional glass melting or powder processing methods.[21] This is made possible by the control of surfaces and interfaces during the earliest stages of production.[22] Drying of modern sol- gel derived materials, such as gel- silica optics,[23] can be carried out in days rather than years. Stresses due to shrinkage during removal of pore liquids from the gel can result in fractures. In the synthesis of small diameter powders, films and fibres, these

stresses are small and normally do not lead to failure. For larger monoliths (>1cm) it is essential to control the chemistry of each step of the sol- gel process very carefully to prevent cracking. For sol- gel synthesis of ceramics, three approaches are utilised:

a) Gelation of a solution of colloidal powders.
b) Hydrolysis and polycondensation of precursors, such as alkoxides or nitrates, followed by hypercritical drying of gels.
c) Hydrolysis and polycondensation of alkoxide precursors followed by ageing and drying under ambient atmospheres.

Sols are dispersions of colloidal particles (diameter 1- 100 nm) in a liquid.[24] A *Gel* is an interconnected, rigid network with pores of submicron dimensions and polymeric chains with average length greater than a micron.[21] When the pore liquid is evaporated under hypercritical conditions (critical point drying, approach b), the network does not collapse and an *Aerogel* is formed with pore volumes as large as 98% and densities as low as 80 Kgm^{-3}.[24] Thermal evaporation (approaches a, c) results in shrinkage and the monolith is referred to as a *Xerogel*.[21] Whichever approach is employed, sol- gel processing of monoliths is a seven stage process:[21]

i) Mixing. Mechanical mixing of colloidal particles in water or hydrolysis of a precursor, Eqn. 8. The hydroxide undergoes condensation reactions, Eqn. 9, and eventually results in networks which behave like colloidal particles *Sols*. Use of metallorganic precursors rather than colloidal particles allows for mixing on the atomic (single precursor) or molecular (multiple precursors) level rather than mixing individual grains of material.

$$Si(OMe)_4 + 4H_2O \rightarrow Si(OH)_4 + 4MeOH \qquad \text{-Eqn.8}$$

$$2Si(OH)_4 \rightarrow (OH)_3Si\text{-}O\text{-}Si(OH)_3 + H_2O \qquad \text{-Eqn.9}$$

ii) Casting. The sol, a low viscosity liquid, is cast into a mold.

iii) Gelation. With time the colloidal particles or condensed species interlink to form a 3- dimensional network. At gelation, viscosity increases sharply and a solid object is formed in the shape of the mold. Fibres can be pulled as gelation occurs.

iv) Ageing. The cast object is kept completely immersed in liquid for hours to days. Polycondensation continues along with localised solution and

reprecipitation of the gel network, which increases the thickness of the interparticle necks and decreases the porosity. Strength is developed to resist fracture during drying.

v) Drying. The liquid is removed from the interconnected network. Large capillary stresses can develop with small pore sizes, resulting in cracking. This is prevented by reducing liquid surface energy using surfactants, hypercritical evaporation or by obtaining monodispersed pore sizes by control of rates of hydrolysis and condensation.

vi) Dehydration or Chemical Stabilisation. Removal of surface hydroxyls from the pore network to yield a chemically stable, ultraporous solid.

vii) Densification. Heating (1000- 1700°C) causes pores to be eliminated and density ultimately can approach theoretical values.

Spherical powders may be obtained by mixing, gelation and spray drying.[25] Spray drying directly into a calcining furnace allows intraparticular sintering to occur and items made from such powders undergo intermolecular sintering with minimal loss of density.[25] The materials produced include oxides (SiO_2, TiO_2, α- Fe_2O_3, Fe_3O_4, $BaTiO_3$, CeO_2), hydroxides (AlOOH, FeOOH, $Cr(OH)_3$), carbonates ($Cd(OH)CO_3$, $Ce_2O(CO_3)_2$, Ce(III)/ $YHCO_3$), sulfides (CdS, ZnS), metals (Fe(III), Ni, Co), composites (Ni/ Co and Sr ferrites) and coated particles (Fe_3O_4 with $Al(OH)_3$ or $Cr(OH)_3$).[2,26-28] Carbides and nitrides are obtained by adding a carbon source at the sol stage and heating the carbon- containing gel in a controlled atmosphere.[4] For example, heating a dried C/SiO_2 gel in a N_2/H_2 atmosphere yields Si_3N_4, in the α- or β- phase for oven dried or spray dried gels respectively.[29]

The major advantage of sol- gel methods is the control of the form of the product. Ceramics may be produced as monoliths, fibres or spherical particles without conventional processing of oxide powders. The technique is limited in the variety of nonoxidic materials which may be produced, however this is a field which is progressing rapidly.

1.4 Precursor Decomposition.

Precursor decomposition reactions are the basis of many sol- gel and chemical vapour deposition syntheses. Thermal decomposition of bulk quantities of compounds may

also be used in ceramics synthesis. The single- source precursor concept has gained popularity on the hypothesis that a molecule with the desired ratio of atoms needed in the target material may be decomposed with product stoichiometry built in at the atomic level.[30] It is, of course, essential that all the other unwanted atoms leave during the transformation from molecule to material. It is also possible to mix two or more precursors at the molecular level and decompose them to homogeneous materials.

The first class of such methods is the use of salts such as carbonates, nitrates, sulfates and hydroxides or complexes such as oxalates, citrates and nitrate/ ethylene diamine tetraacetic acid solutions for decomposition to oxides. Salts are mixed in solution, usually aqueous, and the mixture is dried and calcined to mixed metal oxides. Submicron sized particles of manganese ferrite may be produced in the aerosol spray pyrolysis of solutions of chlorides and nitrates in water.[31] Freeze or spray drying increases the homogeneity of the pre- calcined mixture as any variation in solubility of the salts becomes unimportant. Thus, superconducting $HgBa_2Ca_2Cu_3O_{8+x}$ may be produced from the freeze dried nitrates with a reduced fraction of impurity phases compared with that produced using conventional drying of the nitrates.[32] Nickel- iron hydroxide carbonates may be decomposed to highly dispersed ternary nickel iron oxides, an application of the single source approach to these methods.[33] Yttrium oxide is the product of decomposition of hydrated yttrium acetate, nitrate or oxalate.[34] The materials from these preparations were investigated in terms of temperature of formation, texture and surface area. Nitrate precursors may also be used in methods similar to sol- gel processing techniques. Lead zirconate titanate (PZT) ceramic powder has been synthesised using the EDTA- gel method from nitrate solutions.[35] Nitrate- EDTA complexes were decomposed with crystallisation of PZT at temperatures in the region of 250°C.

Good control of thermal decomposition reactions may be achieved by carrying them out in solution.[36] The product is precipitated from a homogeneous solution, usually aqueous, of a coordination complex by thermal treatment.[37] A complex is formed which is sufficiently stable to prevent spontaneous precipitation at room temperature. Raising the temperature, sometimes in conjunction with a rise in pressure, promotes dissociation of the complex and allows the controlled generation of free metal ions which are precipitated on hydrolysis.[4,37] Such methods are referred to as hydrothermal synthesis and control of particle shape and size may be exercised by variation of ligand, temperature, time, solvent and pressure.[4,37] The use of a non-metallide source can allow synthesis of non- oxidic ceramics. For example, addition of an appropriate chalcogenide source leads to the formation of sulfides and

selenides.[36] Pyrolysis of solutions of zinc nitrate, sulfate, chloride or acetate with a variety of different ligands leads to controlled precipitation of zinc oxide.[37] Addition of thioacetamide allowed synthesis of zinc sufide.

A number of systems exist where reaction in solution leads to precipitates which, upon thermolysis, yield important nonoxidic ceramics.[1] These may produce the desired material which then is sintered to induce crystallinity or they may yield intermediates which decompose to a ceramic. Silane elimination followed by thermolysis of a precipitate may be used to produce 13-15 materials, Eqn. 10, 11.[38]

$$ZnEt_2 + Se(SiMe_3)_2 \rightarrow ZnSe + 2EtSiMe_3 \qquad \text{-Eqn.10}$$

$$CdMe_2 + Te(SiMe_2Pr^i)_2 \rightarrow CdTe + 2Pr^iSiMe_3 \qquad \text{-Eqn.11}$$

ZnS may also be produced by the reaction of the organozinc reagent $[EtZn(SBu^t)]_5$ with H_2S in dichloromethane followed by thermolysis of the solid product under H_2S.[39] MTe (M= Mn, Fe, Ni and Pd) and $FeTe_2$ are obtained by thermolysis of the products of solution reactions of a variety of organometallic compounds with Et_3PTe.[1,40,41] Reactions of early transition metal dialkyl- and silyl- amides with ammonia in benzene yield precipitates which decompose on thermolysis under helium to the nitrides.[42] Thermolysis simply of the amides produces mainly carbides and carbonitrides.[1,43] Treatment with liquid ammonia of $Ti(NMe_2)_4$, $Zr(NEt_2)_4$ and $Nb(NEt_2)_5$ followed by thermolysis of the product gave nitrides with high levels of carbon contamination (2·5 - 7·8 %).[44]

Synthesis of some main group ceramics may be performed by the thermal decomposition of organosilicon polymers.[4] Fig. 1 represents a method for producing silicon carbide fibres.[45] Cross- linking with a metal source may be used to produce composites such as β- SiC·TiC.[46,47] Polysilazane resins, containing Si-N-Si linkages, may be converted to $SiC{\cdot}Si_3N_4$ composites.[46] Heating melt- spun polycarbosilane in ammonia yields silicon oxynitride phases.[48]

Precursor decomposition reactions have the potential to provide low energy routes to a wide variety of materials. The difficulty is in controlling the stages such that the impurities are minimised. This is a field with huge potential for research from a chemical viewpoint.

Figure 1. Synthesis of β- SiC fibres.

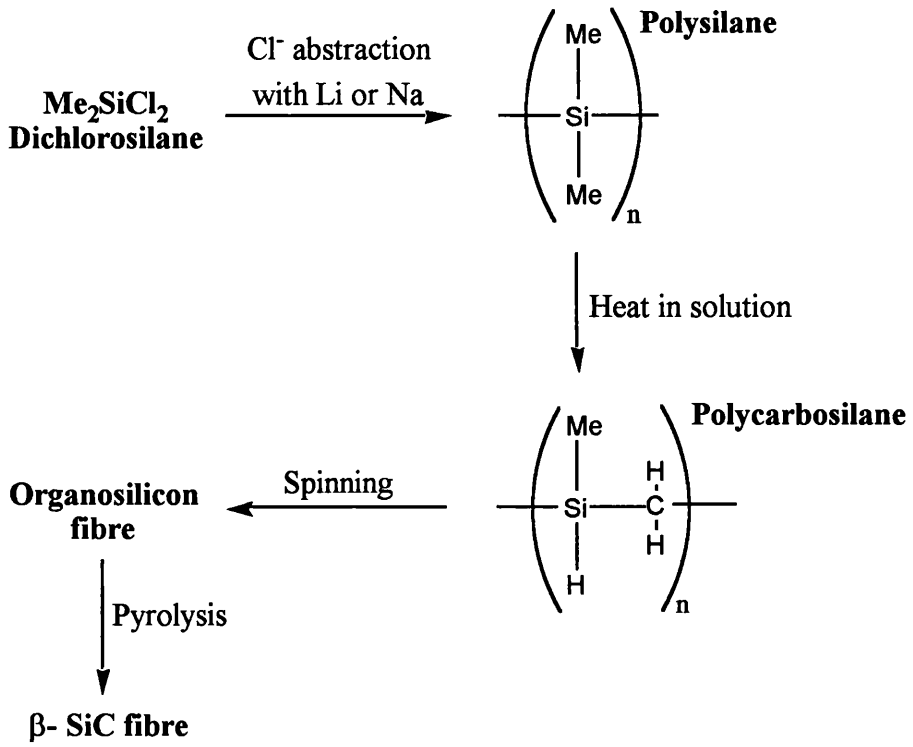

1.5 High Surface Area Syntheses.

Many ceramics are of interest as catalysts.[49] Such utilisation requires the development of high specific surface area (S_g) materials. Classical synthetic methods tend to produce low surface area materials. This has led to some unusual methods. New routes to important catalysts with high surface areas continue to be of great interest.

In 1933, Pfund described the vapourisation of volatile metal compound precursors ($Mo(CO)_6$, $W(CO)_6$, WCl_6) onto an incandescent tungsten coil at 1400- 1700 K in a low pressure hydrocarbon atmosphere.[7] The dark smoky plume of particles which collected on the reactor walls consisted of various carbides or oxycarbides, depending on specific conditions. The method has since been used to produce WC and MoO_xC_y with S_g up to 40 m^2g^{-1}.[50] Unfortunately, the method is poorly controlled and suffers from low yields. Transition metal nitrides with particle sizes of 2- 10 nm have also been prepared by vapourising metals in low pressure N_2 or NH_3 using electron beam heating.[51]

Plasma- jet synthesis combines high temperature combination with very rapid quenching.[49] Carbides and nitrides have been produced as high temperature phases with particle sizes of 5- 50 nm,[52] but only low product yields are attained.

Deposition of a precursor onto a support and subjecting it to a reducing gas stream, Eqn. 12 and 13, offers improvements in control over surface area and pore size distribution.[49,53,54] Reaction of vapourised MoO_3 or WO_2 with ultra- high surface area activated carbon yields carbides with S_g of 100- 400 m^2g^{-1}.[55] The final product appears to retain a memory of the porous structure of the starting material.[49]

$$Mo(CO)_6 + CH_4/ H_2 \rightarrow Mo_2C \text{ (supported)} \qquad \text{-Eqn.12}$$

$$MoO_2 + NH_3/ H_2 \rightarrow Mo_2N \text{ (supported)} \qquad \text{-Eqn.13}$$

Temperature- programmed reactions involve placing an oxide precursor in a reactive gas stream and ramping up the temperature whilst monitoring the exit gas composition and quenching when reaction is complete.[49] MoO_3 with a CH_4/ H_2 gas mixture produced Mo_2C with S_g of 50- 90 m^2g^{-1}.[56] Using NH_3, Mo_2N is obtained with S_g as high as 225 m^2g^{-1}.[57] WO_3 with ammonia yields W_2N with S_g up to 90 m^2g^{-1}.[49]

1.6 Self Propagating Reactions.

Thermite reactions are highly exothermic oxidation- reduction processes. They typically occur between a metal and an oxide, the classic example involves aluminium and iron (III) oxide,[58] Eqn. 14, which has in the past been used for welding railway tracks. This reaction has been reported as achieving temperatures well in excess of 3000°C,[58] sufficient to melt both iron and alumina. Aluminium has been used as reductant to prepare samples of most transition metals, boron, silicon, lead, uranium and plutonium. Other reductants include magnesium, calcium, zirconium, zinc, carbon and silicon but aluminium is normally preferred for cost, product purity and energetic reasons.[59]

$$2Al + Fe_2O_3 \rightarrow 2Fe + Al_2O_3 \qquad \text{-Eqn.14}$$

Self- propagating high- temperature (combustion) synthesis (SHS) is a process which has been developed over the last quarter- century, initially by Merzhanov and co-workers in Russia, as a route to refractory materials such as ceramics, ceramic

composites and intermetallic compounds.[60,61] SHS involves the initiation of an elemental combination reaction in a compacted mixture of powdered reagents, the reaction then being sufficiently exothermic to become self- sustaining. Reactions can be classified as either *Propagating* or *Bulk*.[62] The former occurs when the reactants are ignited locally and a synthesis (combustion) wave then passes through the remainder. Bulk reactions are performed by rapid heating of the compacted reagents in a furnace, such that simultaneous initiation occurs throughout the material, Fig. 2. This is also known as a *Thermal explosion* and is normally used when reactions are not sufficiently exothermic for self- propagation.

Figure 2.[62] *Typical exothermic peak in a thermal explosion mode of combustion.*

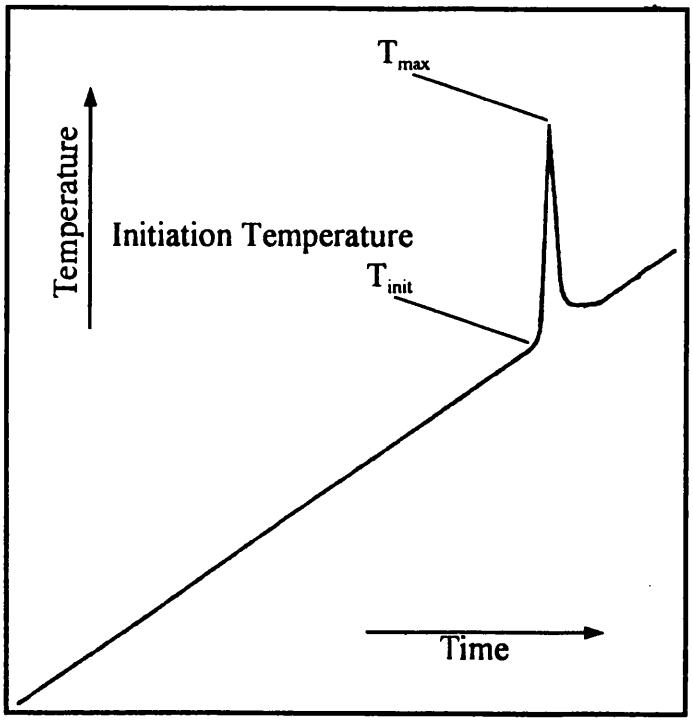

However initiated, a brief period of extreme temperature (1000- 5000°C) is observed, followed by rapid quenching.[62] This leads to a massive potential for the production of metastable materials with high defect concentrations and non- equilibrium structures.[62] The high temperature can vapourise volatile contaminants, leading to high product purity.[63] Products have also been shown to be more active to sintering, at least in the initial period of heating.[64,65] Great savings in time (seconds as opposed to hours or days) and energy compared with conventional preparations may be achieved.

A huge variety of materials have been produced *via* the SHS method. Table 3 gives some indication of the range of these. Where a component is a gas in the elemental form (e.g. in nitride synthesis), it is introduced in gaseous or liquid phase and the

reaction performed in the propagating manner.[62] Complete conversion to nitride requires a significant fraction of nitride added to the precursor as a diluent and a high nitrogen pressure (10 MPa).[66] In this way it has been possible to produce wires and thin sheets of niobium nitride,[67] for superconductor usage. Alternatively, the nitrogen has been incorporated from sodium azide,[62] Eqn. 15. The sodium byproduct was completely volatilised and product purity was found to be very high. This process has also been used in conjunction with a thermite reaction to produce composite ceramics,[62] Eqn. 16.

$$3M_{(s)} + NaN_{3(s)} \rightarrow 3MN_{(s)} + Na_{(g)} \qquad \text{-Eqn.15}$$

$$3TiO_2 + 4Al + NaN_3 \rightarrow 3TiN + 2Al_2O_3 + Na_{(g)} \qquad \text{-Eqn.16}$$

Table 3. Some materials produced by SHS.[62]

Borides	LaB_6, MB_2 (M = Ti, Zr, Hf, Nb, Ta, Mo), VB, CrB
Carbides	MC (M = Ti, Zr, Hf, Nb, Ta, W, Si), Cr_3C_2, B_4C, Al_4C_3
Carbonitrides	M(C,N) (M = Ti, Nb, Ta)
Nitrides	MN (M = Ti, Zr, Hf, Nb, Ta, B, Al), Si_3N_4
Silicides	MSi_2 (M = Zr, Nb, Ta, Mo, W), M_5Si_3 (M = Ti, Zr, V, Nb, Ta)
Hydrides	MH_2 (M = Ti, Zr, Nb)
Intermetallics	MAl (M = Ni, Fe, Cu), TiNi, CoTi, Ni_6Ge
Chalcogenides	NbS_2, $TaSe_2$, MoS_2, WSe_2

1.7 Metathetical Reactions.

Metathetical (exchange) pathways, Eqn. 17, to ceramics require, by definition, two precursors. One is most often a halide, the other contains Group 1 or 2 metals or protons. These reactions have been performed in the gas phase, in solution, at the gas- solid interface or in solution.

$$AB + CD \rightarrow AD + BC \qquad \text{-Eqn. 17}$$

A good example of gas- phase metathesis reactions is that of silicon tetrachloride with ammonia,[68] Eqn. 18. This also illustrates the ease of purification of products from this

type of reaction. The side products will normally be HCl (gaseous) or a Group 1 or 2 halide (easily washed away). Solution reactions are exemplified by the syntheses of Group 4 and 5 disulfides (M= Ti, Zr, Hf and V) in non- aqueous solvents from the tetrachlorides and lithium sulfide,[69] Eqn. 19. Heterogeneous reactions of metal oxides or sulfides with ammonia or phosphine have been used to produce nitrides and phosphides respectively, for example the preparation of boron phosphide at 1200-1400°C,[70] Eqn. 20.

$$3SiCl_{4(g)} + 4NH_{3(g)} \rightarrow Si_3N_{4(s)} + 12HCl_{(g)} \qquad \text{-Eqn. 18}$$

$$MCl_4 + 2Li_2S \rightarrow MS_2 + 4LiCl \qquad \text{-Eqn. 19}$$

$$B_2S_{3(s)} + 2PH_{3(g)} \rightarrow 2BP_{(s)} + 3H_2S_{(g)} \qquad \text{-Eqn. 20}$$

A solid state metathesis, although not referred to as such, reaction was reported by Hilpert and Wille[71] in 1932, who prepared mixed metal ferrites at 400- 500°C, Eqn. 21. A high temperature metathetical combination has also been used as a route to chromium phosphide,[72] Eqn. 22.

$$ZnCl_2 + Li_2Fe_2O_4 \rightarrow ZnFe_2O_4 + 2LiCl \qquad \text{-Eqn.21}$$

$$Ca_3P_2 + 2CrCl_3 \rightarrow 2CrP + 3CaCl_2 \qquad \text{-Eqn.22}$$

These reactions all require high temperature processes, either during the reaction or, in the cases of gas- phase and solution reactions, for the annealing of products where crystalline materials are required.

Kaner and co- workers[73-78] have shown that the adaptation of the SHS technique to SSM (a phrase which they coined) reactions, choosing reagents to make them sufficiently exothermic for self propagation, results in crystalline products at much reduced initiation temperatures. The technique has been used to produce some transition metal dichalcogenides,[73-77] Eqn. 23

$$MCl_x + {}^{x}/_{2}M'_2Ch_y \rightarrow MCh_2 + xM'Cl\ (+zS) \qquad \text{-Eqn.23}$$

(M= Nb, Ta, Mo, W, Ni, Mo/W; M'= Li, Na; Ch= S, Se, Te, S/Se)

The reactions were either self- initiated or hot filament or oven initiation was employed. The advantages of the method include rapidity of reaction, low energy input, highly sinterable products and low external contamination, e.g. from the reaction vessel walls. The two main difficulties lie in containment of the extreme temperatures, especially on scale-

up, and in the need to remove the co- produced alkali- metal halide.

Previous to the start of our work they have also published syntheses of some other materials. These include gallium pnictides from reactions with the sodium pnictides[74,77,78] and refractories such as one nitride (ZrN) from $ZrCl_4$ with Li_3N and one silicide ($MoSi_2$) from $MoCl_5$ with Mg_2Si.[74,75,77] This work was normally carried out with filament initiation and where it has been developed further during the course of our investigations will be mentioned in the appropriate sections.

1.8 Objectives.

SSM reactions have already been shown to possess considerable potential for ceramics synthesis. The intention in the work presented here was to further investigate this potential. The bulk of the work involves metal pnictide formation. This has been concerned with transition metal and rare earth nitride synthesis using a variety of nitrogen sources and transition metal phosphide, arsenide and antimonide synthesis using sodium pnictides. Also included is the synthesis of transition metal and rare earth silicides and transition metal oxides using magnesium silicide and lithium oxide. Attention has been paid to evidence relevant to reaction mechanisms. This tends to rely on end- product analysis since reactions are in general quite fast. Two extremes of reaction mechanism may be envisaged, illustrated for a reaction to produce titanium nitride in Eqn. 24 and 25. Reductive recombination, Eqn. 24, would involve generation of a metal and nitrogen followed by high temperature recombination. Ionic metathesis, Eqn. 25, would occur *via* Ti^{3+} and N^{3-} ions. In this case the transfer of ions in a lithium chloride melt could occur.

$$TiCl_3 + Li_3N \rightarrow Ti + N + 3LiCl \rightarrow TiN + 3LiCl \qquad \text{-Eqn.24}$$

$$TiCl_3 + Li_3N \rightarrow Ti^{3+} + N^{3-} + 3LiCl \rightarrow TiN + 3LiCl \qquad \text{-Eqn.25}$$

The use of the phrase solid state metathesis to describe these reactions is not strictly accurate. The reaction mechanistics are uncertain and it is likely that the reaction actually accurs in an alkali halide melt. However, the phrase is convenient and does describe quite well the overall process, so will be used in this text. Dilution of reaction mixtures could be expected to reduce the voracity of reactions and yield different products or alter their form. Studies were conducted into these possibilities.

2. Metal Nitride Synthesis with Li_3N.

A number of compounds can be envisaged as potential nitrogen sources in metathetical reactions leading to metal nitrides. The metal chlorides or other halides are a convenient source of metal as they are readily available and fairly cheap in a high purity form. Use of an alkali metal or alkaline earth source of nitrogen yields a co-product (alkali metal or alkaline earth halide) which is air stable and easily removed by washing. The high lattice energy of the co- product is the biggest contributor to the exothermicity of the reactions. A number of groups of compounds fulfil these criteria:

i) Nitrides. Li_3N.
Mg_3N_2, Ca_3N_2, Sr_2N.

ii) Azides. LiN_3, NaN_3, KN_3.
$Mg(N_3)_2$, $Ca(N_3)_2$.

iii) Amides. $LiNH_2$, $NaNH_2$, $LiNMe_2$.
$Mg(NH_2)_2$, $Ca(NH_2)_2$.

In this chapter, syntheses using Li_3N will be discussed, Eqn. 26. The following chapter will describe work with NaN_3 and group 2 nitrides. During the course of this study, work has been carried out in our laboratory using lithium and sodium amides in related reactions to produce nitrides.[79,80]

$$MCl_n + {}^{n}/_{3}Li_3N \rightarrow {}^{1}/_{x}M_xN_y + zN_2 + nLiCl \qquad \text{-Eqn.26}$$

2.1 Properties and Applications of Nitrides.

Most transition metals, lanthanides and actinides and many main group elements form nitrides, listed in Table 4.[81,82] Many are of special interest for utilisation in a variety of guises. Many azides also form. The nitrides of groups 1, 2, 11 and 12 are normally regarded as essentially ionic materials, containing N^{3-} ions (~1.4 Å radius) in their crystal lattices.[82] Group 1 and 2 nitrides readily hydrolyse with evolution of ammonia,[83] Eqn. 27.

$$Mg_3N_2 + 3H_2O \rightarrow 3Mg(OH)_2 + 2NH_3 \qquad \text{-Eqn.27}$$

Sodium azide and the group 11 nitrides decompose readily at modest temperatures (e.g. Ag_3N at 25°C).[82] The rare earth nitrides possess the Fm3m (NaCl) structure.

Table 4. Stoichiometric Nitride Phases.*[81,82]

(1)	(2)	(3)	(4)	(5)	(6)	(7)	(8)	(9)	(10)	(11)	(12)	(13)	(14)	(15)
Li_3N	Be_3N_2											BN	C_3N_4	×
Na_3N	Mg_3N_2											AlN	Si_3N_4	P_3N_5 PN
×	Ca_3N_2 Ca_2N	ScN	TiN Ti_4N_3 Ti_3N_2 Ti_2N	VN V_2N	CrN Cr_2N	MnN Mn_3N_2 Mn_2N Mn_4N	Fe_2N Fe_3N Fe_4N	CoN Co_2N Co_3N Co_4N	Ni_3N Ni_4N	Cu_3N	Zn_3N_2	GaN	Ge_3N_4	×
×	SrN Sr_3N_2 Sr_2N	YN	Zr_3N_4 ZrN	NbN Nb_4N_3 Nb_2N	MoN Mo_2N	TcN Tc_4N_3	×	×	×	Ag_3N	Cd_3N_2	InN	Sn_3N_4 Sn_3N_2	×
×	Ba_3N_2		Hf_3N_4 HfN Hf_4N_3 Hf_3N_2	Ta_3N_5 TaN Ta_2N Ta_4N	WN W_2N	Re_2N	×	×	×	Au_3N	Hg_3N_2	TlN	Pb_3N_4 Pb_3N_2	×

LaN	CeN	PrN	NdN	×	SmN	EuN	GdN	TbN	DyN	HoN	ErN	TmN	YbN	LuN
×	Th_2N_3 Th_3N_4 ThN	PaN_2 PaN	UN_2 U_2N_3 UN	NpN	PuN	AmN	CmN	BkN	×	×	×	×	×	×

Molecular nitrides such as S_4N_4 and As_4N_4 have been omitted. × No known nitride phase.

* The interstitial nature of these compounds does make non- stoichiometry rife.
For example, the cubic TiN phase has a composition range from $TiN_{0.6}$ to $TiN_{1.16}$.[7]

Bonding in metal nitrides is generally regarded as between ionic and metallic.[82] Most have magnetic moments which suggest the metal has a 3+ oxidation state,[84] therefore the metallic character is probably due to small deviations from stoichiometry such as vacancies in the N^{3-} population.[85] Most nitrides of groups 4- 10 have historically been referred to as interstitial compounds and are essentially metallic in character.[82] The nitrogen atoms occupy some or all of the interstitial sites in metallic lattices and non-stoichiometry is common.[86] The metal and the nitride share many properties (electrical conductivity, Hall coefficient, magnetic susceptability and heat capacity).[49] They frequently have higher melting points (HfN 3310°C)[87] and hardness values (TiN 1700- 1900 Kg mm^{-1})[88] than the metals, chemical inertness at ordinary temperatures, high thermal conductivity and good mechanical strength.[1,7,89-91] The nitrides of Mn, Fe, Co and Ni, along with the carbides, are important constituents of steels, the hard second phases responsible for higher strength.[7]

Hardness of group 4- 6 nitrides is utilised in machine tools where TiN or ZrN are normally used with a Co, Mo or Ni binder phase.[92] They are also employed in hard-cast alloys, rocket engine coatings and refractory vessel materials.[1] TiN is of great interest as a reflectance coating material, for example in building energy management.[93] Several nitrides and carbonitrides display superconducting properties below *ca.* 15K.[7,90]

The potential of transition metal carbides and nitrides as catalysts is very considerable.[49] Early transition metals are electron defficient and, in their elemental state, are characterised by an aggresive reactivity toward hydrocarbons.[49] Formation of interstitial alloys with essentially covalent bonding increases the electron count and reactivity is tamed, thus the alloys resemble the elements to the right of the d-block.[49,94] For these reasons it has been suggested that, for some reactions, nitrides could provide an inexpensive replacement for the Group VIII metals. In ammonia synthesis, Mo_2N is more active than ruthenium but considerably less active than doubly- promoted iron catalysts.[95] In ammonia decomposition, VN has rate parameters similar to those of iron and platinum.[96] In synthesis gas chemistry (reactions of CO with H_2), Mo_2N and W_2N were found to have similar activity to the best Group VIII metal, ruthenium, and to be immune to small amounts of H_2S.[49,97] Mo_2N was found to be 84% selective to methane, compared with 69% for ruthenium.[49,98] Kinetics and product distributions are found to be dissimilar to those of the Group VIII metal catalysed reactions, which can be taken to indicate different modes of operation.[98] Tolerance to sulfur makes them of great interest as hydrodesulfurisation and hydrodenitrogenation catalysts, Mo_2N has been shown to out perform sulfide systems ($MoS_2{\cdot}Al_2O_3$ and $Ni_xMo_yS_z{\cdot}Al_2O_3$) in coal liquids

processing.[99] The future usage of these systems as catalysts of great industrial importance is very likely.

The group 13, 14 and 15 nitrides listed in Table 4 are strongly bound covalent lattices.[82] There are also a number of molecular p- block nitrides such as As_4N_4 and S_4N_4.[82] Boron nitride is isoelectronic with carbon and occurs in two forms, the hexagonal zinc- blende type phase which is second in hardness only to diamond and a layered structure similar to graphite.[82] β- C_3N_4 is metastable and has only been formed as nitrogen defficient thin films, but has been predicted in computational studies to be harder than diamond.[100] Aluminium, gallium and indium nitride are of interest for their semiconductor properties and Si_3N_4 and AlN are produced on a large scale for engineering applications and for use as abrasives.[82] Actinide nitrides are of interest as alternatives to refractory oxides for nuclear fuel usage.[101]

2.2 Reactions of Lithium Nitride with Transition Metal Chlorides.

Lithium nitride has previously been used as a nitride source in molecular chemistry, such as in the synthesis of S_4N_4.[102] In this work the thermally initiated solid state metathesis reactions of transition metal chlorides with lithium nitride were investigated.

If an intimate mixture of an anhydrous transition metal chloride with lithium nitride is heated, *in vacuo* at *ca.* 400°C in a sealed Pyrex ampoule , then after a few seconds a bright flash of light is observed. The reactions with $CrCl_2$ and $MoCl_3$ required a reaction temperature of 500°C. When cool, the glass ampoules used to perform the reactions were found to contain a black solid, in fused lumps. These crude products were characterised through X- ray powder diffraction (XRD) as metal nitride or metal (Table 5) and lithium chloride. Scanning electron microscopy (SEM), Fig. 3, showed a smooth, continuous surface. Energy dispersive X- ray analysis (EDXA) showed chlorine and metal, Fig. 4. The technique is insensitive to elements with atomic numbers <4, so lithium could not be detected. These data indicate that metal nitride or metal produced by the reaction are coated with lithium chloride which has melted during the reaction. Nitrogen was presumably not observed as the 'soft' (low energy) X- rays it produces would have been reabsorbed by the lithium chloride coating or by the metal itself. In section 2.3 it is shown from constant pressure calculations that the temperatures reached during these reactions are easily sufficient to melt the lithium chloride (and indeed boil some of it) and produce the thermal flash which was observed during reactions.

Table 5. Products of reactions with lithium nitride and their lattice parameters.

Reagent	Product(s)	System, space group	**a** (lit.[81,103] **a**) / Å	**c** (lit.[81,103] **c**) / Å
$TiCl_3$	TiN	Cubic Fm3m	4.237 (4.242)	
$ZrCl_4$	ZrN	Cubic Fm3m	4.572 (4.578)	
$HfCl_4$	HfN	Cubic Fm3m	4.507 (4.525)	
VCl_3	VN	Cubic Fm3m	4.140 (4.139)	
	(V_2N)	Hexagonal P31m		
$NbCl_5$	Nb_4N_3	Tetragonal	4.373 (4.382)	4.309 (4.316)
	Nb_2N	Hexagonal $P6_3/mmc$	3.056 (3.055)	9.987 (9.988)
$TaCl_5$	TaN	Cubic Fm3m	3.362 (3.369)	
	Ta_2N	Hexagonal $P6_3/mmc$	3.051 (3.045)	4.915 (4.914)
$CrCl_2$	Cr_2N	Hexagonal P-31m	4.804 (4.811)	4.442 (4.484)
	Cr	Cubic Im3m	2.885 (2.884)	
$CrCl_3$	Cr_2N	Hexagonal P-31m	4.800 (4.811)	4.452 (4.484)
$MoCl_3$	Mo	Cubic Im3m	3.149 (3.147)	
	(Mo_2N)	Tetragonal $I4_1/amd$		
$MoCl_5$	Mo	Cubic Im3m	3.144 (3.147)	
WCl_4	W	Cubic Im3m	3.165 (3.165)	
$MnCl_2$	Mn_4N	Cubic Pm3m	3.837 (3.846)	
$FeCl_3$	Fe	Cubic Im3m	2.869 (2.866)	
$CoCl_2$	Co	Cubic Fm3m	3.545 (3.545)	
$NiCl_2$	Ni	Cubic Fm3m	3.530 (3.524)	
$CuCl_2$	Cu	Cubic Fm3m	3.606 (3.615)	
$ZnCl_2$	Zn	Hexagonal $P6_3/mmc$	2.672 (2.665)	4.938 (4.947)

Where two phases are listed, greater phase listed first. Parentheses indicate trace amounts only.

Parameters derived using TREOR program.

Grinding the crude product and washing with dry THF or methanol removes LiCl and leaves the pure metal nitride or metal product. Table 5 lists these materials with XRD lattice parameters. SEM indicated agglomerated particles sized 10- 100 μm, Fig. 3. Crystallite sizes, calculated from XRD line broadening,[104] were of the order of 500-

1000 Å. EDXA, Fig. 4, showed only metal and nitrogen for TiN, VN and Cr_2N. This places impurity levels (A. N. >4) below 0.5- 1%, the detection limit of the instrument. Second and third row nitrides, or first row nitrides washed with water, also showed a small oxygen peak. This may be attributed to the formation of a surface layer of oxide. The metals listed in Table 5 showed only metal and sometimes oxygen. Fourier transform infrared (FT-IR) spectra of the nitrides showed only a broad band centred at 400- 500 cm^{-1}. This is consistent with M-N bonds[105] in an infinite lattice. Microanalysis data were often indicative of slightly nitrogen defficient products. This is most likely to be a function of the refractory nature of the compounds rather than an actual defficiency, since the XRD lattice parameters (Table 5) so closely match the literature values.

Fig. 3. Scanning electron micrograph of the crude (top) and washed (bottom) products of the reaction between $TiCl_3$ and Li_3N.

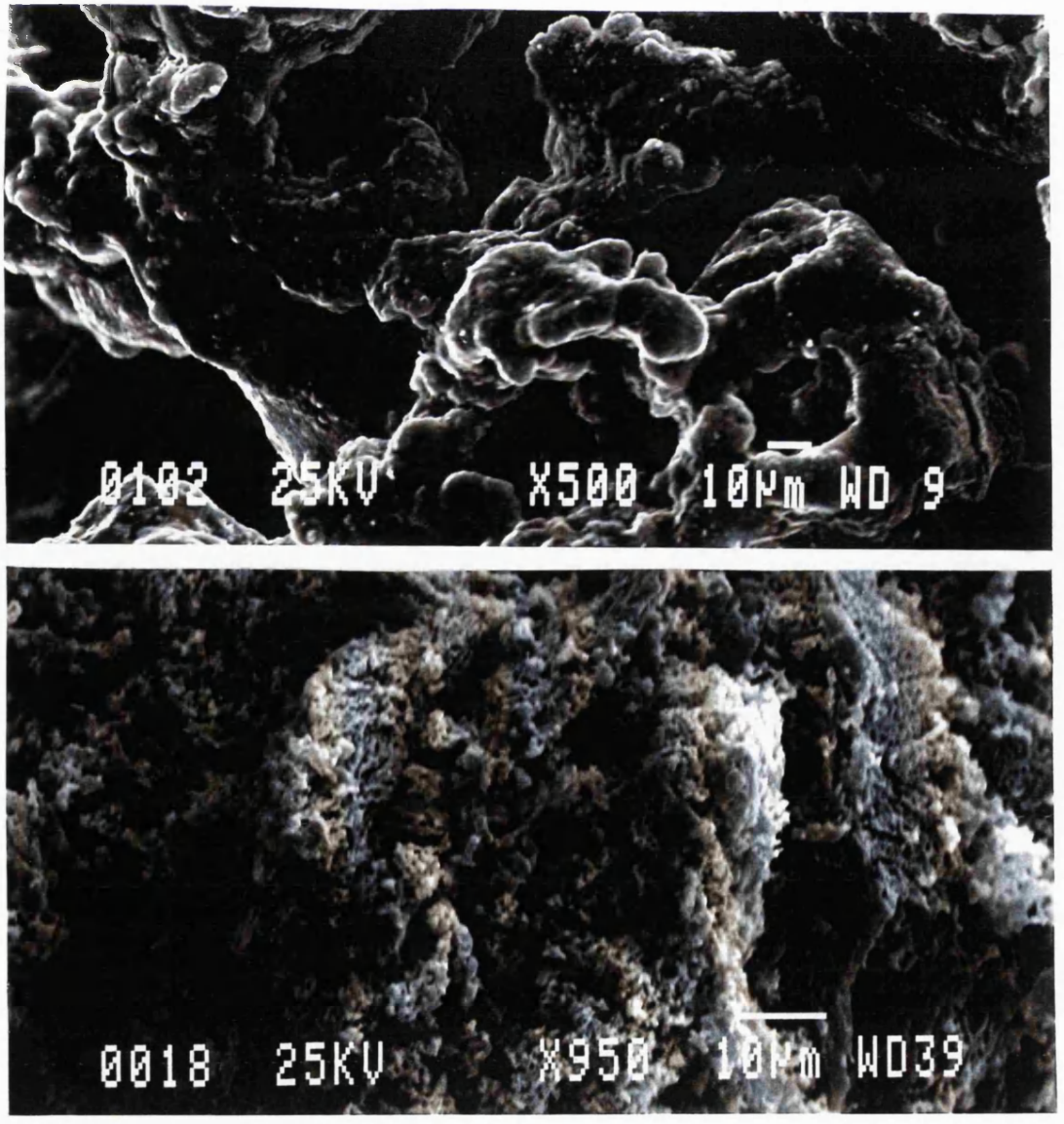

The products of these reactions are remarkably crystalline considering the timescale of the reactions. This is most likely due to the the temperatures reached in such extremely exothermic reactions, Eqn. 28 and 29. It is also worth noting that lithium chloride has been implicated[106] in catalysing the crystallisation of lanthanum nitride by providing a template. A similar effect cannot be ruled out here but the reaction temperatures are too high to have any solid LiCl present, so this is unlikely.

$$TiCl_3 + Li_3N \rightarrow TiN + 3LiCl \qquad \Delta H_r^\circ = -676 \text{ kJ mol}^{-1} \qquad \text{-Eqn.28}$$

$$MoCl_5 + {}^5/_3Li_3N \rightarrow Mo + 5LiCl + {}^5/_6N_2 \qquad \Delta H_r^\circ = -1389 \text{ kJ mol}^{-1} \qquad \text{-Eqn.29}$$

Fig. 4. Energy dispersive X-ray analysis of the crude (top) and washed (bottom) products of the reaction between $TiCl_3$ and Li_3N.

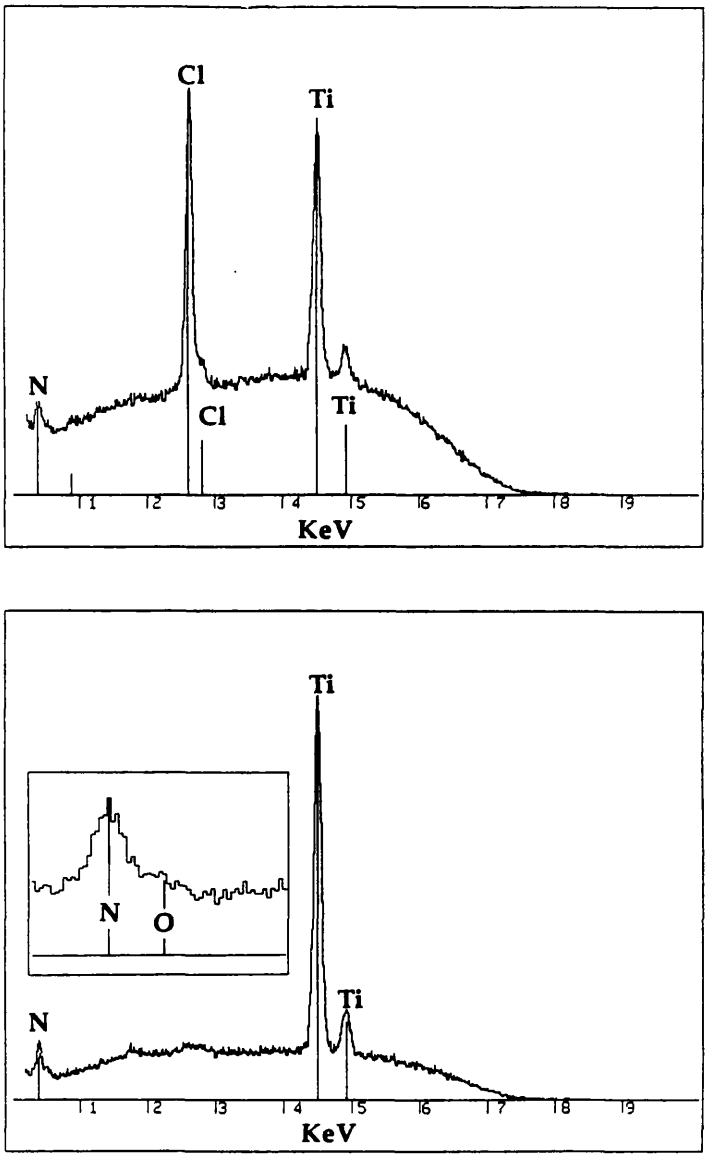

Table 5 illustrates the periodic trend in which, as the transition series are traversed, the degree of nitridation of the products decreases. This may be explained in terms of product stability. The thermal flash observed during reactions indicates temperatures in excess of 1000°C and the calculations in section 2.3 indicate a temperature of 1383°C. Table 6 lists the decomposition temperatures for several nitrides, from which it is clear that stability falls drastically at group 6. This has been rather grandly referred to as the *Chromium enigma*[90] and occurs for carbides as well as nitrides. If a nitride of, say, molybdenum formed through an ionic metathesis process the decomposition to metal and nitrogen would immediately follow since the reaction temperature exceeds the decomposition temperature of molybdenum nitride. If a reductive recombination pathway were followed, nitride formation would not occur at the extreme temperatures and the cooling rate in such reactions would be too fast to allow diffusion of nitrogen to any degree into the metal lattice. The low thermal stability of later transition metal nitrides has also been used in the CVD preparation of high purity transition metal films from the amides.[107]

Table 6. Decomposition temperatures of some nitrides.

Nitride phase	Decomposition temperature / °C
TiN	2930
ZrN	2980
HfN	3310
VN	2050
NbN	2050
TaN	3360
Ta_2N	3090
CrN	1500
Mo_2N	790
WN	650
Fe_2N	200

Many of the reactions which yield nitrides involve a reduction in the formal oxidation state of the transition metal, with concommitant production of nitrogen. Eqn. 30 and 31 show two examples. Gas chromatography (GC) was used to confirm that the expected amount of nitrogen was produced. Reactions were carried out in an evacuated tube of known volume with a sidearm plugged with a gas tight septum. When the reaction was complete the tube was carefully backfilled to atmospheric

pressure with argon and a sample taken for injection into the GC. Table 7 lists the results. They correlate well with the XRD results. Production of this gas could be explained by an ionic metathesis process followed by thermal decomposition to the observed phase, Eqn. 32, or by direct production through a reductive recombination process.

$$HfCl_4 + {}^4/_3Li_3N \rightarrow HfN + 4LiCl + {}^1/_6N_2 \qquad \text{-Eqn.30}$$

$$TaCl_5 + {}^5/_3Li_3N \rightarrow TaN + 5LiCl + {}^1/_3N_2 \qquad \text{-Eqn.31}$$

$$CrCl_3 + Li_3N \rightarrow CrN + 3LiCl \rightarrow {}^1/_2Cr_2N + 3LiCl + {}^1/_4N_2 \qquad \text{-Eqn.32}$$

Table 7. Evolution of nitrogen as detected by gas chromatography.

Reagent	Product	N_2 detected (%)[a]	N_2 expected (%)[a]
$ZrCl_4$	ZrN	25	25
$HfCl_4$	HfN	25	25
$NbCl_5$	Nb_4N_3	60	55
	Nb_2N		70
$TaCl_5$	TaN	45	40
	Ta_2N		70
$MoCl_5$	Mo	100	100
WCl_4	W	100	100
$MnCl_2$	Mn_4N	65	62.5
$ZnCl_2$	Zn	100	100

a. As % of the nitrogen in the starting material, Li_3N.

2.3 Thermal Aspects of Reactions.

In a closed system, the maximum theoretical temperature reached during a reaction is the adiabatic temperature, T_{ad}. This may be calculated from the summation and the integration of the heat capacities of the products, equated to the reaction enthalpy,[62] Eqn. 33 describes this for a two product system. If T_{ad} is above the melting or boiling points of any products, heats of fusion or evaporation must also be taken into account. Heat capacity, C_p, may be used as described in Eqn. 34 and 35 and values of parameters A- D taken from tables.[108]

$$-\Delta H_r^\circ = \int_{T_{init}}^{T_{ad}} \{C_p(\text{product X}) + C_p(\text{product Y})\}.dT \qquad \text{-Eqn.33}$$

$$C_p = A + BT + CT^{-2} + DT^2 \qquad \text{-Eqn.34}$$

$$\int C_p.dT = AT + {}^1/_2BT^2 - CT^{-1} + {}^1/_3DT^3 \qquad \text{-Eqn.35}$$

For example, the maximum theoretical temperature reached in the reaction between titanium trichloride and lithium nitride may be calculated thus:

$$TiCl_3 + Li_3N \rightarrow TiN + 3LiCl \qquad \Delta H_r^\circ = -676 \text{ kJ mol}^{-1} \qquad \text{(Eqn.28)}$$

Assume initiation at 300°C (= 573 K)

Energy required to reach LiCl melting point

$$\int_{573}^{887} \{C_p(TiN) + 3C_p(LiCl)\}.dT$$

$$= \int_{573}^{887} \{49.83 + (3.93 \times 10^{-3})T + (-12.38 \times 10^5)T^{-2} + 3(41.42) + 3(23.39 \times 10^{-3})T\}dT$$

$$= 70{,}800 \text{ J mol}^{-1}$$

Energy required to melt all the LiCl

Enthalpy of fusion of LiCl= 13,400 J mol^{-1}

$3 \times 13{,}400 = 40{,}200$ J mol^{-1}

Energy required to reach LiCl boiling point

$$\int_{887}^{1656} \{C_p(TiN) + 3C_p(LiCl)\}.dT$$

$$= \int_{887}^{1656} \{49.83 + (3.93 \times 10^{-3})T + (-12.38 \times 10^5)T^{-2} + 3(73.39) + 3(-9.46 \times 10^{-3})T\}.dT$$

$= 183{,}100 \text{ J mol}^{-1}$

Energy unused at 1656 K

$676{,}000 - 70{,}800 - 40{,}200 - 183{,}100 = 381{,}900 \text{ J mol}^{-1}$

Energy required to boil all the LiCl

Heat of evaporation of LiCl= $151{,}000 \text{ J mol}^{-1}$

$3 \times 151{,}000 = 453{,}000 \text{ J mol}^{-1}$

$\therefore$ would boil off 84% of the LiCl at 1656 K = 1383°C.

This of course assumes that no energy is lost, however it is probably safe to assume that 1383°C would be reached and some LiCl boiled off since this requires less than half the total energy. This energy is produced in a reaction which in the cases studied is complete within a period of about 5 seconds, normally much less than this, so heat loss will be minimal. The reactions of lithium chloride with $MoCl_3$ and $MoCl_5$ to produce molybdenum metal, when treated as above, are sufficiently exothermic for all the LiCl to be evaporated. The $MoCl_5$ reaction then has a further 215.5 kJ mol^{-1}, thus T_{ad} is calculated[109] as 2387°C. The $MoCl_3$ reaction is 56.7 kJ mol^{-1} more exothermic than would be required to boil off all the LiCl and T_{ad} is 1863°C. It is no surprise that no molybdenum nitrides are observed in the products of the reaction with $MoCl_5$. The small quantity of Mo_2N observed when using $MoCl_3$, Fig. 5, is probably not due to nitridation during cooling as then it should be the same in both cases, unless the metal produced in the more exothermic reaction had a much lower degree of porosity due to rapid sintering at the very high temperature. Otherwise, the results could be explained by incomplete thermal decomposition of a nitride product from the $MoCl_3$ reaction, resulting from the short timescale of the reaction.

In order observe reaction temperatures and timescales, a thermocouple was placed inside reaction mixtures. A thermocouple of composition Pt/ 13% Rh in Pt/ Pt was connected to a chart recorder set to measure mV and data tables[110] were used to convert mV to temperature. The thermocouple was placed into reaction mixtures at the end of a thick walled Pyrex tube, connected *via.* a tap to a Schlenk line open to argon and to a glass feed- through for the wires. The end of the tube containing the reaction mixture was heated in a tube furnace and the chart recorder monitored. Fig. 6 shows a representative trace for a titanium nitride preparation. The maximum

temperature reached, extrapolated to allow for a standard cooling curve, is lower than expected at around 1000°C. This is likely to be due to the small size of the reaction mixture used, neccessary for safety reasons with the available apparatus. The heat capacity of the thermocouple and the ampoule are, therefore, significant. However, it does show the timescale of the reaction, the ampoule contents returned to the furnace temperature in 5- 10 seconds.

Fig. 5. Powder X-ray diffraction pattern of Mo/ Mo_2N produced from $MoCl_3$ with Li_3N.

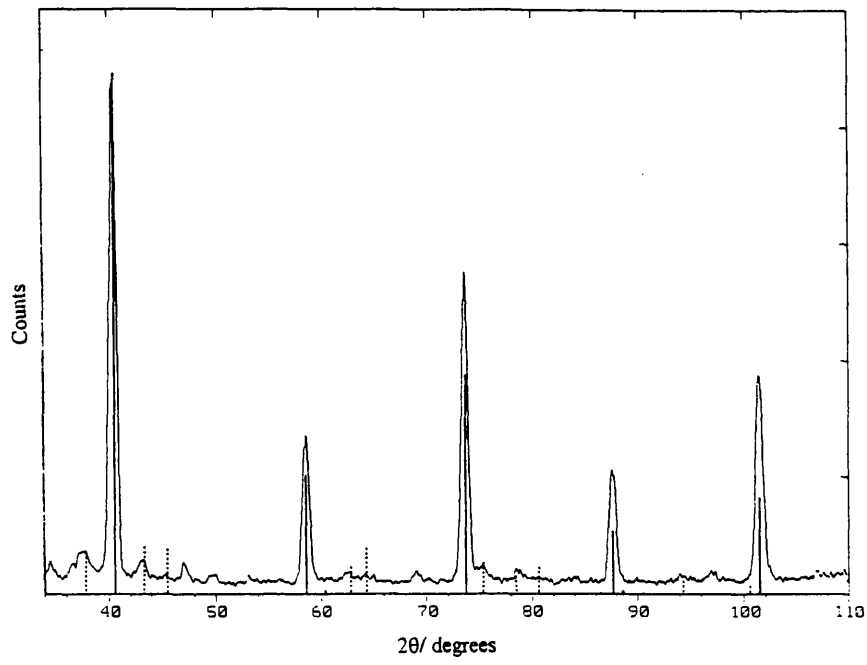

Fig. 6. Thermocouple trace from the reaction between $TiCl_3$ and Li_3N.

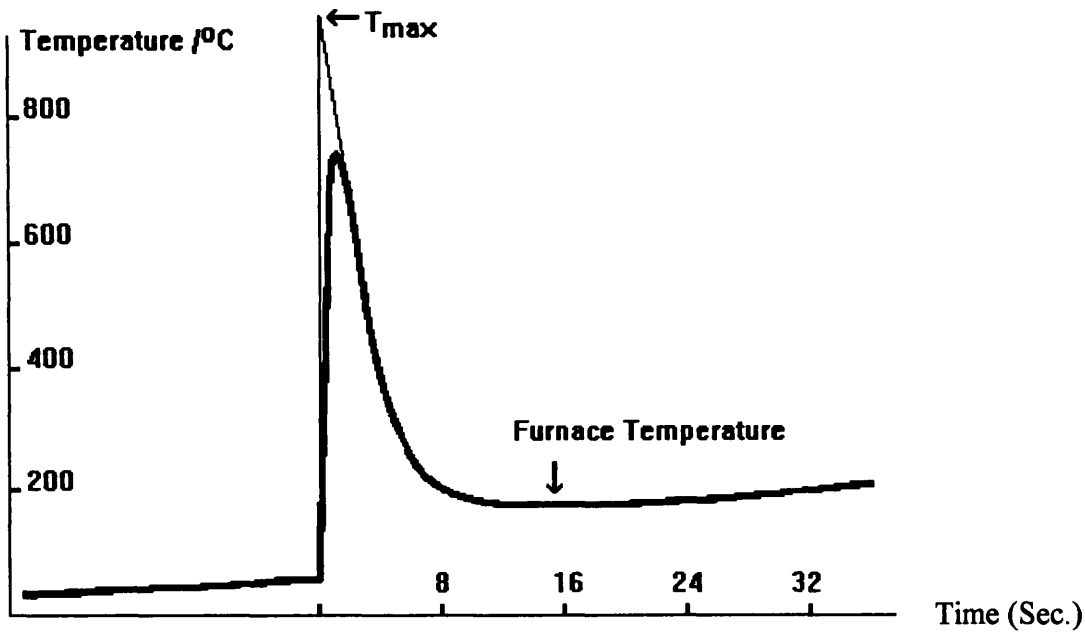

2.4 Synthesis of Rare Earth Nitrides.

The same general procedure was adopted for reactions of the rare earth trichlorides with lithium nitride. Reaction mixtures were ground together with a 1:1 ratio of metal to chloride under an inert atmosphere, sealed into a Pyrex ampoule and initiated by heating rapidly to 400°C. Reactions emitted a flash of light upon initiation. The rare earth nitride products are listed in Table 8 and all crystallise with the Fm3m (NaCl) structure. They oxidise slowly in air to the M_2O_3 rare earth oxide phase and decompose with moisture to the oxide and ammonia.[83,106] Thus, they were handled only under inert atmospheres and were washed with dry THF. Crystallite sizes, as assessed from XRD linewidths,[104] were lower than those of the transition metal nitrides, of the order of 300- 400 Å. A typical XRD pattern is shown in Fig. 7. The reactions to produce rare earth nitrides are considerably less exothermic, which could be responsible for the lower crystallinity of the products. Eqn. 36 illustrates this for the lanthanum nitride preparation.

$$LaCl_3 + Li_3N \rightarrow LaN + 3LiCl \qquad \Delta H_r^\circ = -328 \text{ kJ mol}^{-1} \qquad \text{-Eqn.36}$$

Table 8. XRD data and magnetic susceptabilities for the rare earth nitride products.

Product	a / Å	lit.[81] a / Å	μ / BM	μ (lit.)[84]	Typical μ (Ln^{3+})[84]
YN	4.891	4.894			
LaN	5.327	5.300			
PrN	5.154	5.15	3.6	3.57	3.58
NdN	5.141	5.141	3.7	3.65- 4.0	3.62
SmN	5.034	5.048	1.4	1.60	0.85
EuN	5.012	5.014	4.1	0- 5	0
GdN	4.984	4.999			
TbN	4.937	4.933	9.6	9.5- 10.0	9.72
DyN	4.906	4.905	10.4	10.5- 10.6	10.6
HoN	4.870	4.874			
ErN	4.838	4.839	9.4	9.2- 9.4	9.5
YbN	4.783	4.786	4.4	5.1	4.54

No nitrogen was evolved during these preparations, according to GC studies. Magnetic moment measurements, Table 8, matched reasonably well the literature[84] values.

Fig. 7. XRD pattern of purified DyN produced from $DyCl_3$ and Li_3N.

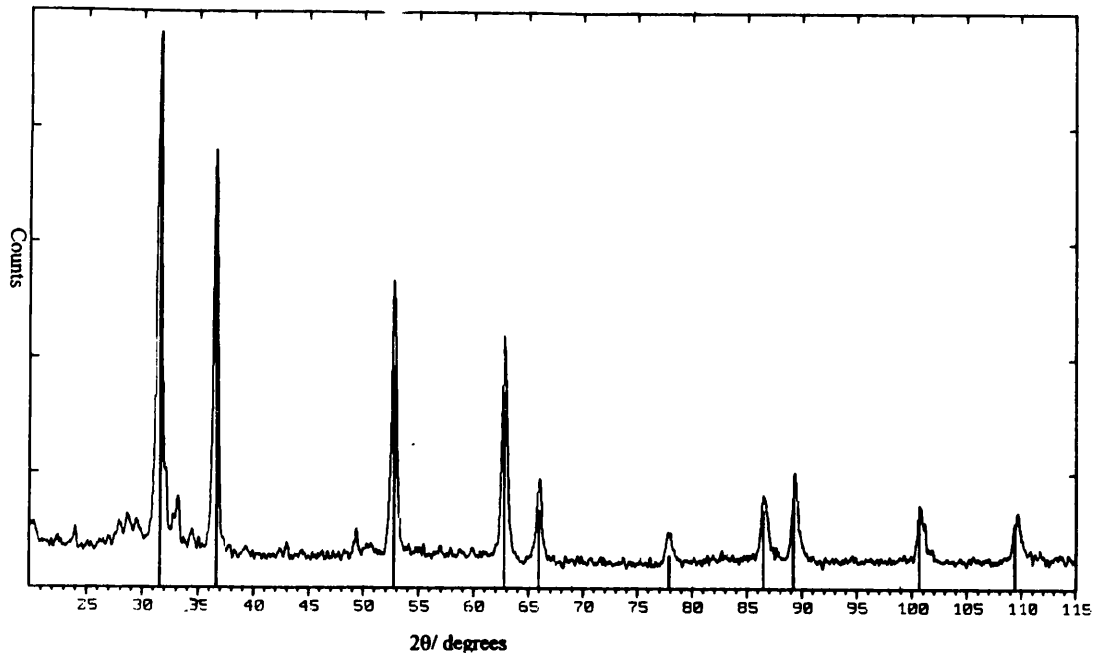

2.5 Reactions Involving Two Metal Chlorides.

Use of a mixture of two metal chlorides in reactions with lithium nitride could be expected to be a good method for the synthesis of ternary nitrides. Ternary sulfides have been produced in this way, such as $(Mo,W)S_2$ from a mixture of $MoCl_5$, WCl_6 and Na_2S.[74] The products of similar reactions with Li_3N are listed in Table 9. Mixtures of rare earth chlorides yielded patterns consistent with solid solutions only when rare earths with similar ionic radii were used. Lines in the XRD patterns were broadened, indicating that the solid solutions were incomplete, although not to an extent which would indicate individual phases with reflections simply overlapping. Mixtures of rare earths with dissimilar ionic radii, however, yielded the individual nitrides.

The same comments are true for the transition metal products. Fig. 8 shows the XRD pattern for (Ti,V)N + V_2N compared with the binary nitrides produced in the same way. Where ionic radii are similar, the XRD patterns are consistent with solid solutions. The exceptions to this are mixtures of Y/Zr and La/ Hf, where the production of individual nitride phases may be due to the large deviations in the chloride melting points (e.g. YCl_3 680°C, $ZrCl_4$ subl. 300°C[87]) as this may allow one chloride to react more rapidly than the other. In all cases, step EDXA (performed on spots at various points over the surface) showed a reasonable degree of homogeneity

Table 9. Products of reactions of equimolar mixtures of metal chlorides with Li_3N.

Chloride reagents	Products observed by XRD.[a]
$LaCl_3$, $ErCl_3$	LaN, ErN
$PrCl_3$, $NdCl_3$	(Pr,Nd)N
$TbCl_3$, $DyCl_3$	(Tb,Dy)N
$DyCl_3$, $HoCl_3$	(Dy,Ho)N
YCl_3, $ZrCl_4$	YN, ZrN
$LaCl_3$, $HfCl_4$	LaN, HfN
$TiCl_3$, $HfCl_4$	TiN, HfN
$ZrCl_4$, $HfCl_4$	(Zr,Hf)N
$TiCl_3$, VCl_3	(Ti,V)N, V_2N
$ZrCl_4$, $NbCl_5$	(Zr,Nb)N, Nb_2N
$HfCl_4$, $TaCl_5$	(Hf,Ta)N, Ta_2N
$ZrCl_4$, $MoCl_5$	ZrN, Mo
VCl_3, $NbCl_5$	(V,Nb)N
$NbCl_5$, $TaCl_5$	(Nb,Ta)N, $(Nb,Ta)_2N$
$MoCl_5$, WCl_6	MoW

Fig. 8. XRD patterns of purified products of reactions of:
Top. (a) $TiCl_3$ + Li_3N, (b) $TiCl_3$ + VCl_3 + $2Li_3N$ and (c) VCl_3 + Li_3N
Bottom. $TiCl_4$ + VCl_4 + $^8/_3Li_3N$, literature patterns[81] for (——) TiN and (·····) VN.

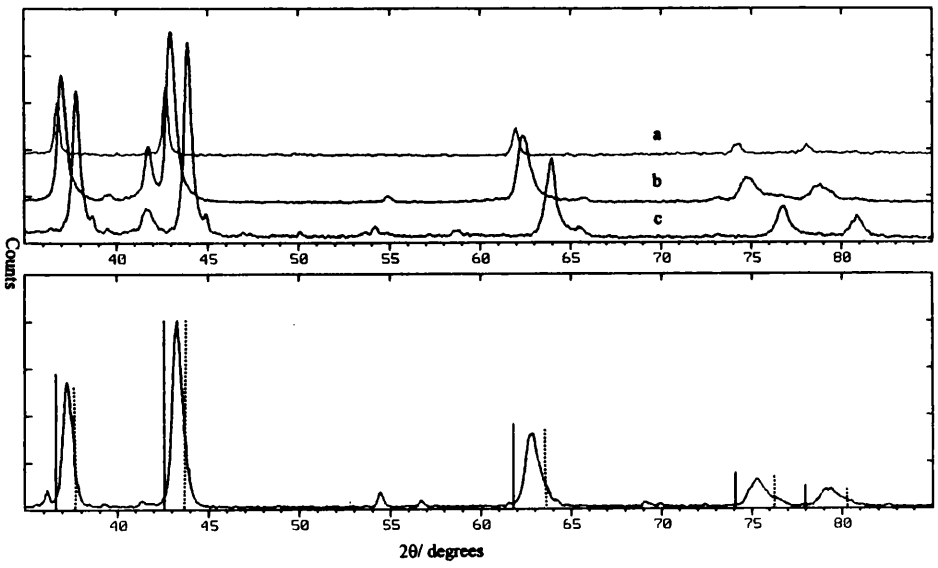

so even where more than one phase is observed by XRD, mixing occurs on the submicron scale.

Solid solutions of nitrides have been found surprisingly difficult to produce by other methods. For example, Chisholm and co- workers[42] found that the ammonolysis of titanium/ vanadium amide mixtures in solution, followed by thermal decomposition of the product yielded poor solid solutions and heating at 1100°C was neccessary to even partially integrate the two phases.

2.6 Reactions with Liquid Chlorides.

The tetrachlorides of titanium and vanadium exist as liquids at room temperature. A different experimental setup was required for their usage. Reactions were carried out in Schlenk tubes under argon. Fig. 9 shows a reaction of a mixture of these chlorides with lithium nitride. The process occurs over a period of about 3-5 sec and the white heat which can be observed in the centre of the mixture indicates a temperature on the scale of about 1000°C. The binary products in both cases are the MN phase, with no V_2N observed. The use of liquid chlorides allows intimate mixing before reaction, hence $Ti_xV_{1-x}N$ ($0<x<1$) may be produced at very high quality. Fig. 8 contains a representative pattern for $Ti_{0.5}V_{0.5}N$. Fig. 10 shows the variation of lattice parameter with x. From Vegard's Law,[104] this should be a linear relationship since Ti^{3+} and V^{3+} have similar ionic radii and TiN and VN both crystallise with the Fm3m structure. Step EDXA showed even ratios of Ti:V within experimental error in each sample, indicative of the intimacy of mixing.

2.7 Dilution Experiments.

The extreme exothermicity of SSM reactions is their most striking feature. It results in rapidity and high temperature. These conditions lead in turn to surprisingly crystalline products, considering the timescale of the synthesis, but also some difficulties. The speed and temperature of the reactions makes scaling up problematic in terms of containment and control. Also, for some applications reduced crystallinity is advantageous.

Most chemical reactions are carried out in solution, which not only overcomes solid state diffusion but tames highly exothermic processes. Lithium nitride is insoluble in all solvents, except alcohols, water and acids in which it decomposes. However,

Fig. 9. Photographs of a reaction of $TiCl_4 + VCl_4 + {}^8/_3Li_3N$ after: (a) 0.7 sec, (b) 1.4 sec, (c) 2.8 sec.

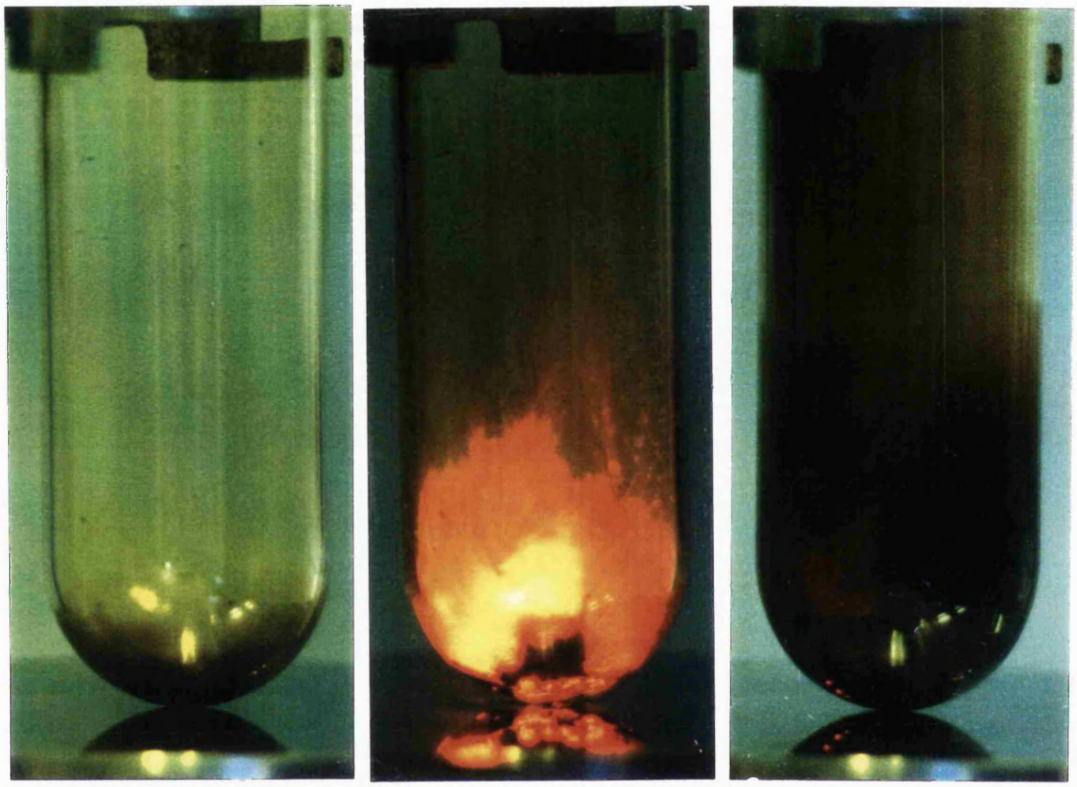

*Fig. 10. Graph of lattice parameter **a** (Å) vs x for $Ti_xV_{1-x}N$ produced from the tetrachlorides.*

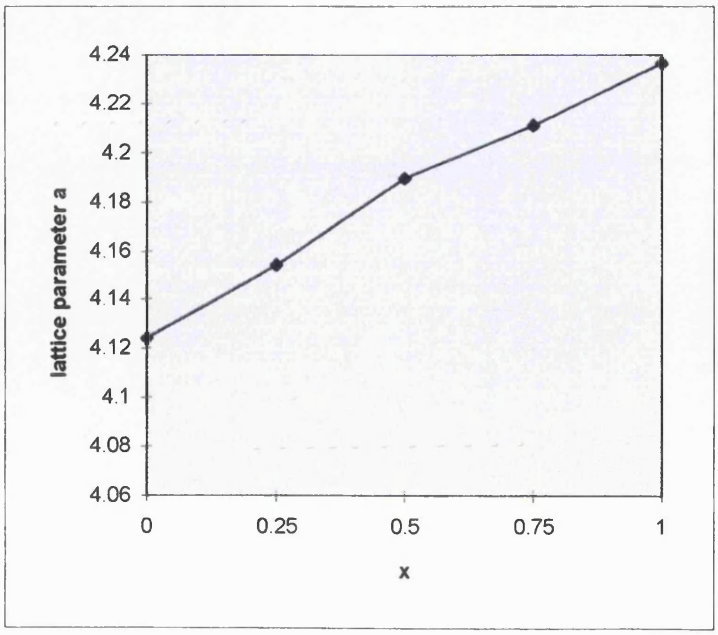

reactions with lithium nitride were attempted in suspension with solutions of metal chlorides in dichloromethane, tetrahydrofuran and toluene. $TiCl_3$, $HfCl_4$ and $TaCl_5$ were stirred in solution with lithium nitride for 24 hours. No reactions were observed to have occurred, so the solutions were heated at reflux for a further 5 hours. The unreacted lithium nitride was recovered from the solutions by filtration. These reactions were, therefore, considered to be of no use in nitride synthesis. Reactions of Li_2S in solvents such as THF do produce TiS_2 quite readily.[69] The difference here is that Li_3N is much more insoluble in such solvents than is Li_2S. Lithium nitride does react in suspension with chlorides such as SCl_2, however.[102]

Alkali halides are better diluents for these reactions. Diluting the reaction of $TiCl_3$ and Li_3N with LiCl reduces the crystallinity of the product and the voracity of the reaction. Fig. 11 shows the broadening of one reflection in the TiN powder pattern with increased dilution. The halfwidths of peaks in diffraction patterns may be related to the crystallite size using the Scherrer equation:[104]

$$L = \frac{k\lambda}{\cos\theta \sqrt{(B^2 - b^2)}}$$

[L = crystallite size, k = constant ($0.89<k<1.1$), λ = wavelength of X-rays, θ = angle of diffraction, B = halfwidth of reflection for sample, b = halfwidth for standard peak (101 of Zn)].

The crystallite sizes obtained in diluted reactions of $TiCl_3$ with Li_3N and calculated in this way are shown in Fig. 12. Products of diluted reactions were less tightly fused and less material was found to coat the walls. Thermocouple studies showed that the dilution causes an increased timescale for the reactions and a lower temperature is ultimately reached compared with that observed with undiluted reaction mixtures. The crystallite sizes of the products will be influenced by the lower reaction temperature and by the increased path lengths which species will travel during reactions.

Reaction of tungsten tetrachlorides with lithium nitride produces tungsten metal as the decomposition temperature of tungsten nitride is below the reaction temperature, section 2.2. Crystallinity of samples produced in diluted reactions was poor so the products were examined by X-ray photoelectron spectroscopy (XPS). Fig. 13a shows the X-ray photoelectron spectrum of the product from an undiluted reaction in the tungsten 4f region. Tungsten metal is observed as a doublet at 30.9 eV and 33.0 eV. Oxide peaks are also observed at about 35.3 eV and 37.3 eV. Dilution of the reaction resulted in nitride formation, observed through peaks at 32.2 eV and 34.2 eV, as

Fig. 11. Broadening of 200 reflection of the TiN powder pattern with dilution. (no added LiCl, 200mg, 400mg).

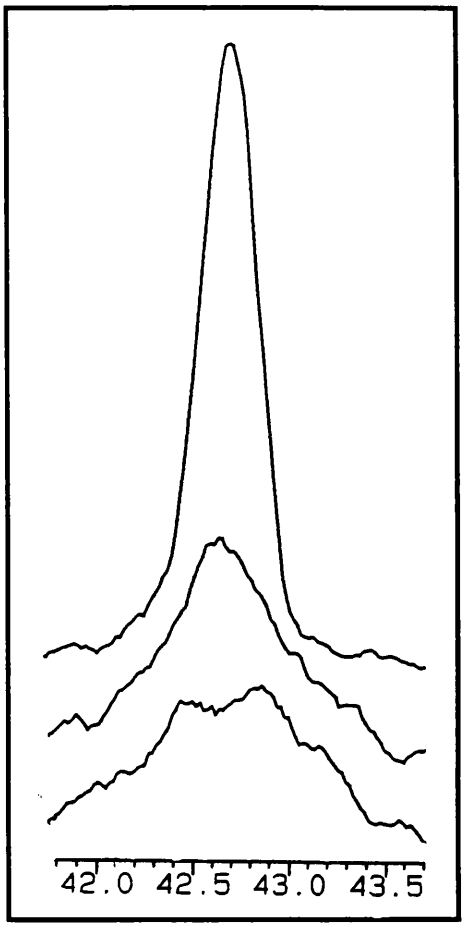

shown in Figs. 13b and 13c. These peaks are asymmetric, which indicates metallic character,[110a] and are shifted from the metal by about the correct amount of energy to support their assignment as nitride.[110a] When a reaction on a scale of 100mg Li_3N is diluted with 300mg of LiCl results in a ratio of metal to metal nitride equal to 1 : 0.48. Dilution with 600mg LiCl increases the amount of nitride and the ratio is 1 : 2.22. Argon etching in all cases reduced the oxide and nitride levels. In the case of the oxide this must mean the oxide is on the surface since tungsten oxides have very high stabilities and must be etching from the surface rather than decomposing. The tungsten nitride, however, is probably decomposing as it has a low thermal stability.

2.8 Summary and Relevance to Mechanistics.

Lithium nitride reacts rapidly after bulk thermal initiation with rare earth and early transition metal chlorides to yield binary nitrides of these metals. Reactions generate extreme temperatures, thus as the transition series is traversed metals are produced

instead of the thermally labile nitrides. Ternary nitrides may be produced, with limited

Fig. 12. Graph of crystallite size L (in Å) of TiN product vs. amount of LiCl diluent added to synthesis of TiN (reaction scale: 220mg of $TiCl_3$).

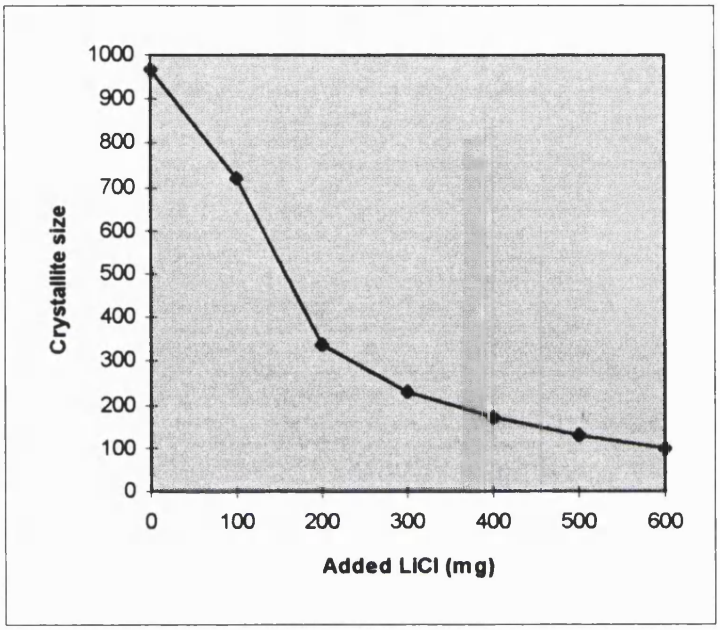

Fig. 13. X-ray photoelectron spectra in the tungsten 4f region of the purified products of reaction between WCl_4 and Li_3N (a) Undiluted at a scale of 100mg Li_3N.

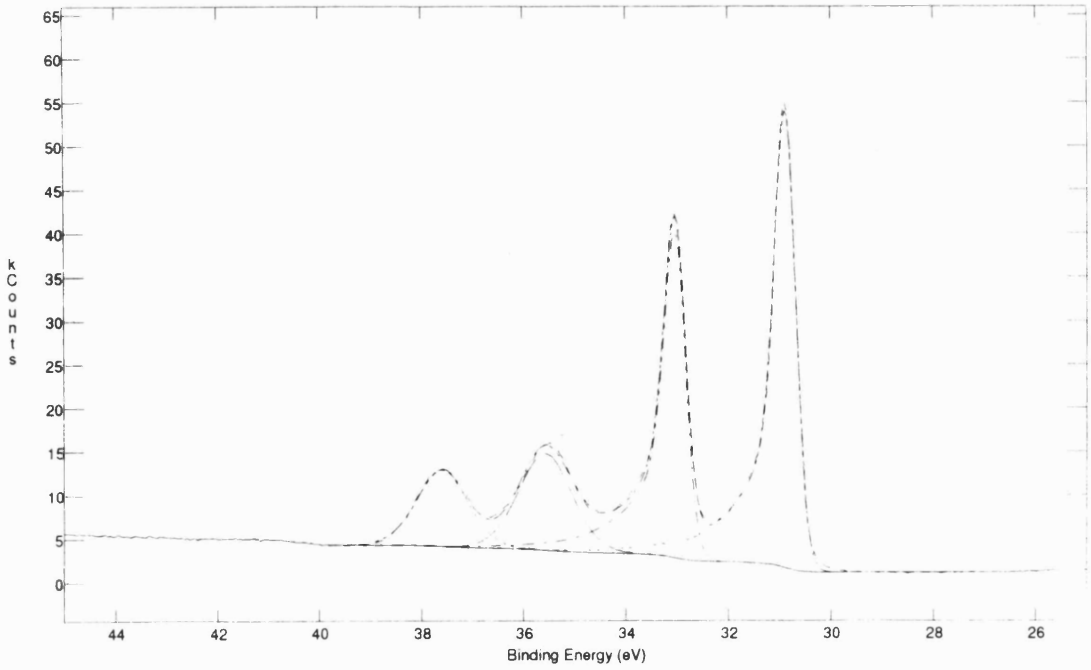

(B) Diluted with 300mg LiCl.

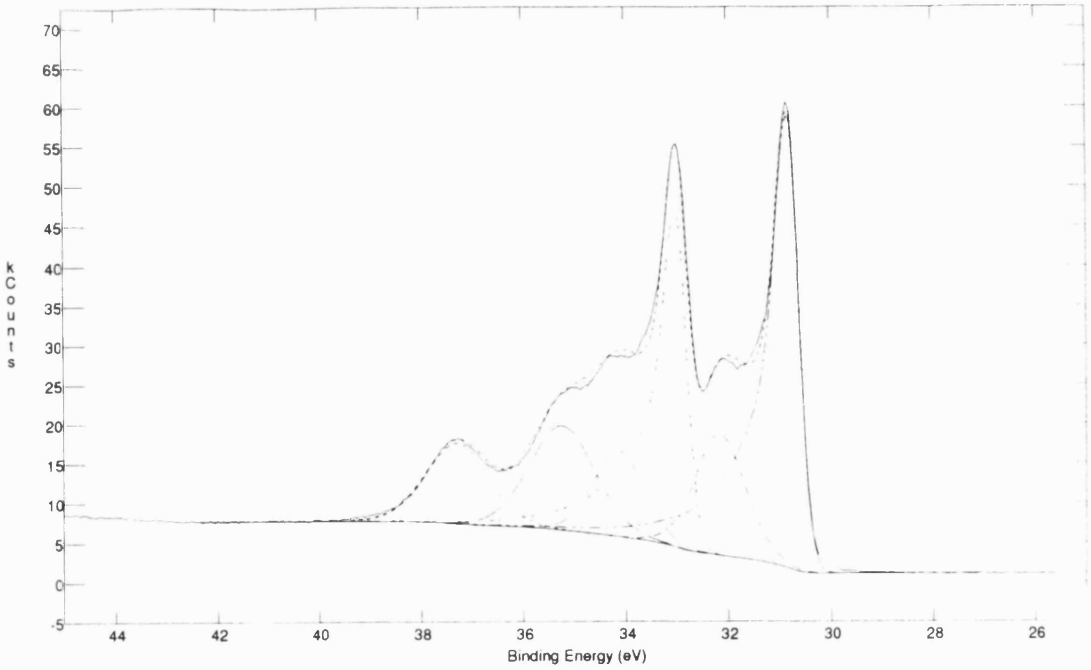

(C) Diluted with 600mg LiCl.

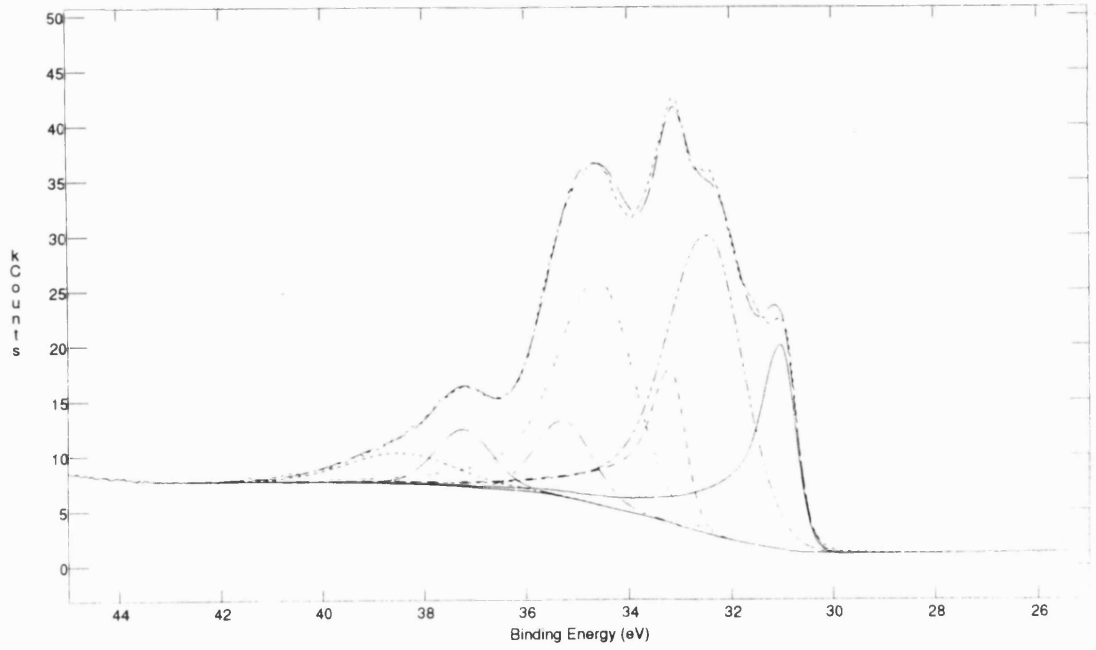

success, from mixtures of metal chlorides. Use of titanium and vanadium liquids at room temperature, allows formation of high quality $Ti_xV_{1-x}N$ ($0<x<1$). Nitrides are formed as agglomerates of crystallites on the order of 0.1 μm. Dilution of reactions with lithium chloride allows some control of crystallite size and reduces the voracity of reactions.

In section 1.8, two extreme mechanistic pathways which could occur in SSM reactions were discussed. Fig. 14 shows the ionic and elemental (reductive recombination) routes for the reactions of $NbCl_5$ and $MoCl_3$ with Li_3N. Ionic metathesis would involve the formation of M^{x+} and N^{3-} from MCl_x and Li_3N, which combine in the lithium chloride melt. The stoichiometric phase so produced (M_3N_x, e.g. Ta_3N_5 from $TaCl_5$, or MN if x = 3) then decomposes, if thermally labile, with a reduction in metal oxidation state to the product.

Fig. 14. Examples of SSM Processes: Ionic vs Elemental Mechanism.

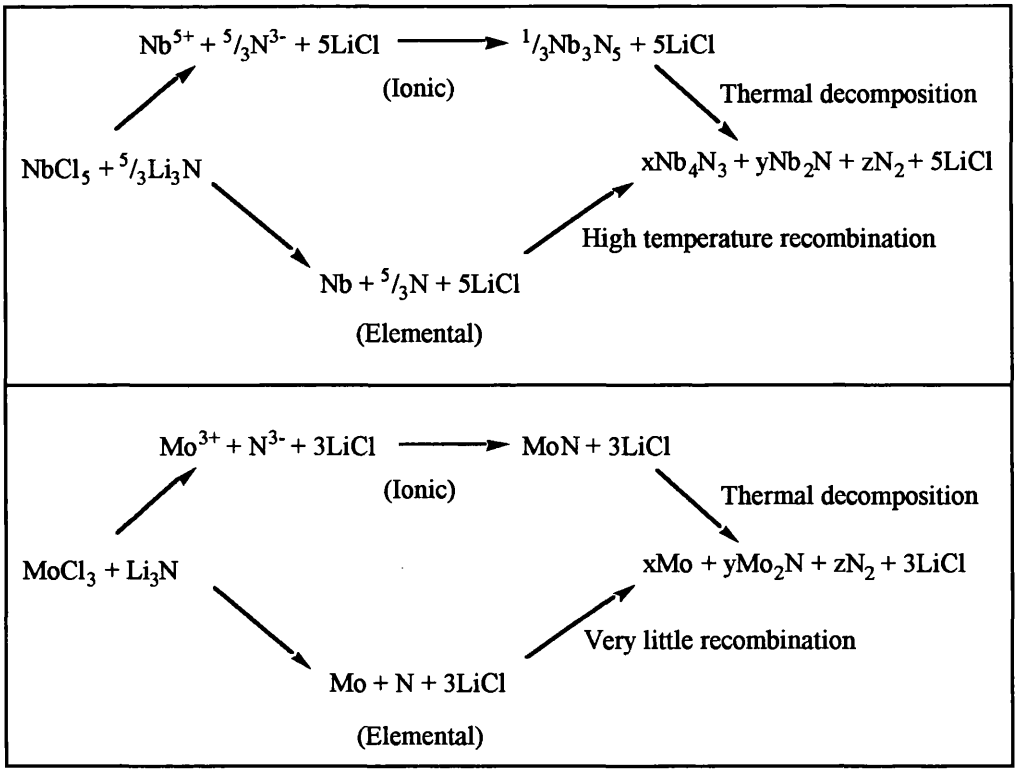

Reductive recombination requires the formation of metal and nitrogen followed by their reaction at high temperature. On the timescale of these processes, nitrogen radicals are a possible species. Metals would be generated with very small particle sizes. The reaction of metal with nitrogen could, therefore, be more favourable and

quicker than in the conventional preparations where dissolution of nitrogen into metals can be a slow process.

These two processes are of course two extremes as both processes could occur in a stepwise manner. Rather than producing the metal atom or ion in one step, sequential loss of chlorines could occur with gain of nitrogen before all the chlorine is lost. One could also envisage a mechanism which had elements of the ionic and the elemental processes, where a partial reduction in the oxidation state of the metal ion occurred during the first stage of the reaction. However, from the evidence available, consisting of end product analysis and possibly some intermediates, the only conclusions likely to be possible will be that a reaction is mainly ionic or elemental in character.

The formation of rare earth nitrides and TiN with no rare earth or titanium metal observed would support an ionic mechanism, since in an evacuated environment some loss of nitrogen would be expected with the observation of some elemental metal in the product. Reductions in formal oxidation state occur with all the chlorides except the rare earths and $TiCl_3$. The phases observed can still be rationalised by an ionic mechanism if the product from an ionic reaction, M_3N_x when the chloride is MCl_x, is thermally unstable. Such nitrogen rich phases are known, for example Zr_3N_4, Hf_3N_4 and Ta_3N_5, and do have low decomposition temperatures. Thus, $HfCl_4$ would produce Hf_3N_4 which would decompose to HfN with a reduction in the formal oxidation state of hafnium from 4 to 3. Where two product phases are observed, such as TaN and Ta_2N from $TaCl_5$, this may still be explained by this mechanism, since the decomposition products of Ta_3N_5 under these conditions are unknown. The exception is the reaction of VCl_3 where V_2N is observed as well as VN, the stoichiometric product. The decomposition temperature of VN is 2050°C, well above T_{ad} for this reaction (1383°C).

A reductive recombination process can also be used to explain all the observed phases, although no loss of nitrogen in the rare earth and $TiCl_3$ reactions would be a surprise. Filament initiated reactions of $TiCl_3$ with Li_3N, published[111] after this work, have been reported to yield some Ti metal as well as TiN. This is a method of initiation where a hot filament is used to start a reaction at one point in the mixture followed by self- propagation through all the reagents. The observation of Ti metal was taken as evidence of the operation of an elemental process, although it could just as easily be from the thermal decomposition of some unreacted $TiCl_3$ at the propagation front or the edge of the mixture. The evidence which most strongly supports either case is that which comes from the dilution experiments. In the case of

the ionic mechanism, a lower degree of thermal decomposition would lead to a higher level of product nitridation. The reverse is true for the elemental process, a greater degree of dilution would be expected to reduce the product nitridation. The XPS results for molybdenum and tungsten, where dilution increases nitrogen content, point to the ionic process having most influence.

This is the first method for producing high quality, crystalline nitrides which does not require a large input of energy. Using SHS methods, high pressures are required to facilitate complete nitridation. Other low energy routes require anealling at high temperatures to provide a crystalline product. Conventional elemental combination or metal oxide/ ammonia reactions also require a large energy input. Lithium nitride is only one potential source of nitrogen for these reactions, other possibilities include alkali metal azides and group 2 nitrides and azides. Some of these will be discussed in the next chapter.

2.9 Experimental.

Anhydrous transition metal chlorides were purchased from Aldrich Chemical Co; rare earth chlorides and lithium nitride from Strem Chemicals. All were purchased at high purity, checked by XRD and EDXA and used as supplied. Methanol was distilled from Mg/ I_2; tetrahydrofuran from Na/ benzophenone; toluene from Na; dichloromethane from P_2O_5. All were stored under dry nitrogen/ argon. Ampoules were made of Pyrex or quartz 2mm thick with an internal volume of approx. $15cm^3$ and were flame dried under vacuum before use. Reaction mixtures were prepared in a Saffron Scientific glove box filled with nitrogen and were heated in a Lenton Thermal Designs or Carbolite tube furnace.

X- ray powder diffraction patterns were recorded at ambient temperature using a Siemens Diffractometer D5000, either in transmission mode using germanium monochromated Cu $k_{\alpha 1}$ radiation (λ= 1.5406Å) or in reflection mode using nickel filtered Cu k_α radiation (λ= 1.5418Å). Scanning electron microscopy was carried out with a Jeol JSM820 instrument and EDXA spectra were recorded with a Kevex Quantum Detector, Delta 4 computer and Quantex 6.2 software, sensitive to elements with atomic numbers greater than 5.[112] Alternatively, a Hitachi SEM S-570 microscope was used with a Link Analytical model 5717 detector (atomic numbers above 10). FT-IR spectra were acquired with a Nicolet 205 spectrometer. Magnetic moment measurements were taken with a Johnson Matthey Evan's balance. Microanalysis was carried out by MEDAC Ltd., Brunel University or by the UCL

chemistry department service by combustion with tin powder. Kjeldahl nitrogen analysis was carried out by Stanger Consultants Ltd. using acid digestion.

Gas chromatography was carried out using a Pye unicam 204 chromatograph with a 5 Å molecular sieves column, helium carrier gas and a thermal conductivity detector. A reaction was carried out in an evacuated tube of known volume which was then allowed to cool and backfilled to atmospheric pressure with argon. A sample of gas was taken by syringe and the ratio of N_2:Ar examined by GC and compared with the ratio present in the argon gas used.

Reaction temperatures were monitored with a Pt/ 13% Rh in Pt/ Pt thermocouple with an iced water cold junction, connected to a chart recorder. Temperatures were calculated from published tables.[110] Differential scanning calorimetry was performed using a Shimadzu DSC- 50 and Perkin Elmer high pressure stainless steel cells with gold seals. Photographs were obtained with 100 a.s.a. colour print film at 0.7sec intervals. X-ray photoelectron spectroscopy was performed on pressed disk samples with a VG ESCALAB 220I XL using focussed (300μm spot) monochromatised Al k_α radiation at a pass energy of 20 eV. Scans were acquired with steps of 50 meV. The binding energies were referenced to an adventitious C 1s peak at 284.8 eV.

Procedure for performing reactions with lithium nitride

The same general procedure was adopted for all the reactions as will be illustrated for hafnium chloride with lithium nitride. Anhydrous $HfCl_4$ (345mg, 1.08mmol) was carefully ground together with Li_3N (50mg, 1.44mmol, 1:1 ratio of Cl:Li) under nitrogen using an agate pestle and mortar. This mixture was sealed under vacuum into an ampoule, placed into a furnace and heated rapidly to the desired temperature (400°C or 500°C). After a short period of time, a bright flash emanated from the ampoule. When cool, the crude product, consisting of fused black lumps and a black, powdery coating on the ampoule walls, was removed from the ampoule under nitrogen and ground to a powder. Washing with degassed methanol or thf (40 + 20cm^3) under an inert atmosphere followed by drying *in vacuo* yielded the pure metal nitride or metal products listed in Tables 5 and 8.

Microanalysis:
HfN, %N= 6.41 (calcd. 7.28), %C= 0.42, %H= 0.43, %Li= 0.11.
Mn_4N, %N= 5.81 (calcd. 5.98), %C= 0.28, %H= 0, %Li= 0.23.
TaN/ Ta_2N, %N= 5.95 (calcd. 7.19/ 3.73), %C= 0.57, %H= 0.63.
ErN, %N= 6.5 (calcd. 7.7), %C= 0.12, %H= 0.32.

TbN, %N= 5.77 (calcd. 7.9), %C= 0.42, %H= 0.57.
SmN, %N= 7.5 (calcd. 8.5), %C= 0.27, %H= 0.32.
DyN, %N= 5.55 (calcd. 7.94), %C= 0.43, %H= 0.53.
PrN, %N= 6.47 (calcd. 9.04), %C= 0.42, %H= 0.57.
Kjeldahl analysis:
HfN, %N= 6.59 (calcd. 7.28).

When two chlorides or a diluent were used, these were ground together before the addition of lithium nitride. When reactions were performed with liquid chlorides, the chloride was measured by syringe into a dry Schlenk tube under a flow of argon. Lithium nitride was added with stirring. The majority of reactions initiated spontaneously upon addition of the Li_3N. If not, stirring was stopped and a piece of wire which had been dipped in water was touched onto the side of the mixture. This initiated a reaction which was caused to spread to the rest of the mixture by recommencing stirring.

Caution!

The reactions described here spontaneously reach extreme temperatures and should be treated with caution. When mixing, reactions may very occasionally self- initiate, especially those involving the more volatile chlorides. Hydrated metal halides normally cause self- initiation as well as high levels of oxygen in the products, so should be avoided. When heating sealed ampoules a safety screen should be used to guard against pressure explosion, especially when reactions are expected to produce nitrogen. It is beneficial to calculate the maximum likely pressure before reactions are performed.

3. Reactions of Metal Chlorides with NaN_3 and Group 2 Nitrides.

This chapter will discuss the use of sodium azide and the Group 2 nitrides Mg_3N_2 and Ca_3N_2 in reactions with rare earth and transition metal chlorides. Calcium nitride has previously been used in high temperature synthesis of ternary nitrides by combination with binary transition metal nitrides. DiSalvo and co- workers[113,114] have produced Ca_3VN_3 and Ca_3CrN_3 in this way, consisting of planar $(MN_3)^{6-}$ anions separated by Ca^{2+} ions.

3.1 Reactions with Sodium Azide.

These reactions were carried out in a similar way to those in section 2.2. Sodium azide and anhydrous metal chloride were mixed together by grinding in an inert atmosphere with a 1:1 ratio of sodium to chloride. Heating in a vacuum sealed Pyrex ampoule to 400°C resulted in a thermal flash and yielded the products listed in Table 10 plus sodium chloride. When cool, the ampoule was found to contain a fine black powder distributed throughout, none of which was fused into lumps, as in the lithium nitride reactions. Larger ampoules (internal volume ~35 cm^3) were also required to avoid pressure explosions. Scanning electron micrographs, Fig. 15, showed much more open structures than those found for the products of Li_3N reactions both in the crude products, where the open structure was coated with sodium chloride, and in the methanol washed product. All of these observations may be explained by the large quantities of nitrogen gas produced in the reactions, Eqn. 37- 39. FT- IR and EDXA results were the same as described in section 2.2, except that the crude products showed sodium in the EDXA spectra.

$$TiCl_3 + 3NaN_3 \rightarrow TiN + 3NaCl + 4N_2 \qquad \Delta H_r^\circ = -912 \text{ kJ mol}^{-1} \qquad \text{-Eqn. 37}$$

$$TaCl_5 + {}^5/_3Li_3N \rightarrow xTaN + {}^{1-x}/_2Ta_2N + 5LiCl + {}^{7-3x}/_{12}N_2 \qquad \text{-Eqn. 38}$$

$$TaCl_5 + 5NaN_3 \rightarrow xTaN + {}^{1-x}/_2Ta_2N + 5NaCl + {}^{29-x}/_4N_2 \qquad \text{-Eqn.39}$$

The sodium azide reactions are more exothermic than those of Li_3N, since the contribution from the heat of formation of sodium azide ($n \times +22$ kJ mol^{-1} when using MCl_n) is of opposite sign to that of lithium nitride ($^n/_3 \times -165$ kJ mol^{-1}).[108] Thus, for TiN formation the reaction is 236 kJ mol^{-1} more exothermic than using Li_3N ($\Delta H_r^\circ = -676$ kJ mol^{-1}, Eqn. 28). T_{ad} is a little higher, reaching 1465°C (the sodium chloride boiling point) rather than 1383°C (boiling point of lithium chloride). These data make it surprising, at first glance, that the products are less crystalline. Calculations from XRD linewidths[104] for titanium nitride yielded crystallite sizes of 490Å using lithium

nitride and 250Å using sodium azide. Both reactions were carried out using the same scale (50 mg of $TiCl_3$) and crystallite sizes were calculated as described in section 2.7. XRD patterns for the two samples are shown in Fig. 16. Several moles of nitrogen are also evolved in each reaction. The lower crystallinity may be attributed to the spraying of the product as a fine powder throughout the ampoule, rather than the bulk of it remaining in a fused lump, due to the large amounts of N_2 produced in the reactions. Cooling will, therefore, be even quicker and the opportunity for annealing will be reduced.

Table 10. Phases detected by XRD from reactions of sodium azide with anhydrous metal chlorides.

Reagent	Product(s)	System, space group	**a** (lit.[81,103] **a**) / Å	**c** (lit.[81,103] **c**) / Å
$LaCl_3$	LaN	Cubic Fm3m	5.302 (5.300)	
$SmCl_3$	SmN	Cubic Fm3m	5.072 (5.048)	
$TiCl_3$	TiN	Cubic Fm3m	4.243 (4.242)	
$ZrCl_4$	ZrN	Cubic Fm3m	4.578 (4.578)	
$HfCl_4$	HfN	Cubic Fm3m	4.541 (4.525)	
VCl_3	VN	Cubic Fm3m	4.136 (4.139)	
	V_2N	Hexagonal P-31m	4.902 (4.917)	4.559 (4.568)
$TaCl_5$	TaN	Cubic Fm3m	3.371 (3.369)	
	Ta_2N	Hexagonal $P6_3/mmc$	3.052 (3.045)	4.929(4.914)
$CrCl_2$	Cr	Cubic Im3m	2.888 (2.884)	
	Cr_2N	Hexagonal P-31m	4.789 (4.811)	4.475 (4.484)
$MoCl_3$	Mo	Cubic Im3m	3.148 (3.147)	
	(Mo_2N)	Tetragonal $I4_1/amd$		
WCl_6	W	Cubic Im3m	3.163 (3.165)	
	(W_2N)	Cubic F		
$MnCl_2$	Mn_4N	Cubic Pm3m	3.857 (3.846)	
	Mn	Cubic Im3m	3.085 (3.081)	
$FeCl_3$	Fe	Cubic Im3m	2.860 (2.866)	

Where two phases are listed, the major phase is listed first. Parentheses indicate trace amounts only.

No differences in product distribution compared with those from Li_3N were observed for La, Sm, Ti, Zr, Hf, Ta or Mo. The reaction of VCl_3 produced VN as the major phase in both cases but the NaN_3 reaction yielded a considerable amount of V_2N whereas only traces were observed from Li_3N. The $CrCl_2$ reaction yielded the metal and a lesser amount of Cr_2N, the reverse of the distribution with Li_3N. Reaction of NaN_3 with $MnCl_2$ produced Mn as well as Mn_4N, from Li_3N only Mn_4N was produced.

Fig. 15. SEM of crude (top) and washed (bottom) TiN produced from $TiCl_3$ and NaN_3.

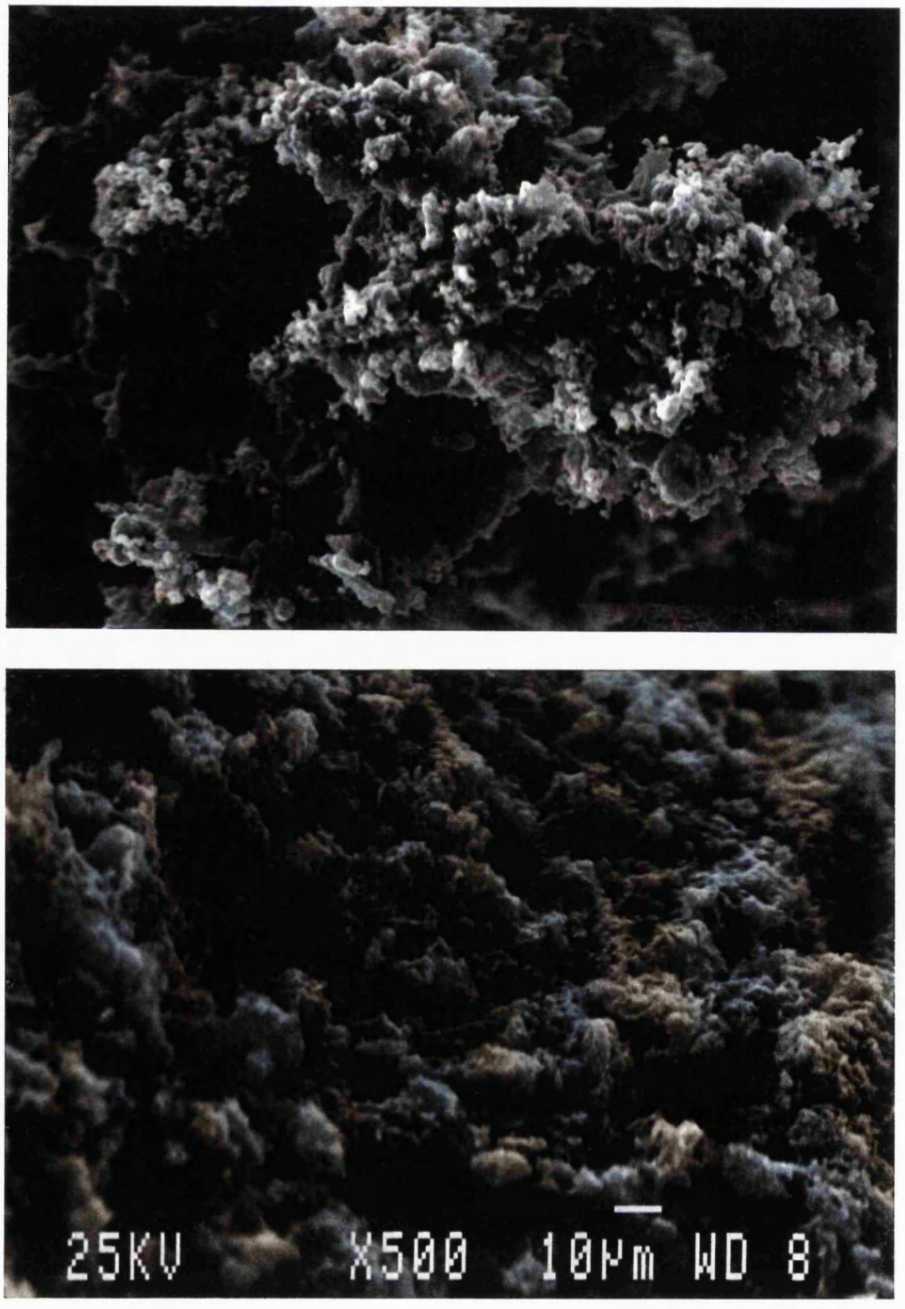

Fig. 16. XRD of TiN produced using $TiCl_3$ with Li_3N (top) and NaN_3 (bottom).

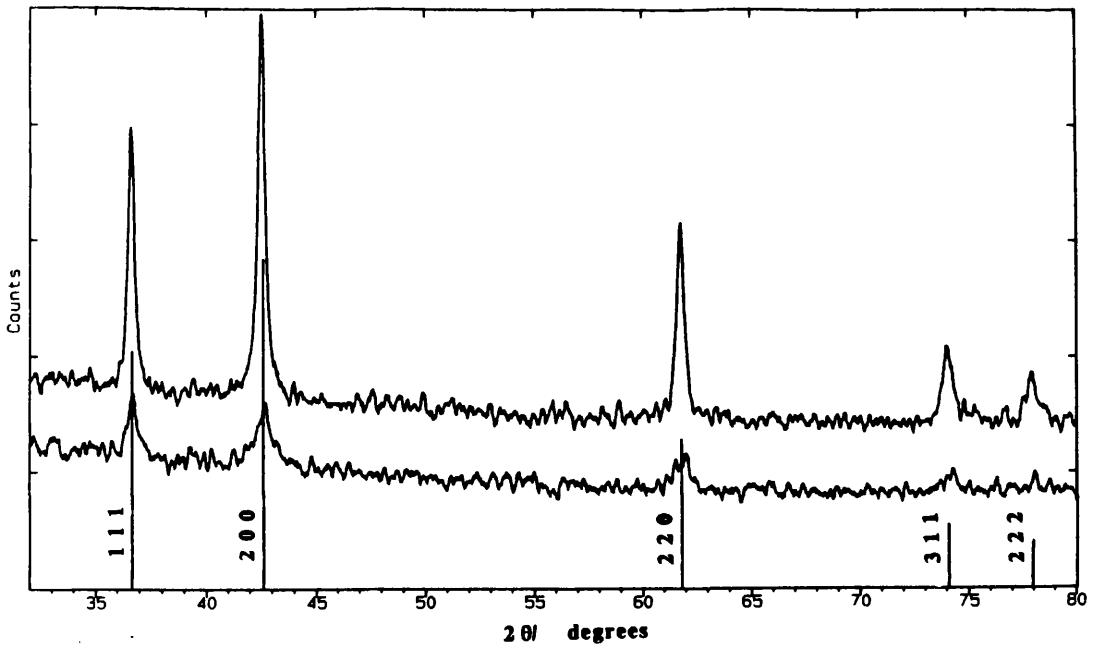

3.2 Thermally Initiated Reactions with Calcium and Magnesium Nitride.

The thermally initiated reactions of magnesium and calcium nitride with rare earth chlorides were carried out and products were characterised similarly to those described in section 2.2. Magnesium or calcium nitride was ground together with anhydrous metal chloride (ratio of magnesium/ calcium to chloride was 1:2) under nitrogen or argon and vacuum sealed into a Pyrex ampoule. This was placed in a furnace and heated as stated in Tables 11 and 12. The fused, black products were ground in an inert atmosphere and washed with methanol or tetrahydrofuran.

A general trend is observed, Fig. 17, of reactions of calcium nitride occurring more readily than those of magnesium nitride. The main barrier to reaction can be expected to be solid state diffusion. Calcium nitride decomposes at 900°C whereas magnesium nitride decomposes at 1500°C[87] which would mean that propagation would occur more readily, once initiated, in the calcium case. The ease of reaction of sodium azide with rare earth chlorides also supports this reasoning since it decomposes at 300°C. Lithium nitride decomposes at 850°C, so would not be expected to be so reactive just from it s decomposition temperature. Lithium ions are, however, quite mobile so solid- state diffusion would be faster than with magnesium or calcium ions. Another explanation comes from the examination of the reaction energetics, Eqn. 40 and 41. The reactions of rare earth chlorides with magnesium nitride are actually slightly endothermic (although entropy favoured: A first approximation taking room

temperature values gives ΔS_r= 11 J deg^{-1} mol^{-1}. This does not take into account phase changes). Powder XRD data for the products are listed in Table 11.

$$GdCl_3 + {}^1/_2Mg_3N_2 \rightarrow GdN + {}^3/_2MgCl_2 \qquad \Delta H_r^\circ = +41 \text{ kJ mol}^{-1} \qquad \text{-Eqn.40}$$

$$GdCl_3 + {}^1/_2Ca_3N_2 \rightarrow GdN + {}^3/_2CaCl_2 \qquad \Delta H_r^\circ = -202 \text{ kJ mol}^{-1} \qquad \text{-Eqn.41}$$

Reactions of calcium and magnesium nitride are considerably slower those of Li_3N and NaN_3. Heating a mixture of rare earth chloride and either magnesium or calcium nitride to 900°C for one hour formed only rare earth nitride and magnesium or calcium chloride. Reducing the reaction time to *ca.* 10 minutes at 900°C enables a trace of Ln_2Cl_3N (Ln= rare earth) to be observed in most reactions. Reaction of Ca_3N_2 with $LnCl_3$ for two hours at 500°C produces LnN, Ca_2NCl and Ln_2Cl_3N. Reaction of magnesium nitride under the same conditions predominantly yielded Ln_2Cl_3N and some $MgCl_2$, Fig. 18. The observation of Ln_2Cl_3N and Ca_2NCl is important as these are possible intermediates, the implications of which will be discussed in section 3.4.

Fig. 17. Products of reactions of rare earth chlorides with magnesium and calcium nitride.

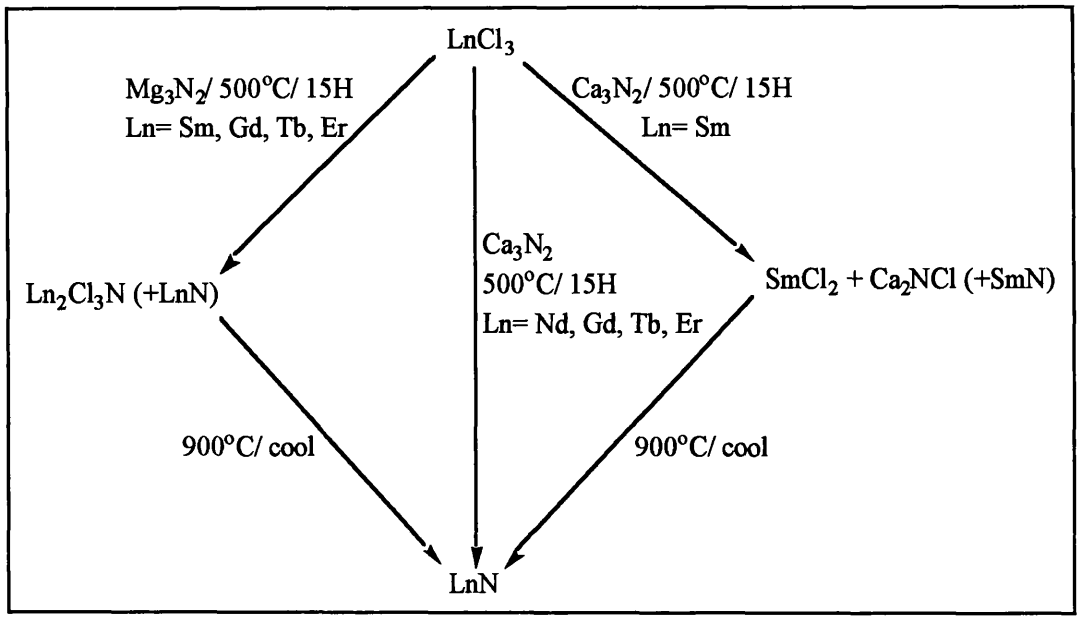

The products of reactions with transition metal chlorides are summarised in Table 12. The difference in reactivity between Mg_3N_2 and Ca_3N_2 is again demonstrated by examination of the products with $TiCl_3$ at 500°C. The calcium nitride reaction goes to

Table 11. XRD data for the rare earth nitride products.

Reagents		Conditions	Product	**a** (ref.[81] **a**) / Å
$NdCl_3$	Ca_3N_2	500°C / 15H	NdN	5.136 (5.141)
$SmCl_3$	Mg_3N_2	900°C / 1H	SmN	5.042 (5.048)
	Ca_3N_2	900°C / 1H	SmN	5.044 (5.048)
$GdCl_3$	Mg_3N_2	900°C / 1H	GdN	4.991 (4.999)
	Ca_3N_2	500°C / 15H	GdN	5.003 (4.999)
$TbCl_3$	Mg_3N_2	900°C / 1H	TbN	4.924 (4.933)
	Ca_3N_2	500°C / 15H	TbN	4.930 (4.933)
$ErCl_3$	Mg_3N_2	900°C / 1H	ErN	4.836 (4.839)
	Ca_3N_2	500°C / 15H	ErN	4.835 (4.839)

completion within 15 hours whereas reagents are also observed in the products of the magnesium nitride reaction performed with the same conditions. Also similar to the findings with the rare earth reactions, these reactions occurred over longer time periods than those of Li_3N or NaN_3. At 500°C they do not propagate after initiation but react slowly with thermolysis. This is especially true with the magnesium nitride reactions and is attributable to the lower reaction exothermicity. Unlike with the rare

*Fig. 18. XRD pattern of the product of $GdCl_3$ with Ca_3N_2 after two hours at 500°C; Stick pattern: Gd_2Cl_3N. * $MgCl_2$.*[81]

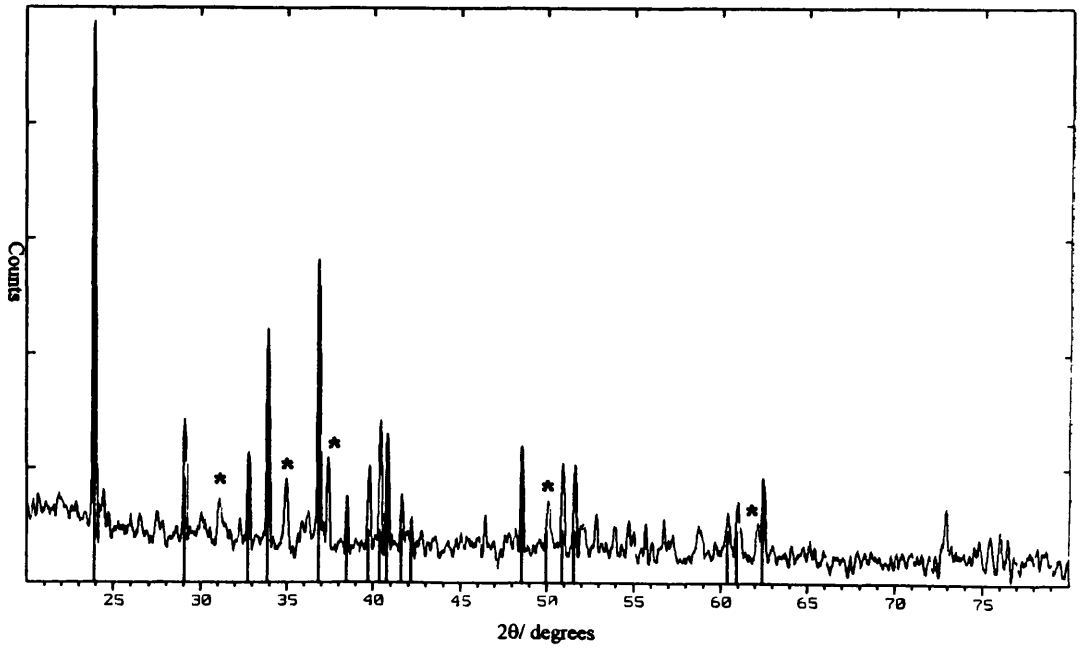

earths, potential intermediates were not observed in any of these reactions. This does not neccessarily imply a different process to that occurring with the rare earths. It could be due to a faster reaction of the intermediate to yield the product. The transition metal chlorides generally have lower melting/ decomposition temperatures than the rare earth chlorides, thus the solid state diffusion barrier to activation will be removed by the occurrence of a change of phase. The reactions are also more exothermic, Eqn. 40- 43, which would make propagation of the transition metal reactions more favourable than those of the rare earths after initiation.

$$TiCl_3 + {}^1/_2Mg_3N_2 \rightarrow TiN + {}^3/_2MgCl_2 \qquad \Delta H_r^\circ = -345 \text{ kJ mol}^{-1} \qquad \text{-Eqn.42}$$

$$TiCl_3 + {}^1/_2Ca_3N_2 \rightarrow TiN + {}^3/_2CaCl_2 \qquad \Delta H_r^\circ = -588 \text{ kJ mol}^{-1} \qquad \text{-Eqn.43}$$

Table 12. Products of reactions of transition metal chlorides with magnesium and calcium nitride.

Reagents		Conditions	Products
$TiCl_3$	Mg_3N_2	500°C / 15H	TiN, Mg_3N_2, $TiCl_3$
		900°C / cool	TiN
	Ca_3N_2	500°C / 15H	TiN
		900°C / cool	TiN
$HfCl_4$	Mg_3N_2	900°C / cool	HfN
	Ca_3N_2	900°C / cool	HfN
VCl_3	Mg_3N_2	500°C / 15H	VN (poorly crystalline)
		900°C / cool	VN
	Ca_3N_2	900°C / cool	VN, V_2N
$TaCl_5$	Mg_3N_2	500°C / 15H	Ta_2N, TaN (poorly crystalline)
	Ca_3N_2	500°C / 15H	Ta_2N, TaN
$MoCl_3$	Mg_3N_2	500°C / 15H	Mo
	Ca_3N_2	500°C / 15H	Mo
WCl_4	Mg_3N_2	500°C / 15H	W
	Ca_3N_2	500°C / 15H	W
$MnCl_2$	Ca_3N_2	500°C / 15H	Mn_4N (poorly crystalline)

$MgCl_2$ and $CaCl_2$ omitted. Lattice parameters within 0.02 Å of lit.[81,103] values.

The reaction of VCl_3 with Mg_3N_2, at 500°C or 900°C, produces phase pure VN. The product from reactions of VCl_3 with Li_3N, NaN_3 or Ca_3N_2 always contains some V_2N.

The tantalum chloride reactions with either nitride produce Ta_2N in the greater proportion whereas the Li_3N and NaN_3 reactions yield TaN as the major phase with some Ta_2N. The $MoCl_3$ reactions could have been expected to produce more nitride than with Li_3N since they are less exothermic, however no Mo_2N was observed in the products. Molybdenum and tungsten nitrides decompose below 790°C (Mo_2N[7]), less than the temperatures produced in the reactions.

3.3 Filament Initiation of Reactions.

Some of the reactions studied could alternatively be initiated by touching the reaction mixture with an electrically heated metal filament glowing yellow (~1000°C). Reaction mixtures were made up in the usual way by grinding the reagants together under nitrogen or argon in a glove box, but then were touched with a hot metal filament whilst still in the agate pestle and mortar. No initiation or propagation was found to occur between rare earth chlorides and magnesium or calcium nitride. The reaction products and the ease of propagation are summarised in Table 13. No changes in reactivity or composition of products was observed using an argon atmosphere instead of nitrogen. Under air, reactions were more vigourous and products were found to contain considerable amounts of oxide (of the order of 30%) in addition to the products in Table 13.

Table 13. Products of filament initiated reactions with magnesium and calcium nitride.

Reagents		Propagation	Product(s)
$TiCl_3$	Mg_3N_2	none	—
	Ca_3N_2	fast	TiN, Ca_2NCl_3, Ca_3N_2
	$1Ca_3N_2 : 2Mg_3N_2$	none	—
VCl_3	Mg_3N_2	none	—
	Ca_3N_2	fast	V_2N, VN
	$1Ca_3N_2 : 2Mg_3N_2$	slow	V_2N
$NbCl_5$	Mg_3N_2	none	—
	$1Ca_3N_2 : 2Mg_3N_2$	slow	Nb_2N, NbN
$TaCl_5$	Mg_3N_2	none	—
	$1Ca_3N_2 : 2Mg_3N_2$	slow	Ta_2N (TaN)
$MoCl_5$	Mg_3N_2	slow	Mo
WCl_5	Mg_3N_2	slow	W

$MgCl_2$ and $CaCl_2$ omitted. Lattice parameters within 0.02 Å of lit.[81,103] values.

Filament initiated reactions of Ca_3N_2 and Mg_3N_2 with transition metal chlorides showed different rates of propagation. Reactions of magnesium nitride with niobium or tantalum chloride could be initiated at the tip of the filament but the reaction failed to propagate through the solid. Similar reactions with calcium nitride were easily initiated and spread through the reaction mixture very quickly. Reaction times were less than a second and accompanied by a bright thermal flash indicating a temperature of the order of 1000°C. The reactions cool rapidly and approach ambient temperature

Fig. 19. Photographs of the filament initiated reaction of VCl_3 with a mixture of $1Ca_3N_2$: $2Mg_3N_2$ after 0.7 (top left), 1.4 (top right), 3.5 (bottom left) and 4.9 (bottom right) seconds.

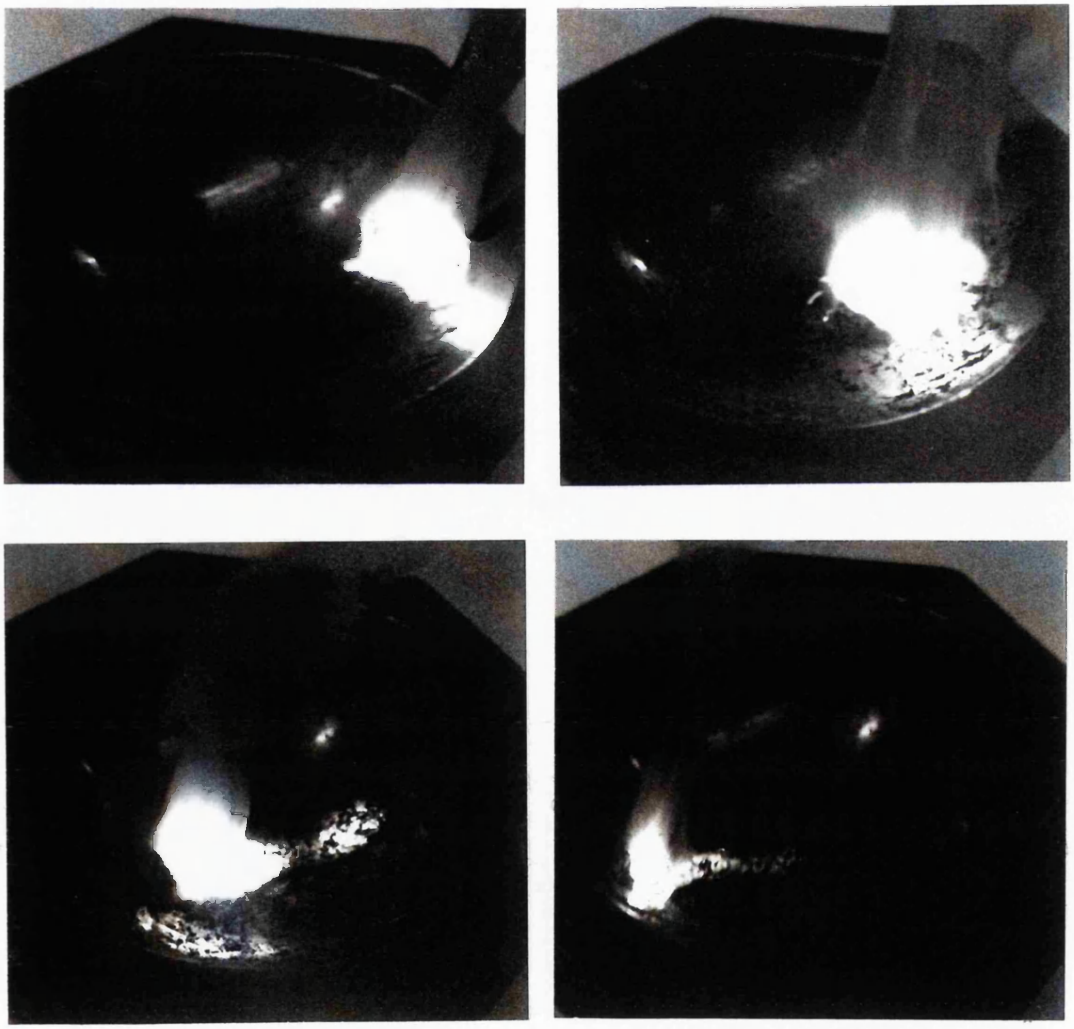

in about 30 seconds. Using mixtures of Mg_3N_2 and Ca_3N_2 it was possible to modulate the reactions so that only a slow propagation occurred. This is demonstrated in Fig. 19 which contains photographs of a slow propagation wave with a velocity of *ca.* 1 cm s^{-1} generated by a reaction of VCl_3 with a 1:2 mixture of Ca_3N_2 and Mg_3N_2. It is

to be expected that factors such as particle size, reaction exothermicity, degree of mixing and melting and vapourisation temperatures of components would influence the rate of propagation as has been extensively reported for SHS processes, where propagation velocities from 1 mm s^{-1} to 0.5 m s^{-1} are common.[62]

In some cases, reactions initiated by a hot filament and those performed by heating in a sealed ampoule show some differences in the phases of product observed. Filament initiated reactions of $TiCl_3$ and Li_3N have been reported to produce TiN and some Ti metal,[111] whilst the same reaction carried out in a sealed ampoule produces only the TiN phase. The reaction of VCl_3 with Mg_3N_2 in a sealed ampoule produced VN, whilst with Ca_3N_2 the major phase was VN with some V_2N also present. Modifying the nitriding component of the reaction mixture to a 1:2 mixture of calcium: magnesium nitride allowed the isolation of phase pure V_2N. Thermally initiated reactions in sealed ampoules were found to favour more highly nitrided products than the filament initiated reactions. Modification of the conditions allowed isolation of VN or V_2N at high purity, Fig. 20.

Fig. 20. XRD patterns of VN (top) and V_2N (bottom) produced from the thermally initiated reaction of VCl_3 with Mg_3N_2 and the filament initiated reaction of VCl_3 with $1Ca_3N_2$: $2Mg_3N_2$ respectively. Stick pattern: V_2N.[81]

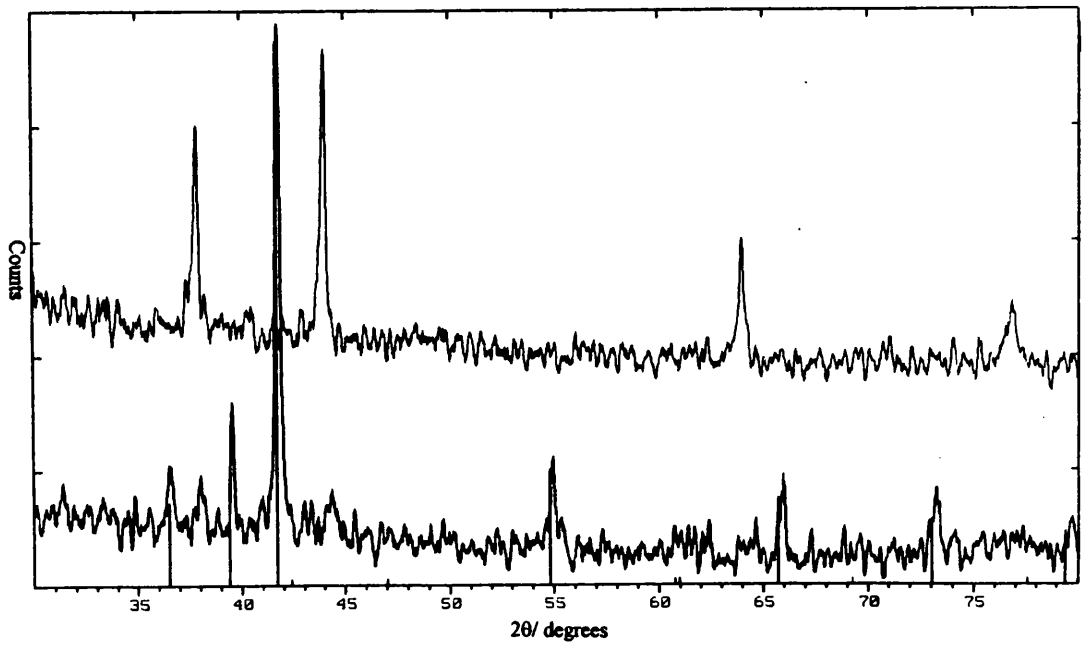

Kaner and co- workers have recently shown, by considering reactions of MgB_2 and Li_3N,[115] that self- propagation in filament initiated SSM reactions is dependent on the overall reaction enthalpy and crucially on T_{ad}, the adiabatic combustion temperature. For SHS reactions a value of $T_{ad} > 1800$ K is required for propagation,[62] whilst in considering SSM reactions to form transition metal borides $T_{ad,s}$ (the adiabatic combustion temperature for salt formation only, i.e. in a magnesium nitride reaction this would be calculated for the reaction $MCl_n + Mg_3N_2 \rightarrow MgCl_2 + M + N$) was found to be a more useful parameter and $T_{ad,s}$ needed to be greater than the melting point of the salt co- product $MgCl_2$. The correlation with the temperature required to produce the salt in the liquid phase was taken as evidence that self- propagation relied on mediation by the molten salt, which would also imply that salt formation was the most likely first step in the reactions. If these findings hold for this work then values of $T_{ad,s}$ corresponding to the melting point of $MgCl_2$ and $CaCl_2$, 987 K and 1055 K respectively, would be expected to be important.

From Table 13 it is clear that reactions of Ca_3N_2 propagated far more readily than those involving Mg_3N_2. The reactions of VCl_3 propagated very quickly with Ca_3N_2, but not at all with Mg_3N_2. A 1:2 mixture of these two reagents led to a reaction which propagated slowly through the reaction mixture, the reaction being only just self sustaining. The values of $T_{ad,s}$ given in Eqn. 44- 46 explain this data well. The 1:2 mixture is sufficiently exothermic to melt some of the $MgCl_2$ and allow salt mediation of the reaction. The reactions of $MoCl_5$ and WCl_4 with Mg_3N_2 also self-propagate slowly. These reactions are more exothermic than those of Mg_3N_2 with VCl_3 or $TiCl_3$ and in both cases $T_{ad,s}$= 987 K. For all the reactions of the lanthanide chlorides with calcium or magnesium nitride the reactions involving salt formation only are endothermic so $T_{ad,s}$ is below room temperature, hence the complete lack of propagation in these cases.

$$VCl_3 + {}^1/_2Mg_3N_2 \rightarrow V + {}^1/_2N_2 + {}^3/_2MgCl_2 \qquad T_{ad,s}= 351\ K \qquad \text{-Eqn.44}$$

$$VCl_3 + {}^1/_3Mg_3N_2 + {}^1/_6Ca_3N_2 \rightarrow V + {}^1/_2N_2 + MgCl_2 + {}^1/_2CaCl_2 \qquad T_{ad,s}= 987\ K \qquad \text{-Eqn.45}$$

$$VCl_3 + {}^1/_2Ca_3N_2 \rightarrow V + {}^1/_2N_2 + {}^3/_2CaCl_2 \qquad T_{ad,s}= 1611\ K \qquad \text{-Eqn.46}$$

3.4 Summary and Relevance to Reaction Mechanism.

Rare earth and early transition metal nitrides may be produced from reactions of metal

chlorides with sodium azide and Group 2 nitrides. Differences in product distributions from lithium nitride reactions are observed in the transition metal nitrides. Sodium azide reactions are more exothermic than those of lithium nitride, but also produce large amounts of nitrogen gas so yield nitrides with smaller crystallite sizes and more open morphologies. Calcium and magnesium nitride reactions occur more slowly, often requiring periods of thermolysis. The ease with which the reactions occur is related to the melting/ decomposition temperatures of the reagents and reaction exothermicity. Hence, calcium nitride reactions occur more readily than those of magnesium nitride. Under filament initiation conditions the ability of reactions to propagate can be related to $T_{ad,s}$, the theoretical temperature which would be reached if calcium or magnesium chloride was formed with metal and nitrogen. $T_{ad,s}$ must equal or exceed the melting point of the salt by- product for propagation to occur.

Section 2.8 discussed the mechanistic pathways which could operate in SSM reactions. These can simply be described as ionic, elemental or a combination of ionic/ elemental. The comments made about lithium nitride reactions may also, generally, be applied to those of transition metal chlorides with sodium azide and the group 2 nitrides. Either process can explain the observed phases. The case in which this becomes strained is when ionic arguments are applied to the sodium azide reactions. An azide ion, N_3^-, would replace each chloride ion so that MCl_n would react to give $M(N_3^-)_n$ as an intermediate species. A reductive recombination mechanism or a combination of the two processes is easier to imagine. For example, one azide ion could replace one chloride, then decompose to N^{3-}, liberating two atoms of chlorine which could go on to react further with sodium ions.

The reactions of rare earth chlorides with magnesium or calcium chloride could only be promoted thermally and the reaction was slow. Uniform heating of the reaction mixture at 550°C for 1 hour yields a mixture of products as identified by XRD including some rare earth nitride but largely nitride chlorides, Ca_2NCl and Ln_2Cl_3N. Heating the reaction mixture for a longer time period increases the amount of nitride and diminishes the amount of rare earth chloride such that, for most Ca_3N_2 reactions, after 15 hours at 550°C only rare earth nitride and calcium chloride are observed. The rare earth chloride reactions, when heated to 900°C and allowed to cool, produced rare earth nitride and magnesium or calcium chloride only. The observation of intermediate species, Ln_2Cl_3N and Ca_2NCl, in the reaction pathway gives strong evidence of an ionic mechanism. No changes of oxidation state are observed in any of the elements, the rare earth retains the +3 oxidation state from $LnCl_3 \rightarrow Ln_2Cl_3N \rightarrow LnN$. In no cases were the elements observed in the products by XRD.

The previously mentioned work of DiSalvo and co- workers[113,114] is also worth mentioning at this point. The ternary nitrides Ca_3VN_3 and Ca_3CrN_3 consist of $(MN_3)^{6-}$ anions separated by Ca^{2+} ions. The synthesis of these compounds must involve the transfer of N^{3-} ions from Ca_3N_2 to MN, showing that such transfers are possible.

3.5 Experimental.

Reagents, solvents and instumentation were as described previously. In addition sodium azide, magnesium nitride and calcium nitride were purchased from Aldrich Chemical Co. Photographs were obtained with Ilford XP2 film at 0.7 sec intervals. Filament initiation was carried out with a nichrome wire heated using a 6 volt battery.

Thermally Initiated Reactions.

These were carried out in a similar way to those of lithium nitride. Sodium azide reaction mixtures were made up on a scale of 50mg sodium azide with a 1:1 ratio of sodium to chloride, sealed into large pyrex ampoules (~30cm^3 internal volume), heated to 400°C and allowed to cool. Group 2 nitrides were mixed with metal chlorides on a scale of 50- 100mg magnesium or calcium nitride with a 1:2 ratio of alkaline earth to chloride. Mixtures were heated to 500°C in pyrex or 900°C in quartz ampoules for the time periods listed in Tables 11 and 12. All the products were ground and washed with methanol or tetrahydrofuran.

Filament Initiated Reactions.

Reaction mixtures were prepared in an agate pestle and mortar under nitrogen or argon. A hot metal filament was placed in the mixture and removed after initiation. The products were then treated in the same way as those from thermally initiated reactions.

4. Reactions of Transition Metal Chlorides with Na_3Pn (Pn= P, As, Sb, Bi).

Solid state metathesis reactions to produce transition metal pnictides M_xPn_y (Pn= P, As, Sb, Bi) can most easily be performed with Group 1 or 2 pnictide reagents. The available phosphides include Li_3P, Na_3P, NaP, Na_2P_5, K_3P, Mg_3P_2, Ca_3P_2 and Sr_3P_2.[116] The trisodium pnictides were chosen for ease of preparation. This choice also allows work in a nitrogen atmosphere without the likelihood of nitride contamination (since sodium nitride has a low thermal stability decomposing below 300°C). These were synthesised by direct high temperature combination of the elements. The compounds so produced were checked for phase purity by XRD, sample results are presented in Table 14. The crystal structure of these compounds shows two layers, hexagonal nets of composition NaPn are sandwiched by layers of sodium, Fig. 21.[117] Their properties show ionic and metallic characteristics.

Table 14. XRD data for sodium pnictides.

Sodium pnictide	**a** (lit.[81,103] **a**) / Å	**c** (lit.[81,103] **c**) / Å
Na_3P	4.972 (4.990)	8.821 (8.815)
$Na_3P_{0.5}As_{0.5}$	5.058	8.982
Na_3As	5.053 (5.088)	9.011 (8.982)
Na_3Sb	5.356 (5.355)	9.497 (9.496)
Na_3Bi	4.454 (5.448)	9.667 (9.655)

All crystallise with the hexagonal $P6_3/mmc$ space group.

Fig. 21. The unit cell of Na_3As.[117]

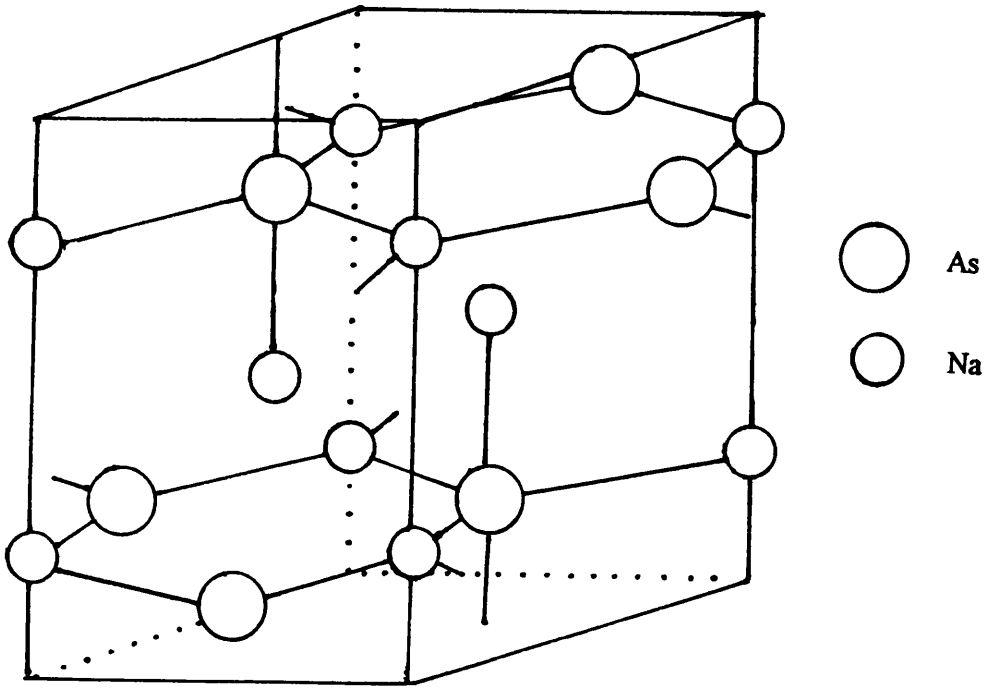

This chapter will discuss the reactions of the trisodium pnictides with d- block chlorides. Simultaneously to this work, preparations by similar methods of lanthanide phosphides,[118] arsenides, antimonides and bismuthides[119] (LnPn; Pn= P, As, Sb, Bi) were carried out in our laboratory. Group 13 pnictides (MPn; M= Al, Ga, In; Pn= P, As, Sb) have also been prepared in this way[120] and the magnetic characterisation of gadolinium phosphide, arsenide and antimonide from this route has been carried out.[121]

4.1 Properties of Phosphides.

Phosphides are known for almost all metals and occur in a very wide range of stoichiometries, from M_4P to MP_{15}.[122] Many metals form five or six distinct phosphide phases, nickel forms at least eight (Ni_3P, Ni_5P_2, $Ni_{12}P_5$, Ni_2P, Ni_5P_4, NiP, NiP_2 and NiP_3).[122] They are sometimes divided into two general classes:

- Reactive phosphides which hydrolyse readily.

- Phosphides with a metallic nature which do not easily hydrolyse.

The former class includes those of Groups 1-3 and other electropositive metals. They possess a considerable degree of ionic character but are not generally considered to contain fully ionised P^{3-} and there are considerable metallic or covalent interactions.[122] Reactions with water yield phosphine. The transition metal phosphides and those of the more noble metals are metallic in nature. They are characterised by hardness, high melting point, high thermal and electrical conductivity, metallic lustre and resistance to attack by dilute acids and alkalis.[123] Some will react with hot nitric acid.

It is also informative, especially for the transition metal phosphides, to classify as metal- rich phosphides, monophosphides or phosphorus- rich phosphides.[122] The metal- rich compounds have the most metallic character. The monophosphides adopt a variety of structures under the influence of size and electronic effects. The phosphorus- rich compounds have lower melting and decomposition temperatures. They are not adequately described as reactive or metallic. Often they are semiconductors and feature increasing catenation of phophorus atoms. Structures contain P_2 units in MP_2 (M= Fe, Ru, Os, Pt), planar P_4 units in MP_3 (M= Co, Ni, Rh, Pd, Ir), chains (PdP_2, NiP_2, CdP_2, BaP_3), double chains in $MPbP_{14}$ (M= Zn, Cd, Hg) or layers. These form with a regular fusion of puckered 10- membered rings of phosphorus with metal atoms in the interstices (CuP_2, AgP_2, CdP_4).[122]

Relatively few industrial applications for transition metal phosphides have been found. Monophosphides of tantalum, tungsten and niobium are extremely resistant to oxidation at high temperatures and have been suggested as nose cone surface materials for space re- entry vehicles.[70] Reactive phosphides release phosphine upon hydrolysis, hence zinc phosphide has been used as a rodent poison.[124] Calcium phosphide hydrolyses with evolution of spontaneously flammable phosphines and is a component of some naval flares.[70] Aluminium, gallium and indium phosphides are important semiconductors[120] whereas lanthanide phosphides are semiconductors with ferromagnetic or antiferromagnetic behaviour.[121]

4.2 Reactions of Sodium Phosphide.

Reactions of sodium phosphide with anhydrous metal chlorides were performed with mixtures made up with a 1:1 ratio of sodium to chloride. The products are listed in Table 15 together with reaction conditions. A number of reactions were found to self- initiate during mixing or grinding together of the reagents. These tended to be those which involved the more volatile chlorides ($MoCl_5$ melts at 194°C and boils at 268°C[87]). Initiation probably occurs because some NaCl forms and the heat produced is sufficient to cause propagation. It has previously been shown[125] that a mixture of GaI_3 and Na_3As produces NaCl at room temperature without initiation.

Those reactions which required more energy to overcome the solid state diffusion barrier were heated to 500°C (800°C with YCl_3 or $LaCl_3$) in vacuum sealed Pyrex (quartz) ampoules and allowed to cool. Powder XRD of the crude products indicated sodium chloride and the phases listed in Table 15. EDXA showed strong sodium and chlorine peaks with weaker transition metal and phosphorus peaks. SEM data were similar to those of the products with lithium nitride, a smooth continuous surface was observed indicative of a coating of sodium chloride which had melted during the reaction.

Sodium chloride was removed from the crude products, after grinding, using distilled methanol. Phosphides of Groups 4-11 could alternatively be washed with water, however this decomposed YP, LaP and Zn_3P_2. No elemental phosphorus was normally observed by XRD or SEM/ EDXA, presumably because it sublimed out during reactions. If any was present it was sublimed out under static vacuum at 500°C.

Primary characterisation of the purified products was carried out by powder XRD,

SEM, EDXA and microanalysis. The X- ray diffraction data are presented in Table 15. A typical XRD pattern is shown in Fig. 22. SEM revealed aggregated particles,

Table 15. Products of reactions of metal chlorides with sodium phosphide.

Reagent	Initiation	Product	System, space group[81,103]
YCl_3	800°C	YP	Cubic Fm3m
$LaCl_3$	800°C	LaP	Cubic Fm3m
$TiCl_3$	500°C	TiP	Hexagonal $P6_3/mmc$
$ZrCl_4$	500°C	ZrP	Cubic Fm3m
$HfCl_4$	500°C	HfP	Cubic Fm3m
VCl_3	500°C	VP	Hexagonal $P6_3/mmc$
		(VP_2)	Monoclinic C2/m
$NbCl_5$	r.t.	NbP	Tetragonal $I4_1md$
$TaCl_5$	r.t.	TaP	Tetragonal $I4_1md$
$CrCl_2$	500°C	CrP	Orthorhombic Pbnm
		($Cr_{12}P_7$)	Hexagonal P6
$MoCl_3$	500°C	MoP	Hexagonal P6m2
		(Mo)	Cubic Im3m
$MoCl_5$	r.t.	MoP	Hexagonal P6m2
WCl_4	r.t.	WP	Orthorhombic Pnma
$FeCl_3$	r.t.	FeP	Orthorhombic Pbnm
		(FeP_2)	
$CoCl_2$	500°C	CoP	Orthorhombic Pbnm
$NiCl_2$	500°C	Ni_2P	Hexagonal P62m
K_2PtCl_4	r.t.	PtP_2	Cubic Pa3
		(Pt_5P_2)	Monoclinic C2/c
$ZnCl_2$	500°C	Zn_3P_2	Tetragonal $P4_2/nmc$

r.t. Initiated on mixing or grinding.
Structural data are listed in Appendix 1.

on the scale of 10- 100 μm. Crystallite sizes, calculated from XRD linewidths,[104] were generally on the order of 500- 700Å for self- initiated reactions and 1000Å for ampoule reactions. EDXA showed metal and phosphorus, with a small oxygen peak in the water washed Group 4-11 phosphides. No sodium or chlorine peaks were observed (detection limit ~0.5%). FT-IR spectra were featureless in the range 4000-200 cm^{-1}.

Solid state magic angle spinning (MAS) ^{31}P nuclear magnetic resonance (NMR)

spectroscopy was carried out for YP, LaP and Zn_3P_2. The spectrum of YP contained a single sharp resonance with a chemical shift of +565ppm and no resolvable ^1J ^{89}Y-^{31}P coupling (^{89}Y; I= $^1/_2$, 100% abundant[126]). Spinning side bands were negligible, presumeably due to the highly symmetric environment of the phosphorus atoms in the

Fig. 22. XRD pattern of Ni_2P produced from $NiCl_2$ and Na_3P.

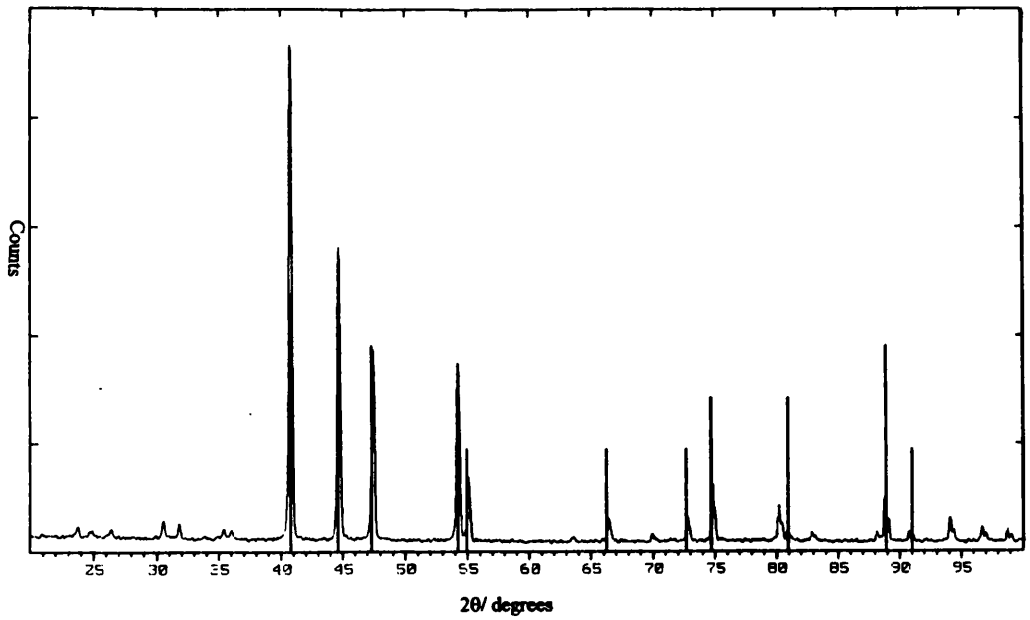

Fm3m lattice. The LaP spectrum contained a broad resonance at +657ppm. The broadening is attributable to a quadrupolar contribution from ^{139}La (I= $^7/_2$, 99.9% abundant[126]) or to relaxation effects. The solid state MAS ^{31}P NMR spectrum of Zn_3P_2, Fig. 23, contains two sharp resonances at -193ppm and -227ppm with relative intensity of 1:0.86 (^{67}Zn; I= $^5/_2$, 4.1% abundant[126]). Two phosphorus environments would be expected to be observed as two different phosphorus lattice sites are present with equal populations. Spinning side bands are also clearly apparent, plus a broad peak of low signal intensity observed at -50ppm. No previous solid state ^{31}P NMR measurements of d- block metal phosphides could be found.

The major phase of phosphide products from the reactions of Group 3-9 chlorides were the monophosphides. In all reactions of these chlorides the amount of phosphide ions equalled or exceeded the number of metal ions and phosphorus was often a by- product, Eqn. 47 and 48. Considering the thermal instability of the phosphorus- rich compounds it is unsurprising that the monophosphides form and that phosphorus is sometimes lost. The products from these reactions are by no means totally obvious, however. Eqn. 49-51 show idealised equations where either metal or

phosphorus is lost, or a product is obtained with the ratio of metal to phosphorus governed by the reagent mixture (although no cobalt metal was observed it is needed to balance the equation).

Fig. 23. Solid state MAS ^{31}P NMR spectrum of Zn_3P_2.

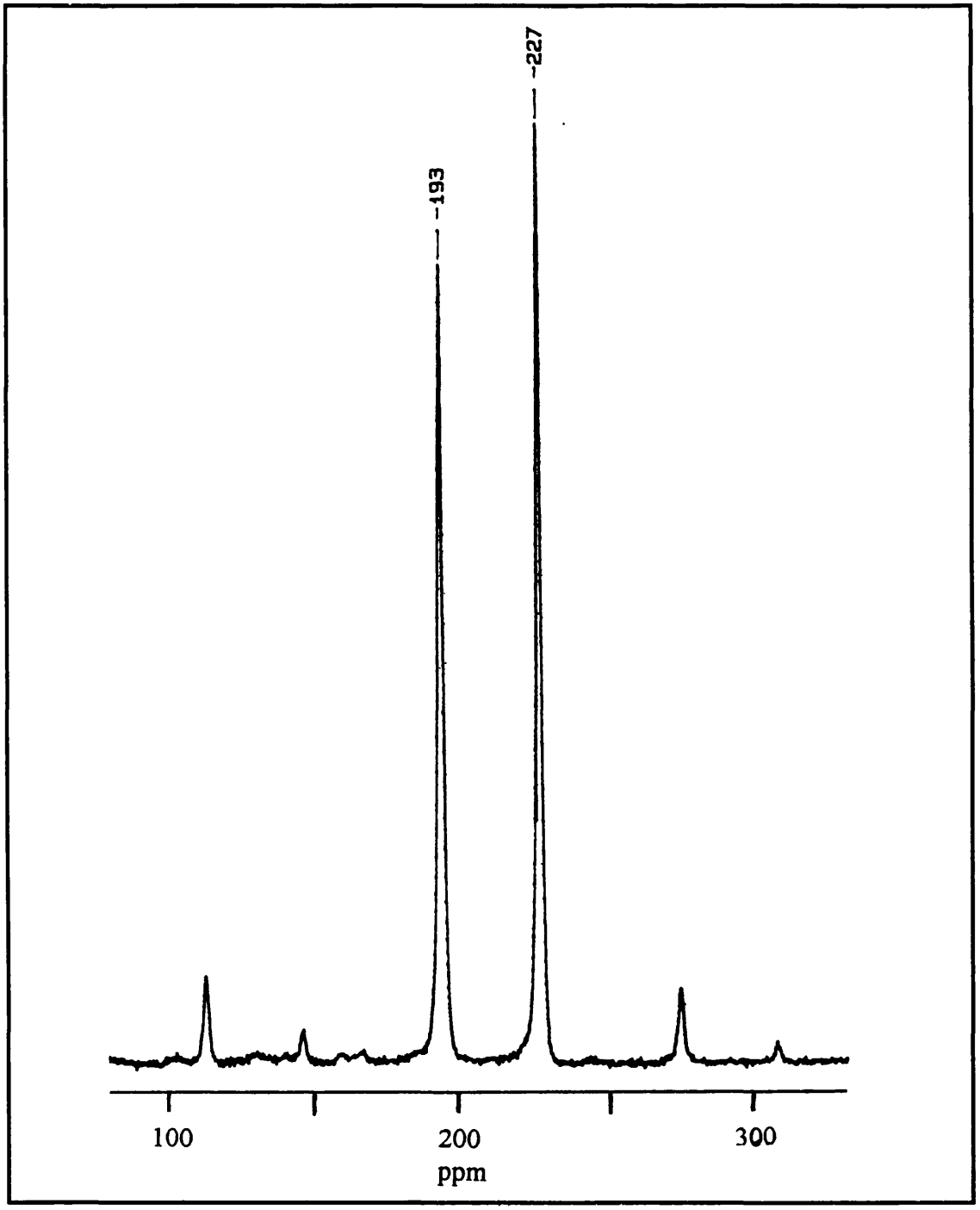

$$LaCl_3 + Na_3P \rightarrow LaP + 3NaCl \qquad \text{-Eqn.47}$$

$$MoCl_5 + {}^5/_3Na_3P \rightarrow MoP + 5NaCl + {}^1/_6P_4 \qquad \text{-Eqn.48}$$

$$CoCl_2 + {}^2/_3Na_3P \rightarrow {}^2/_3CoP + {}^1/_3Co + 2NaCl \quad \Delta H_r^\circ = -532.4 \text{ kJ mol}^{-1} \quad \text{-Eqn.49}$$

$$NiCl_2 + {}^2/_3Na_3P \rightarrow {}^1/_2Ni_2P + {}^1/_{24}P_4 + 2NaCl \quad \Delta H_r^\circ = -548.8 \text{ kJ mol}^{-1} \quad \text{-Eqn.50}$$

$$ZnCl_2 + {}^2/_3Na_3P \rightarrow {}^1/_3Zn_3P_2 + 2NaCl \quad \Delta H_r^\circ = -398.8 \text{ kJ mol}^{-1} \quad \text{-Eqn.51}$$

Likewise, the main product with $CrCl_2$ is CrP and the resulting phosphorus deficiency is balanced by the presence of some metal- rich $Cr_{12}P_7$ in the product. The reactions with VCl_3 and $FeCl_3$ also produce some of the MP_2 phase. This is unexpected since the stoichiometry of the reagent mixtures would point to the monophosphide, Eqn. 52. However, if any excess phosphorus can be obtained under the right conditions, formation of the diphosphide is energetically favourable, Eqn. 53 and 54.[116]

$$FeCl_3 + Na_3P \rightarrow FeP + 3NaCl \quad \Delta H_r^\circ = -861.7 \text{ kJ mol}^{-1} \quad \text{-Eqn.52}$$

$$VP + {}^1/_4P_4 \rightarrow VP_2 \quad \Delta H_r^\circ = -238 \text{ kJ mol}^{-1} \quad \text{-Eqn.53}$$

$$FeP + {}^1/_4P_4 \rightarrow FeP_2 \quad \Delta H_r^\circ = -69 \text{ kJ mol}^{-1} \quad \text{-Eqn.54}$$

The reactions with Group 4 chlorides produce hexagonal TiP and cubic ZrP or HfP, Eqn. 55 and 56. Zirconium and hafnium monophosphide also form as hexagonal phases isostructural with TiP which transform to the cubic phase at 1425°C and 1600°C respectively.[117,127] The adiabatic combustion temperature, T_{ad}, for all three reactions is 1465°C, the boiling point of NaCl.[128] Thus ZrP would be expected to form in the cubic phase but for HfP the hexagonal phase would be more likely. Formation of the cubic phase for HfP could be explained by a small phosphorus deficiency from $MP_{1.00}$ caused by carrying out the reaction under vacuum. The more compact cubic form would then become more favourable. An alternative explanation would be a templating effect from the co- produced, cubic NaCl encouraging the cubic phase, although this is counter intuitive since NaCl would be in the gas/ liquid states at the reaction temperature. The β- phases of NbP and TaP, the phases obtained in this study, form above 900°C.

$$TiCl_3 + Na_3P \rightarrow TiP_{(Hex)} + 3NaCl \quad \Delta H_r^\circ = -682 \text{ kJ mol}^{-1} \quad \text{-Eqn.55}$$

$$HfCl_4 + {}^4/_3Na_3P \rightarrow HfP_{(Cub)} + 4NaCl + {}^1/_{12}P_4 \quad \Delta H_r^\circ = -830 \text{ kJ mol}^{-1} \quad \text{-Eqn.56}$$

Dilution of reactions with lithium or sodium chloride resulted in reduction in crystallite and particle sizes, as per the lithium nitride reactions. In addition, where

self- initiation occurred this could be controlled. A reaction of $MoCl_5$ with Na_3P on a scale of 200mg $MoCl_5$ was carried out with increasing degrees of dilution. With no LiCl added the reaction initiated during mixing with a spatula and the average crystallite size (calculated using the Scherrer equation[104] with the half- width of the 101 reflection of the MoP XRD pattern) was 760Å. With 160mg and 320 mg LiCl added the reactions were less voracious and initiated when ground in a pestle and mortar. Average crystallite sizes were 650Å and 480Å respectively. When 480mg of LiCl was added, gentle warming with a hairdryer was needed to cause initiation and the average crystallite size was 320Å.

4.3 Properties of Arsenides, Antimonides and Bismuthides.

Most metals form compounds or alloys with the heavier pnictogen elements. Many demand attention for their interesting structures or physical properties.[122] Like most nonoxidic ceramics a multitude of stoichiometries (M_9As, M_5As, M_4As, M_3As, M_2As, M_5As_3, M_3As_2, M_4As_3, M_5As_4, MAs, M_3As_4, M_2As_3, MAs_2 and M_3As_7 is a typical range for the arsenides, a similar variety for antimony and bismuth) and many different structures occur.[122] Many compounds also occur over a range of composition and non- stoichiometry is rife. A great deal of electrical and magnetic data is available about these compounds, reviewed by J. D. Smith,[117] and the structural data have been comprehensively reviewed by Hulliger.[129]

Most binary compounds of arsenic, antimony and bismuth with transition metals can generally be regarded as intermetallics. Transition metals with similar electronic structures generally form pnictides with similar stoichiometries and structures. Group 3 metals form monopnictides (MPn) with the Fm3m (f.c.c. NaCl) structure, as per the nitrides and phosphides. The most common monopnictide structures for the other d-block metals are the closely related $P6_3/mmc$ (hexagonal NiAs) and Pnma (orthorhombic MnP) structures.[117] The other stoichiometries crystallise with a wide variety of structures.

Group 3 pnictides are used as semiconductors (especially GaAs) and magnetic materials (lanthanide pnictides).[120,121] The pnictogen rich transition metal compounds (e.g. $FeSb_2$ and $PtAs_2$) are often semiconductors.[117] Many compounds have interesting magnetic properties, for example CrAs and CrSb are antiferromagnetic whereas MnAs, MnSb and MnBi are ferromagnetic. The manganese- bismuth compound is ferromagnetic with a strong coersive force up to 357°C and has possibilities for use in permanent magnets.[130]

4.4 Reactions of Sodium Arsenide.

The reactions of sodium arsenide with anhydrous metal chlorides were carried out in the same way as those of sodium phosphide. Anhydrous metal chloride and sodium arsenide (1:1 ratio of sodium to chloride) were mixed in an inert atmosphere and ground together in an agate pestle and mortar. Some mixtures initiated on mixing or grinding. Those which did not were sealed under vacuum into a Pyrex (quartz for >500°C) ampoule and heated as stated in Table 16. The product was ground and washed with methanol, thf or water. The resulting materials were characterised by XRD, Fig. 24, and SEM/ EDXA. EDXA showed even ratios of metal to arsenic and semiquantitative analysis was close to the theoretical values for the phases observed by XRD. Sodium and chlorine were below the detection threshold (~0.5%). Only YAs and LaAs were decomposed by water washing. The products of these reactions are listed in Table 16.

Those reactions where the products can be directly compared have reaction enthalpies lower than the phosphide reactions, Eqn. 57 and 58. The analogous phosphide reactions have $\Delta H_r°$ values of -682 kJ mol^{-1}, Eqn. 55, and -398.8 kJ mol^{-1}, Eqn. 51, respectively. A general trend is observed of the products being more pnictogen rich than the phosphides. This would have to be due to higher decomposition temperatures of the diarsenides, compared with the diphosphides, or the diarsenides being considerably more thermodynamically favourable. The data to assess the thermochemical factors which could be responsible are unavailable. The diarsenides tend to be semiconductors[117] so must possess some covalent bonding as with the diphosphides. One would, therefore, expect them to be thermally labile with respect to the monoarsenides.

$$TiCl_3 + Na_3As \rightarrow TiAs + 3NaCl \qquad \Delta H_r° = -457.0 \text{ kJ mol}^{-1} \quad \text{-Eqn.57}$$

$$ZnCl_2 + {}^2/_3Na_3As \rightarrow {}^1/_3Zn_3As_2 + 2NaCl \qquad \Delta H_r° = -317.5 \text{ kJ mol}^{-1} \quad \text{-Eqn.58}$$

These reactions occur in four different ways. Some involve no change in the formal oxidation state of the metal and yield only an arsenide and NaCl, Eqn. 59. Some involve a disproportionation and yield two arsenide phases, Eqn. 60. Others involve an increase in formal oxidation state and yield some metal as a by- product, Eqn. 61, or a decrease in oxidation state and some arsenic by- product, Eqn. 62. Some reactions involve an increase in oxidation state but no metal was observed, such as the reaction of WCl_4 to yield WAs_2. In this case either the product must have been arsenic deficient, possible since the lattice parameters do deviate from the literature

Table 16. Products of reactions of metal chlorides with sodium arsenides.

Reagent	Initiation	Product	System, space group[81,103]
YCl_3	800°C	YAs	Cubic Fm3m
$LaCl_3$	800°C	LaAs	Cubic Fm3m
$TiCl_3$	500°C	TiAs	Hexagonal $P6_3/mmc$
$ZrCl_4$	500°C	ZrAs	Hexagonal $P6_3/mmc$
$HfCl_4$	500°C	HfAs	Hexagonal $P6_3/mmc$
		$HfAs_2$	Orthorhombic Pnam
VCl_3	500°C	VAs	Orthorhombic Pnma
		(V_5As_3)	Tetragonal I4/mcm
$NbCl_5$	r.t.	NbAs	Tetragonal $I4_1md$
		($NbAs_2$)	Monoclinic C2/m
$TaCl_5$	r.t.	TaAs	Tetragonal $I4_1md$
		$TaAs_2$	Monoclinic C2/m
$CrCl_3$	500°C	CrAs	Orthorhombic Pnma
$MoCl_3$	500°C	Mo_5As_4	Tetragonal I4/m
		MoAs	Orthorhombic Pnma
WCl_4	r.t.	WAs_2	Monoclinic C2
$MnCl_2$	500°C	MnAs	Hexagonal $P6_3/mmc$
		(Mn)	Cubic I-43m
$FeCl_3$	r.t.	$FeAs_2$	Orthorhombic Pnnm
$CoCl_2$	r.t.	CoAs	Orthorhombic Pmcn
		Co_2As	Hexagonal P62m
$NiCl_2$	r.t.	$Ni_{11}As_8$	Tetragonal $P4_12_12$
		Ni_5As_2	Hexagonal $P6_322$
K_2PtCl_4	r.t.	Pt	Cubic Fm3m
		$PtAs_2$	Cubic Pa3
$ZnCl_2$	500°C	Zn_3As_2	Tetragonal $I4_1/acd$

r.t. Initiated on mixing or grinding.
Structural data are listed in Appendix 2.

values, or another product could have been present but amorphous. This could be metal, Eqn. 63, or a less arsenic rich phase such as WAs. Where arsenic is a by-product this was not observed in the XRD patterns but this was assumed to be due to sublimation of the excess.

$$YCl_3 + Na_3As \rightarrow YAs + 3NaCl \qquad \Delta H_r^\circ = -353 \text{ kJ mol}^{-1} \text{ -Eqn.59}$$

$$CoCl_2 + {}^2/_3Na_3As \rightarrow {}^1/_3CoAs + {}^2/_3Co_2As + 2NaCl \quad \Delta H_r^\circ = -400 \text{ kJ mol}^{-1} \quad \text{-Eqn.60}$$

$$MnCl_2 + {}^2/_3Na_3As \rightarrow {}^2/_3MnAs + {}^1/_3Mn + 2NaCl \quad \Delta H_r^\circ = -243 \text{ kJ mol}^{-1} \quad \text{-Eqn.61}$$

$$ZrCl_4 + {}^4/_3Na_3As \rightarrow ZrAs + {}^1/_3As + 4NaCl \quad \text{-Eqn.62}$$

$$WCl_4 + {}^4/_3Na_3As \rightarrow {}^2/_3WAs_2 + {}^1/_3W + 4NaCl \quad \text{-Eqn.63}$$

Fig. 24. XRD pattern of YAs produced from YCl_3 and Na_3As.

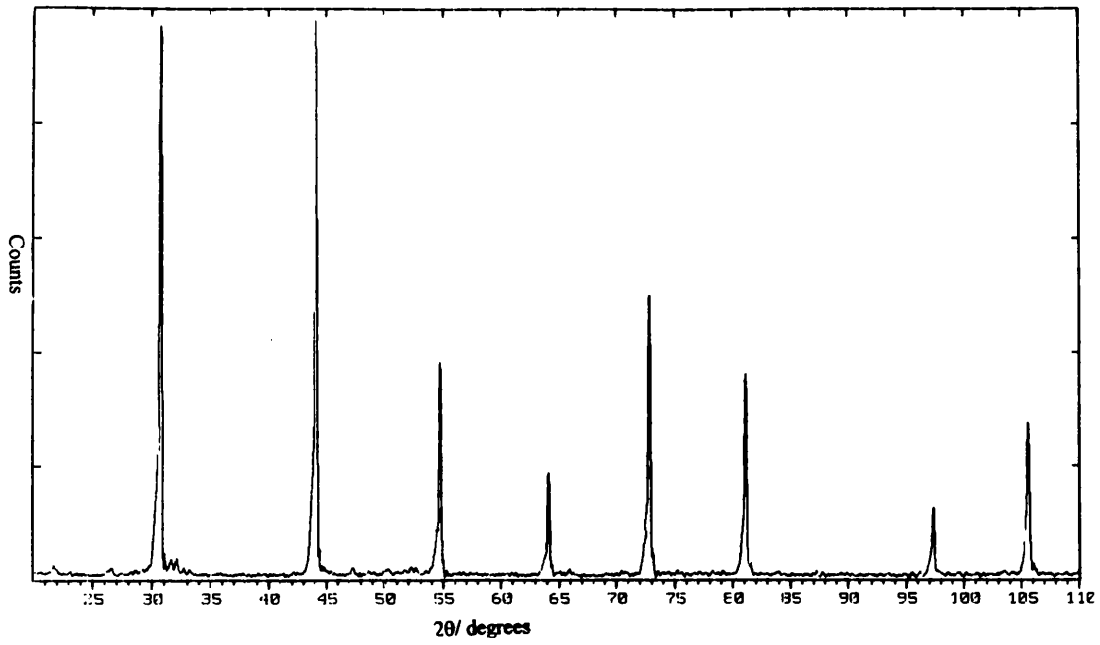

To study changes in reactivity with sodium arsenide composition, compounds with variable sodium content were prepared. Sodium arsenides made by elemental combination in liquid ammonia occur with a wide range of compositions. Materials were produced with stoichiometries Na_2As, Na_3As and Na_4As. These reagents were amorphous and no attempt was made to induce crystallinity, although a short period of thermolysis was used to drive off any excess ammonia. They were used without characterisation. Using these compounds in reactions with $HfCl_4$, Na_3As yielded a mixture of HfAs and $HfAs_2$, similar to the product from the conventionally produced reagent, Eqn. 65. Reactions with Na_4As yielded mostly HfAs and a trace of $HfAs_2$, Eqn. 64, whereas Na_2As yielded $HfAs_2$ and a trace of HfAs, Eqn. 66. The Na_4As reactions self- initiated when grinding together the reaction mixtures. The Na_3As reaction mixtures normally required heating but could be caused to initiate by pressing a small piece of sodium metal into the mixture. Thus the self- initiation with Na_4As could be due to some free sodium.

$$HfCl_4 + Na_4As \rightarrow HfAs + 4NaCl \qquad \text{-Eqn.64}$$

$$HfCl_4 + {}^4/_3Na_3As \rightarrow {}^2/_3HfAs + {}^1/_3HfAs_2 + 4NaCl \qquad \text{-Eqn.65}$$

$$HfCl_4 + 2Na_2As \rightarrow HfAs_2 + 4NaCl \qquad \text{-Eqn.66}$$

The effect of dilution with LiCl on the self- initiation of the reaction of $MoCl_5$ with Na_3As was very similar to that with Na_3P. On a scale of 200mg $MoCl_5$, undiluted reactions initiated during mixing, 160mg or 320mg of LiCl caused initation to be delayed until grinding and gentle heating was needed when 480mg of LiCl was added. These reactions yielded too many phases to draw other conclusions. Reactions with $NbCl_5$ initiated in the same way for each degree of dilution. The undiluted reaction yielded NbAs and a little $NbAs_2$. With 160mg added LiCl, the amount of $NbAs_2$ increased and a little As metal was observed. With 320mg and 480mg of diluent the amount of $NbAs_2$ and As continued to increase relative to the amount of NbAs. The amount of arsenic in the products was, therefore, seen to increase with increasing dilution and lower reaction temperature.

Reactions of manganese dichloride with Na_3As produced MnAs and some manganese metal. A reaction with MnF_2 on the same scale yielded MnAs and some arsenic. The reaction with MnI_2 produced MnAs, As and unidentified phases. The products from the $MnCl_2$ reaction are as expected from the reagents, Eqn. 67. The products from MnF_2 can be explained either from some MnF_2 not reacting or some manganese metal being co- produced, although neither was observed in the products.

$$MnCl_2 + {}^2/_3Na_3As \rightarrow {}^2/_3MnAs + {}^1/_3Mn + 2NaCl \qquad \text{-Eqn.67}$$

4.5 Reactions of Sodium Antimonide and Bismuthide.

The reactions between sodium antimonide and metal chlorides yielded the products listed in Table 17. The experimental methods were similar to those used for reactions of sodium arsenide. Reactions which self initiated were less voracious, they tended to emit yellow- red light rather than white- yellow. The products were generally more pnictogen rich than the arsenides. This could be due to the greater metallic character of the antimonides, causing greater thermal stability in the pnictogen rich phases. Some reactions are represented in ideallised form in Eqn. 68- 76. The reactions with $TiCl_3$, $NbCl_5$, $FeCl_3$ (Eqn. 73), $CoCl_2$ (Eqn. 74), $NiCl_2$ and $ZnCl_2$ (Eqn. 76) only balance if transition metal or a transition metal rich phase is present in the products

although these were not observed. Reactions with $MoCl_3$, WCl_4, $ZnCl_2$ and $HgCl_2$ were found to yield elements either exclusively or as a component of the products.

Table 17. Products of reactions of metal chlorides with sodium antimonide.

Reagent	Initiation	Product	System, space group[81,103]
YCl_3	800°C	YSb	Cubic Fm3m
$LaCl_3$	800°C	LaSb	Cubic Fm3m
$TiCl_3$	500°C	$TiSb_2$	Tetragonal I4/mcm
		TiSb	Hexagonal $P6_3/mmc$
VCl_3	500°C	VSb_2	Tetragonal I4/mcm
		(V_3Sb_2)	Hexagonal $P6_3/mmc$
$NbCl_5$	r.t.	$NbSb_2$	Monoclinic C2/m
$TaCl_5$	r.t.	$TaSb_2$	Monoclinic C2/m
		(Ta_5Sb_4)	Tetragonal I4/m
$MoCl_3$	500°C	Mo	Cubic Im3m
		Mo_3Sb_7	Cubic Im3m
WCl_4	r.t.	W	Cubic Im3m
		Sb	Hexagonal R-3m
$FeCl_3$	r.t.	$FeSb_2$	Orthorhombic Pnnm
		(FeSb)	Hexagonal $P6_3/mmc$
		(Sb)	Hexagonal R-3m
$CoCl_2$	500°C	CoSb	Hexagonal $P6_3/mmc$
		$(CoSb_2)$	Monoclinic $C2_1/c$
$NiCl_2$	500°C	NiSb	Hexagonal $P6_3/mmc$
		$NiSb_2$	Orthorhombic Pnnm
K_2PtCl_4	500°C	PtSb	Hexagonal $P6_3/mmc$
		Pt_3Sb_2	Orthorhombic
		(Pt)	Cubic Fm3m
$ZnCl_2$	500°C	Zn_4Sb_3	Hexagonal
		Sb	Hexagonal R-3m
$HgCl_2$	r.t.	Hg	Observed droplets
		Sb	Hexagonal R-3m

r.t. Initiated on mixing or grinding.
Structural data are listed in Appendix 3.

$$YCl_3 + Na_3Sb \rightarrow YSb + 3NaCl \qquad \text{-Eqn.68}$$

$$VCl_3 + Na_3Sb \rightarrow {}^1/_4VSb_2 + {}^1/_4V_3Sb_2 + 3NaCl \qquad \text{-Eqn.69}$$

$$TaCl_5 + {}^5/_3Na_3Sb \rightarrow {}^{13}/_{18}TaSb_2 + {}^1/_{18}Ta_5Sb_4 + 5NaCl \quad \text{-Eqn.70}$$

$$MoCl_3 + Na_3Sb \rightarrow {}^4/_7Mo + {}^1/_7Mo_3Sb_7 + 3NaCl \quad \text{-Eqn.71}$$

$$WCl_4 + {}^4/_3Na_3Sb \rightarrow W + {}^4/_3Sb + 4NaCl \quad \text{-Eqn.72}$$

$$FeCl_3 + Na_3Sb \rightarrow xFeSb_2 + yFeSb + zSb + (1\text{-}x\text{-}y)Fe + 3NaCl \quad (2x + y + z = 1) \quad \text{-Eqn.73}$$

$$CoCl_2 + {}^2/_3Na_3Sb \rightarrow xCoSb + yCoSb_2 + (1\text{-}x\text{-}y)Co + 2NaCl \quad (x + 2y = {}^2/_3) \quad \text{-Eqn.74}$$

$$K_2PtCl_4 + {}^2/_3Na_3Sb \rightarrow {}^x/_3Pt_3Sb_2 + {}^{2(1-x)}/_3PtSb + {}^{(1-x)}/_3Pt + 2KCl + 2NaCl \quad \text{-Eqn.75}$$

$$ZnCl_2 + {}^2/_3Na_3Sb \rightarrow xZn_4Sb_3 + ({}^2/_3\text{-}3x)Sb + (1\text{-}4x)Zn + 2NaCl \quad \text{-Eqn.76}$$

Reactions with sodium bismuthide were found to yield the metal and bismuth as the major products. Other phases could not generally be identified. PtBi was formed, in addition to Pt and Bi metals, from the reaction of K_2PtCl_4 with Na_3Bi. YBi and LaBi were formed, with the metals, using YCl_3 and $LaCl_3$ but decomposed when washed with rigourously distilled and degassed methanol under dry argon. With $TiCl_3$ or $ZrCl_4$ with Na_3Bi the main phase observed was bismuth metal. The voracity of reactions which self initiated was lower still than those of sodium antimonide, mixtures glowed red. To be useful for bismuthide synthesis, the products from this method would need a period of sintering to combine the elements.

4.6 Reactions of Titanium and Vanadium Tetrachlorides.

As was described in section 2.6, these metal chlorides are liquids at room temperature and the reactions need to be carried out under different conditions. Reactions were self initiating and performed in Schlenk tubes under flowing argon. The liquid metal tetrachloride was first added to the tube followed by the solid sodium pnictide. The sodium pnictides (Na_3Pn; Pn= P, As, $P_{0.5}As_{0.5}$, Sb, Bi) were prepared as previously described, except that for $Na_3P_{0.5}As_{0.5}$ all three elements were mixed together. Reactions always initiated on or just after mixing. Voracity of reactions visibly decreased from phosphide to bismuthide as with the solid state reactions. The products from these reactions are listed in Table 18.

Table 18. Products of reactions of titanium and vanadium tetrachlorides with sodium pnictides.

Reagents	Phase Detected by XRD	System, space group[81,131]
$TiCl_4 + Na_3P$	TiP	Hexagonal $P6_3/mmc$
$TiCl_3 + VCl_4 + Na_3P$	$Ti_{0.5}V_{0.5}P$	Hexagonal $P6_3/mmc$
$VCl_4 + Na_3P$	VP	Hexagonal $P6_3/mmc$
$TiCl_4 + Na_3As$	TiAs	Hexagonal $P6_3/mmc$
$3TiCl_4 + 1VCl_4 + Na_3As$	$Ti_{0.75}V_{0.25}As$[a]	Hexagonal $P6_3/mmc$
$TiCl_4 + VCl_4 + Na_3As$	$Ti_{0.5}V_{0.5}As$[a]	Hexagonal $P6_3/mmc$
$1TiCl_4 + 3VCl_4 + Na_3As$	$Ti_{0.25}V_{0.75}As$[a]	Orthorhombic Pnma
$VCl_4 + Na_3As$	VAs	Orthorhombic Pnma
$TiCl_4 + Na_3P_{0.5}As_{0.5}$	$TiAs_{0.5}P_{0.5}$	Hexagonal $P6_3/mmc$
$TiCl_4 + Na_3Sb$	Sb	Hexagonal R-3m
	$TiSb_2$	Tetragonal I4/mcm
	(TiSb)	Hexagonal $P6_3/mmc$
$VCl_4 + Na_3Sb$	Sb	Hexagonal R-3m
	VSb_2	Tetragonal I4/mcm
$TiCl_4 + Na_3Bi$	Bi	Hexagonal R-3m
$VCl_4 + Na_3Bi$	Bi	Hexagonal R-3m
	(V)	Cubic Im3m

[a] Ref. 132. Structural data are listed in Appendix 4.

Reactions with Na_3P, Na_3As and $Na_3P_{0.5}As_{0.5}$ yielded binary pnictides of formula MPn or ternary pnictides $Ti_xV_{1-x}Pn$ ($0 < x < 1$) or $TiP_{0.5}As_{0.5}$, Eqn. 77- 79. For $Ti_xV_{1-x}As$, compounds were made with x= 0, 0.25, 0.5, 0.75, 1, Fig. 25. Lattice parameters closely matched literature[131,132] values (Appendix 4). For $Ti_{0.75}V_{0.25}As$ the pattern was weak and the lattice parameters determined in this study were compared with values determined from the literature[132] assuming a linear Vegard's law[104] relationship between lattice parameter and composition for the range between x= 0.6 and 0.8. The previous work[132] describes this composition range as a "nonequilibrium" region and the powder patterns as made up of "fairly sharp and rather diffuse" reflections. Such nonequilibrium compositions may represent a nonuniform distribution of Ti and V in the MnP- type lattice.

$$TiCl_4 + {}^4/_3Na_3P \rightarrow TiP + {}^1/_3P + 4NaCl \qquad \Delta H_r^\circ = -998 \text{ kJ mol}^{-1} \qquad \text{-Eqn.77}$$

$$TiCl_4 + {}^4/_3Na_3As \rightarrow TiAs + {}^1/_3As + 4NaCl \qquad \Delta H_r^\circ = -715 \text{ kJ mol}^{-1} \qquad \text{-Eqn.78}$$

$$TiCl_4 + {}^4/_3Na_3P_{0.5}As_{0.5} \rightarrow TiP_{0.5}As_{0.5} + {}^1/_6P + {}^1/_6As + 4NaCl \qquad \text{-Eqn.79}$$

Reactions of MCl_4 (M= Ti, V) with Na_3Sb yielded Sb and MSb_2 plus TiSb in the titanium case. The main phase observed with Na_3Bi was bismuth metal. This is the same trend as was observed with the solid state reactions, where the tendency to yield the elements increases toward the heavier pnictogens.

Fig. 25. X- ray powder diffraction patterns of (a) TiAs, (b) $Ti_{0.75}V_{0.25}As$, (c) $Ti_{0.5}V_{0.5}As$, (d) $Ti_{0.25}V_{0.75}As$ and (e) VAs produced from $TiCl_4$, VCl_4 and Na_3As.

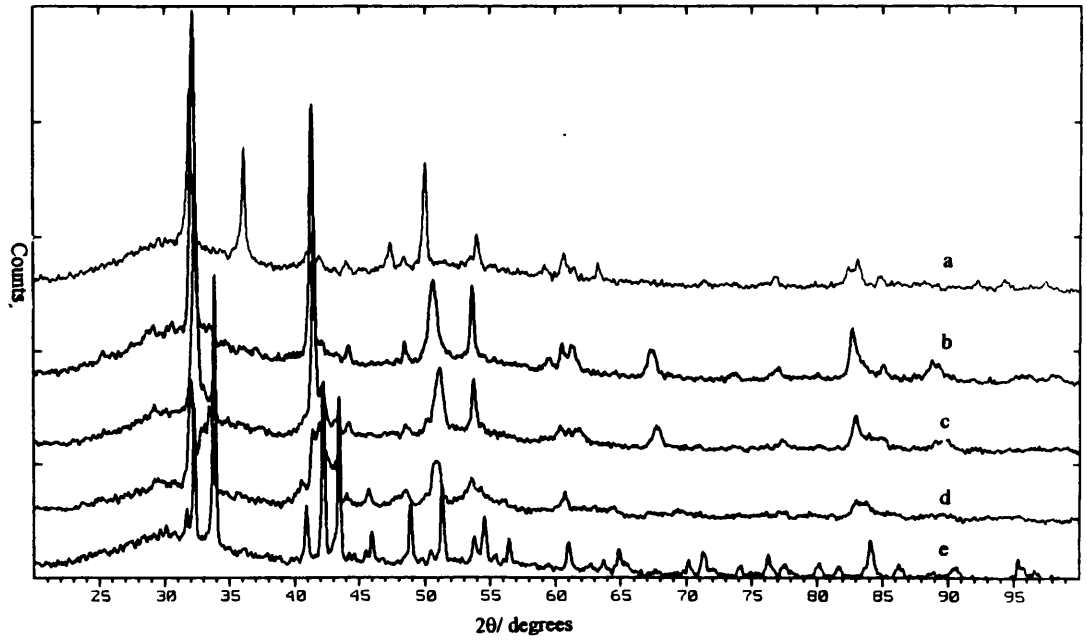

4.7 Summary and Mechanistic Discussion.

Sodium phosphide is a useful source of phosphide for SSM reactions. Many reactions, generally those of the more volatile chlorides, initiate on mixing or grinding together the reagents. Sodium arsenide is an efficient reagent for the synthesis of metal arsenides, although the tendency to produce more than one phase is greater than with the phosphides. Many reactions co- produced phosphorus or arsenic, but this was sublimed out during reaction and no free pnictogen was observed in the products. Reactions with sodium antimonide and bismuthide were progressively lower in voracity. The tendency to observe free pnictogen or transition metal in the products increased toward the heavier pnictides. The solid- liquid metathesis reactions were again shown to be very useful for the synthesis of ternary compounds. These

compounds are normally produced from elemental combination reactions. The obvious advantage of SSM reactions is the ease of preparation since elemental combinations often require long periods of heating at high temperature to achieve complete conversion. The particle sizes from the SSM reactions are also smaller and subject to some control.

Sections 2.8 and 3.4 contain discussion of the mechanistic possibilities in SSM routes to nitrides. For reactions with Group 2 nitrides, the evidence points strongly toward influence of an ionic mechanism whereas with Li_3N and NaN_3 an ionic or elemental process is possible. The ionic mechanism is supported by the lack of any elemental metal in the products, except where the nitride is thermally unstable.

The reactions of Na_3Pn (Pn= P, As, Sb, Bi) with transition metal chlorides show an increasing tendency to yield elemental metal and pnictogen as products on progressing from P→As→Sb→Bi. Reactions forming metal pnictides will always be more exothermic than those which yield the elements if ΔH_f° of the metal pnictide is negative. This is illustrated in Eqn. 78, 80- 82 for reactions of $TiCl_4$ with Na_3As and Na_3Sb.

$$TiCl_4 + {}^4/_3Na_3As \rightarrow TiAs + {}^1/_3As + 4NaCl \qquad \Delta H_r^\circ = -715 \text{ kJ mol}^{-1} \quad \text{(Eqn.78)}$$

$$TiCl_4 + {}^4/_3Na_3Sb \rightarrow TiSb + {}^1/_3Sb + 4NaCl \qquad \Delta H_r^\circ = -847 \text{ kJ mol}^{-1} \quad \text{-Eqn.80}$$

$$TiCl_4 + {}^4/_3Na_3As \rightarrow Ti + {}^4/_3As + 4NaCl \qquad \Delta H_r^\circ = -548 \text{ kJ mol}^{-1} \quad \text{-Eqn.81}$$

$$TiCl_4 + {}^4/_3Na_3Sb \rightarrow Ti + {}^4/_3Sb + 4NaCl \qquad \Delta H_r^\circ = -575 \text{ kJ mol}^{-1} \quad \text{-Eqn.82}$$

Factors other than thermodynamic ones must apply, since TiSb formation would be more favourable than TiAs formation. The reactions actually yielded TiAs and a mixture of Sb, $TiSb_2$ and a trace of TiSb. Thermodynamic data for $TiSb_2$ were unavailable. The metallic character of the sodium pnictides may be expected to increase with the heavier pnictogens. They also exhibit some ionic behaviour. They readily hydrolyse with evolution of phosphine, arsine or stibine.[117] It has also been suggested that Na_3Sb and Na_3Bi form dilute solutions in molten sodium halides, with formation of Sb^{3-} and Bi^{3-} anions.[133] The solubility in the Na_3Bi case, however, was very small (2 mol% at 600°C compared with 11 mol% of Na_3Sb).

If, for the sake of argument, one accepts that sodium phosphide is the most saltlike and sodium bismuthide the most metallic of the reagents, this fits the results. Since

the reactions self- propagate, the most likely first step is sodium chloride formation as this is responsible for such a large fraction of the heat produced. A more ionic Na_3Pn could be expected to yield pnictide ions from this step whereas a more metallic Na_3Pn could produce the elemental pnictogen. The elemental route is more likely to yield products containing the elements. For the ionic route to produce elemental products, a metal pnictide product would have to thermally decompose back to the elements. This becomes increasingly unlikely for the heavier pnictogens as the pnictogen- rich compounds are effectively alloys and will become increasingly thermally stable. Thus, increasing influence of a redox recombination type mechanism and decreasing influence of the ionic from P→As→Sb→Bi explains the observed products very well. The premise of sodium phosphide being the most saltlike of these sodium pnictides is supported by examination of the electronegativities of the pnictogens. The Pauling electronegativities (on a scale where for F, χ_p= 3.98 and for Cs, χ_p= 0.79) are χ_p= 3.04, 2.19, 2.18, 2.05 and 2.02 for N, P, As, Sb and Bi respectively.[133a] Thus Bi is considerably less electronegative than P and hence more likely to form an intermetallic sodium pnictide.

4.8 Experimental.

Reagents, solvents and instrumentation have been previosly described. In addition, solid state MAS- ^{31}P- NMR spectra were obtained by Dr. Apperly of the EPSRC service at Durham university at a frequency of 121.4 MHz, 100 kHz spectral width, 600 sec. relaxation delay, 45 degrees pulse width and 9840 Hz spin rate referenced to H_3PO_4.

Synthesis of Sodium Pnictides.

Sodium pnictides (Na_3Pn) were synthesised by direct, high temperature combination of the elements. Sodium metal was cut into small pieces under an inert atmosphere, mixed with red phosphorus or arsenic, antimony or bismuth metal and sealed under vacuum into a thick walled Pyrex ampoule. This was placed into a furnace, heated slowly to 500°C and maintained at this temperature for four hours. The ampoule was removed, broken open in an inert atmosphere and the contents ground with an agate pestle and mortar. These were then sealed into another ampoule, heated to 500°C for ten hours and reground before use. Purity was checked by XRD and EDXA.

Sodium arsenides of various compositions (Na_xAs; x= 2, 3, 4) were made by combination in liquid ammonia. A thick walled Pyrex tube, sealed with a sidearm by a

Teflon "Young's" tap, was flame dried and connected to a Schlenk line. Ammonia was condensed at -78°C, under flowing argon, until ~15 cm^3 of liquid ammonia was contained in the tube. Powdered arsenic metal was added with stirring followed by sodium metal which had been cut into pieces under dry diethyl ether. The tube was sealed and allowed to warm slowly to room temperature. Stirring was continued for a further twelve hours. The mixture was cooled to -78°C, the tap opened and the ammonia allowed to evaporate. The product was heated to 200°C to drive off any remaining ammonia and stored in an inert atmosphere.

Caution! The sodium pnictides, especially in finely divided forms, are spontaneously flammable and extremely toxic. The maximum pressure of ammonia should be calculated to ensure apparatus is sufficiently strong and apparatus should be sheilded in case of pressure explosion.

Reactions with Sodium Pnictides.

Reaction mixtures were made up under an inert atmosphere, such that the ratio of sodium to pnictide was 1:1, and ground together with a pestle and mortar. Some reactions initiated on mixing or grinding. Those which did not were placed into a thick walled Pyrex ampoule, sealed under vacuum, heated to 500°C (800°C in quartz for YCl_3 and $LaCl_3$) and allowed to cool. Products from either mode of initiation were ground under an inert atmosphere before washing.

Microanalysis:

MoP (from $MoCl_3$)	%P= 27.22 (calcd. 24.41)
Ni_2P	%P= 22.29 (calcd. 20.88)
Zn_3P_2	%P= 26.71 (calcd. 24.00)

5. Reactions of Metal Chlorides with Mg_2Si.

Use of a Group 1 or 2 silicide reagent in solid state metathesis reactions aimed at producing metal silicides from the chlorides results in a high reaction exothermicity with an easily removable salt by- product. Magnesium silicide, Mg_2Si, is formed from the elements at 650°C to 1200°C and is readily available commercially. It is only a weak conductor of electricity and reacts with dilute acids to evolve monosilane (SiH_4). This indicates some salt- like character although it is by no means an ionic material.

This chapter will discuss the reactions of magnesium silicide with transition metal and rare earth chlorides, carried out by heating the reagent mixtures in sealed ampoule inside a furnace. This study was undertaken to determine the scope of SSM reactions. Plans to form analogous metal carbides were thwarted by a lack of suitable precursors such as Mg_2C, since acetylides are the only compounds which usually form between carbon and Group 1 or 2 metals. A filament initiated reaction to produce molybdenum disilicide has previously been reported,[75] Eqn. 83

$$MoCl_5 + {}^5/_4Mg_2Si \rightarrow {}^5/_8MoSi_2 + {}^3/_8Mo + {}^5/_2MgCl_2 \qquad \text{-Eqn.83}$$

5.1 Properties of Silicides.

Bonding and formulae of metal silicides cannot be rationalised by the application of valency rules and bonding varies from essentially metallic to ionic and covalent.[122,134,135] Observed stoichiometries include M_6Si, M_5Si, M_4Si, $M_{15}Si_4$, M_3Si, M_5Si_2, M_2Si, M_5Si_3, M_3Si_2, MSi, M_2Si_3, MSi_2, MSi_3 and MSi_6,[122] the greatest range in Groups 4- 10 and uranium. Silicides are known for all Group 1- 10 elements, except beryllium, and some other metals. Metals which don't form silicides usually form simple eutectic mixtures with silicon, except Hg, Tl, Pb and Bi which are completely immiscible with molten silicon.[122] Silicides are normally prepared by combination of the elements, or by co- reduction of SiO_2 and a metal oxide with C or Al, in an arc furnace.[122] These processes require extreme temperatures, around 1600°C, to be maintained for some time and therefore are very costly in energy and equipment.

Common characteristics of metal silicides include high thermal stability, chemical inertness, hardness and high thermal and electrical conductivity.[136] Some show great promise as interface diffusion barriers[137] and several are significant in very large scale integrated (VLSI) circuit technology.[138] Molybdenum disilicide forms a glossy film of oxide at 1700°C which prohibits further oxidation and thus it may be used for furnace heating elements.[134] Ternary molybdenum- tungsten disilicides are extremely

oxidation resistant, $Mo_{0.7}W_{0.3}Si_2$ shows no weight change after four hours at 1500°C in air.[134] Ferrosilicon, FeSi, is used for the deoxidising of low carbon steel.

As with the phosphides, metal- rich silicides tend to have isolated Si atoms, with increasing catenation toward the silicon- rich compounds. The metal- rich compounds occur with either metallic structures which are good electrical conductors (Cu_5Si, M_3Si; M= V, Cr, Mo, Mn, Fe) or with more polar, non- metallic structures which are poorly conducting (M_2Si; M= Mg, Ca, Ru, Ni, Rh, Ge, Sn).[122] The more silicon rich compounds commonly contain Si_2 and Si_4 units, chains, layers and three dimensional networks of silicon atoms. Transition metal silicides are normally inert to aqueous reagents except HF, but are attacked by molten KOH or, at red heat, by F_2 or Cl_2.[122] Group 1 and 2 silicides are more polar and are attacked by water or dilute acids.

5.2 Reactions of Magnesium Silicide.

Reactions of magnesium silicide with anhydrous metal chlorides were made up on a scale of 100mg Mg_2Si, in an inert atmosphere, with a 1:2 ratio of magnesium to chloride. The mixtures were sealed under vacuum into a quartz ampoule and heated to 850°C for ten hours. Products were then ground and purified with methanol or water.

The metal oxidation state governs the ratio of metal: silicon from which the product is formed since reaction mixtures need to be made up such that all the magnesium and chlorine will be removed as the salt by- product $MgCl_2$. For example, if a metal trichloride is used then a 4:3 ratio of metal: silicon will be available to form a silicide product, Eqn. 84. Table 19 lists the ratios which would be expected from the reagents compared with the known silicide phases if all the metal and silicon was incorporated into the metal silicide product, i.e. if an ionic process occurs with no redox chemistry.

$$MCl_3 + {}^3/_4Mg_2Si \rightarrow {}^1/_4M_4Si_3 + {}^3/_2MgCl_2 \qquad \text{-Eqn.84}$$

The products obtained from reactions of metal chlorides with magnesium silicide are listed in Table 20. They could be explained by reference to published phase diagrams, many of which are included in a recent review.[139]

Reactions of rare earth chlorides and titanium trichloride with magnesium silicide would, if all the metal and silicon combined into one discrete silicide phase, form a material of composition M_4Si_3 (i.e. $MCl_3 \Rightarrow 4M{:}3Si$). However, from Table 19 it can be observed that no phases of this composition are known. Only MSi_2 and M_5Si_3 were observed as products. This is of no surprise for the rare earths since these are the only two silicides which normally form. Considering the composition of the mixture, Eqn. 84 balances if MSi_2 and M_5Si_3 are produced with M_5Si_3 as the major product. We actually observe MSi_2 as the major phase and with yttrium observe no M_5Si_3. For $TiCl_3$, however, Ti_5Si_4 would be expected to be the main product as it most closely matches the composition of the metal- silicon mixture from the reagents, Fig. 26, and Ti_5Si_4 does exist. $TiSi_2$ was the major phase with less Ti_5Si_3 whereas Ti_5Si_3 needs to be the major product to balance Eqn 85. One likely factor in this is the greater heat of formation of $TiSi_2$ (ΔH_f°= -579.5 kJ mol^{-1}) compared with that of Ti_5Si_3 (ΔH_f°= -133.9 kJ mol^{-1}). The reactions of $ZrCl_4$ and $HfCl_4$ ($MCl_4 \Rightarrow 1M{:}1Si$) would be expected to produce MSi but actually disproportionate to MSi_2 and M_2Si, Eqn. 86.

Table 19. Product composition predicted from ratio of metal: silicon in reagent mixture (of MCl_n with Mg_2Si) and of observed silicide product.

Reagent metal chloride	Ratio of metal : silicon	Known silicide phases
	3 : 1	M_3Si
	2.5 : 1	M_5Si_2
MCl_2	2 : 1	M_2Si
	1.67 : 1	M_5Si_3
	1.5 : 1	M_3Si_2
MCl_3	1.33 : 1	No known phase
	1.25 : 1	M_5Si_4
MCl_4	1 : 1	MSi
MCl_5	1 : 1.25	No known phase
	1 : 1.5	M_2Si_3
	1 : 2	MSi_2
	1 : 3	MSi_3

$$MCl_3 + {}^3/_4Mg_2Si \rightarrow {}^3/_{28}MSi_2 + {}^{25}/_{28}M_5Si_3 + {}^3/_2MgCl_2 \qquad \text{-Eqn.85}$$

(M= Y, Gd, Dy, Ho, Ti)

Table 20. Products of reactions of metal chlorides with magnesium silicide.

Reagent	Product	System, space group[81,103]
YCl_3	YSi_2	Hexagonal P6/mmm
$GdCl_3$	$GdSi_2$	Orthorhombic Imma
	(Gd_5Si_3)	Hexagonal $P6_3/mcm$
$DyCl_3$	$DySi_2$	Tetragonal $I4_1/amd$
	(Dy_5Si_3)	Hexagonal $P6_3/mcm$
$HoCl_3$	$HoSi_2$	Hexagonal P6/mmm
	(Ho_5Si_3)	Hexagonal $P6_3/mcm$
$TiCl_3$	$TiSi_2$	Orthorhombic Fddd
	Ti_5Si_3	Hexagonal $P6_3/mcm$
$ZrCl_4$	$ZrSi_2$	Orthorhombic Cmcm
	Zr_2Si	Tetragonal I4/mcm
$HfCl_4$	$HfSi_2$	Orthorhombic Cmcm
	Hf_2Si	Tetragonal I4/mcm
$NbCl_5$	$NbSi_2$	Tetragonal $P6_222$
	Nb_5Si_3	Tetragonal I4/mcm
$TaCl_5$	Ta_5Si_3	Tetragonal I4/mcm
$MoCl_5$	Mo_5Si_3	Tetragonal I4/mcm
	$MoSi_2$	Tetragonal I4/mmm
WCl_4	W	Cubic Im3m
	WSi_2	Tetragonal I4/mmm
	W_5Si_3	Tetragonal I4/mcm
$FeCl_3$	FeSi	Cubic $P2_13$
$NiCl_2$	Ni_5Si_2	Hexagonal P321
	Ni	Cubic Fm3m
	Si	Cubic Fd3m
K_2PtCl_4	Pt	Cubic Fm3m
	Pt_2Si	Tetragonal I4/mmm
	Pt_3Si	Monoclinic F2/m
$ZnCl_2$	Zn	Hexagonal $P6_3/mmc$
	Si	Cubic Fd3m

Structural data are listed in Appendix 5.

$$MCl_4 + Mg_2Si \rightarrow {}^1/_3MSi_2 + {}^1/_3M_2Si + 2MgCl_2 \qquad \text{-Eqn.86}$$

(M= Zr, Hf)

The amounts of each silicide phase in this discussion were estimated from X-ray diffraction line intensities. This is obviously dangerous since it does not take account of X-ray absorption or the presence of amorphous phases. Linewidths were checked to be about equal where more than one phase was present, however, which means that average crystallite sizes would also similar and reduces the inaccuracy from amorphous material.

The reactions of $NbCl_5$, $TaCl_5$ and $MoCl_5$ with Mg_2Si ($MCl_5 \Rightarrow 4M{:}5Si$) would be expected to behave as described in Eqn. 87. According to the phase diagrams,[139] the MSi_2 and M_5Si_3 phases are the closest compositions to the reagent mix since none of the intermediate compositions form for these metals. The $NbCl_5$ reactions yielded MSi_2 as the major phase with M_5Si_3, as expected. With tantalum, only Ta_5Si_3 was observed. With molybdenum, Mo_5Si_3 was the major phase with a lesser amount of $MoSi_2$. For these three metals, M_5Si_3 has a heat of formation about three times higher than that of MSi_2.

Fig. 26. Titanium- silicon phase diagram.[139] Arrow shows composition expected from the reagent mixture of $TiCl_3$ with $^3/_4Mg_2Si$.

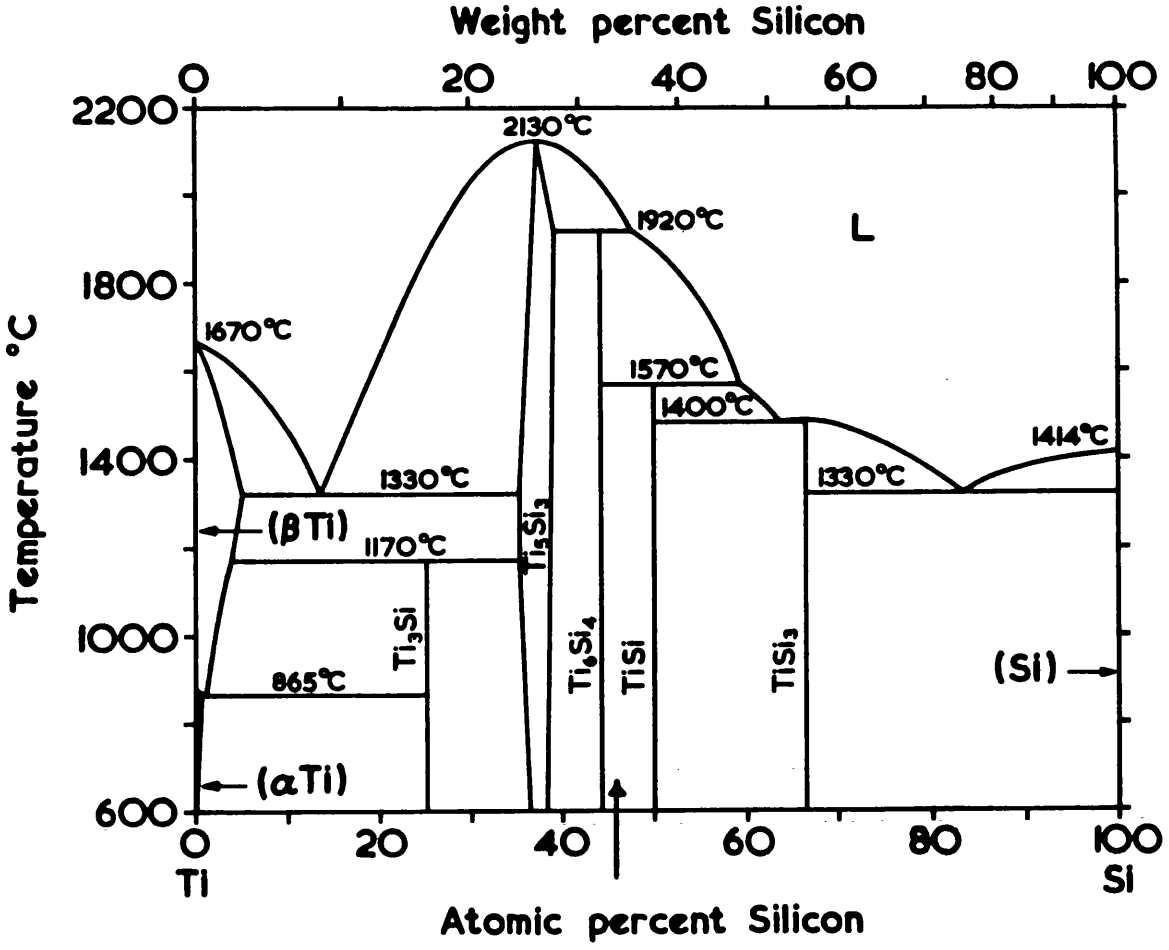

$$MCl_5 + {}^5/_4Mg_2Si \rightarrow {}^{13}/_{28}MSi_2 + {}^3/_{28}M_5Si_3 + {}^5/_2MgCl_2 \quad \text{-Eqn.87}$$
(M= Nb, Ta, Mo)

The reaction with WCl_4 ($MCl_4 \Rightarrow$ 1M:1Si) similarly produces the two phases, WSi_2 and W_5Si_3, Eqn. 88, which are either side of the reagent mixture composition in the phase diagram.[139] In addition, tungsten metal was observed. The reaction of $FeCl_3$ yielded FeSi. To balance Eqn. 89, some iron metal or an iron rich phase must also be produced although none was found in the products. This could be explained by some loss of iron to, or gain of silicon from, the ampoule walls (indeed the ampoules were damaged during reactions). The $NiCl_2$ reaction ($MCl_2 \Rightarrow$ 2M:1Si) would be expected to yield Ni_2Si but produces Ni_5Si_2, Ni and Si, Eqn. 90. The reaction of K_2PtCl_4 requires some silicon produced for Eqn. 91 to balance, although none was observed. The zinc reaction, Eqn. 92, produced the elements, unsurprising since no zinc silicides are known.[122]

$$WCl_4 + Mg_2Si \rightarrow xW + yWSi_2 + zW_5Si_3 + 2MgCl_2 \quad \text{-Eqn.88}$$

$$FeCl_3 + {}^3/_4Mg_2Si \rightarrow {}^3/_4FeSi + {}^1/_4Fe + {}^3/_2MgCl_2 \quad \Delta H_r^\circ = -563.0 \text{ kJ mol}^{-1} \quad \text{-Eqn.89}$$

$$NiCl_2 + {}^1/_2Mg_2Si \rightarrow xNi_5Si_2 + (1\text{-}5x)Ni + ({}^{1-4x}/_2)Si + MgCl_2 \quad \text{-Eqn.90}$$

$$K_2PtCl_4 + {}^1/_2Mg_2Si \rightarrow xPt + yPt_2Si + zPt_3Si + ({}^1/_2\text{-}2y\text{-}z)Si + MgCl_2 \quad \text{-Eqn.91}$$

$$ZnCl_2 + {}^1/_2Mg_2Si \rightarrow Zn + {}^1/_2Si + MgCl_2 \quad \Delta H_r^\circ = -186.7 \text{ kJ mol}^{-1} \quad \text{-Eqn.92}$$

Some reactions require loss of silicon or transition metal to balance equations. For the reactions to produce FeSi, for example, some loss of iron is needed to explain the product. This could occur by combination with the area of ampoule wall in contact with the mixture. No iron was found by XRD in the products or by EDXA on the other inner faces of the ampoule. SEM/ EDXA studies, Fig. 27 and 28, generally showed fused, angular particles of product with even metal: silicon ratios. The zinc/ silicon product was found to contain spheres of material, Fig. 29, with a strong silicon peak in the EDXA and a weak zinc one. This is consistent with silicon coating spheres of zinc.

The reactions with magnesium silicide were exothermic to variable degrees. Heats of reaction, Eqn. 89 and 92- 96, varied from about -200 to -1100 kJ mol^{-1}. These were calculated assuming the amounts of products which would be dictated by stoichiometry of the reaction mixture. They may be higher, for example the titanium

reaction yielded $TiSi_2$ as the major product and it's heat of formation is greater than that of Ti_5Si_3. The major product of this reaction would have been Ti_5Si_3 if Eqn. 93 was correct, so the reaction will in fact be more exothermic than stated in the equation.

Fig. 27. Scanning electron micrograph of the product of $HfCl_4$ and Mg_2Si.

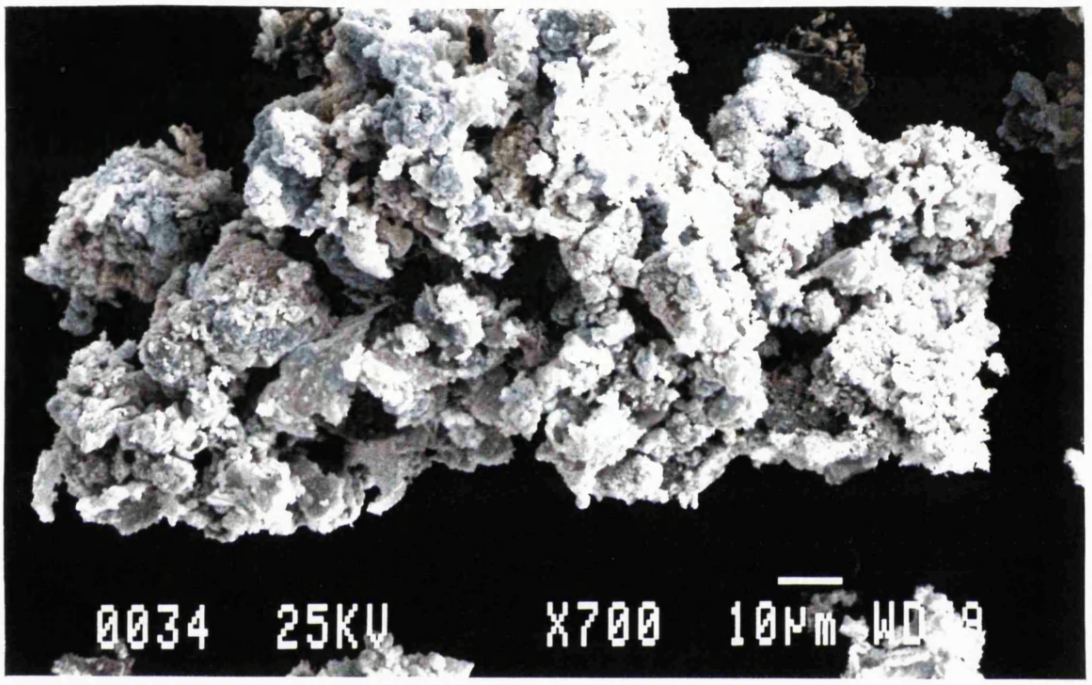

Fig. 28. EDXA spectrum of YSi_2 produced from YCl_3 and Mg_2Si.

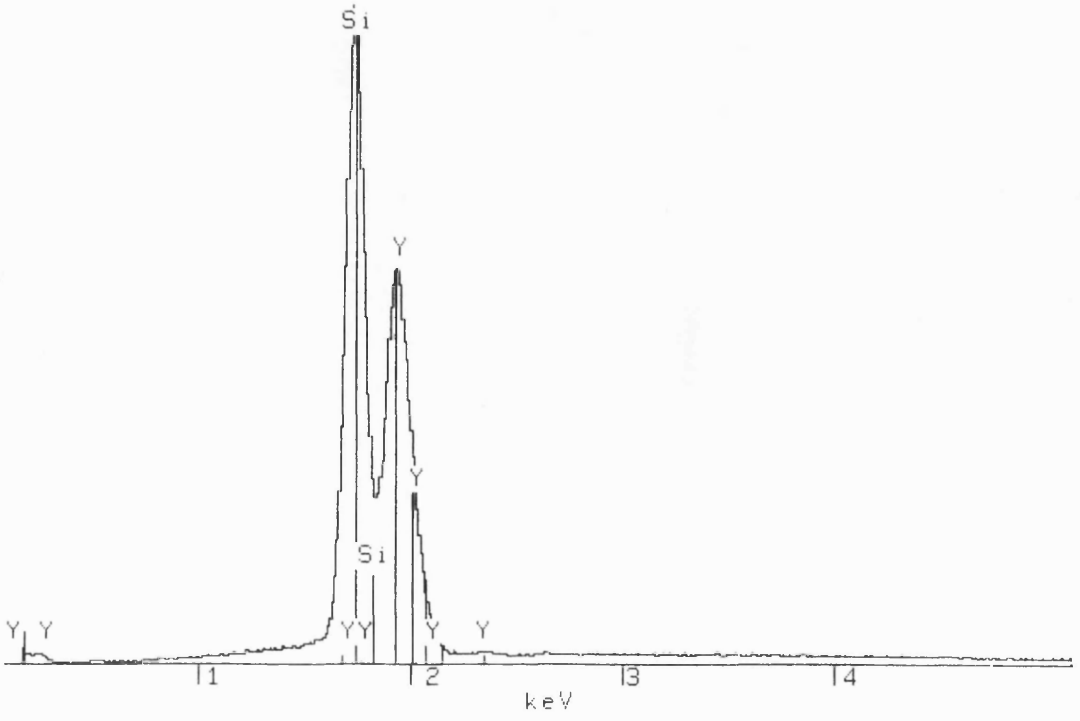

$$TiCl_3 + {}^3/_4Mg_2Si \rightarrow {}^3/_{28}TiSi_2 + {}^{25}/_{28}Ti_5Si_3 + {}^3/_2MgCl_2$$

$\Delta H_r° = -362.8$ kJ mol^{-1} -Eqn.93

$$MCl_5 + {}^5/_4Mg_2Si \rightarrow {}^{13}/_{28}MSi_2 + {}^3/_{28}M_5Si_3 + {}^5/_2MgCl_2$$

M= Nb; $\Delta H_r° = -819.6$ kJ mol^{-1} -Eqn.94

M= Ta; $\Delta H_r° = -736.8$ kJ mol^{-1} -Eqn.95

M= Mo; $\Delta H_r° = -1072.2$ kJ mol^{-1} -Eqn.96

Fig. 29. Scanning electron micrograph the Zn/ Si product from $ZnCl_2$ with Mg_2Si.

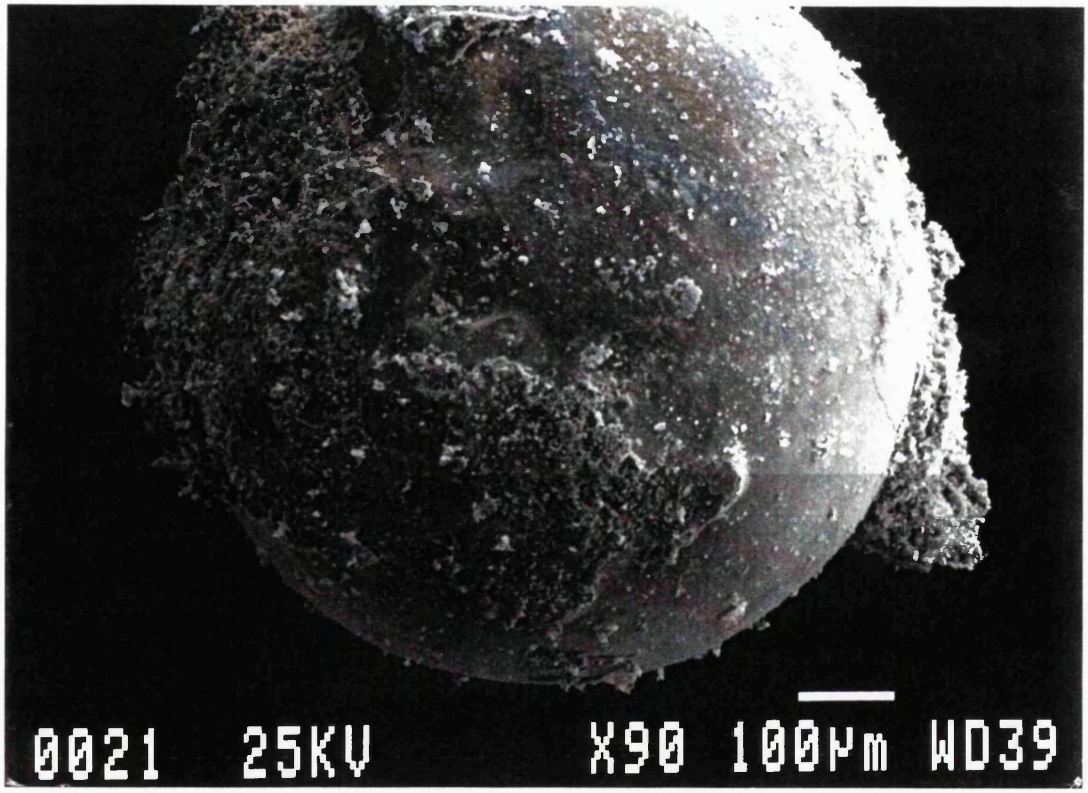

Applied reaction conditions were harsher than those generally employed in those systems discussed in previous chapters. These conditions were needed to produce the phases listed in Table 20. Shorter periods of heating yielded different products. Thermolysis of rare earth chlorides with magnesium silicide at 550°C for ten hours yielded mainly Mg_2Si and some $MgCl_2$ by XRD, indicating only partial reaction had occurred. Thermolysis of the same mixture at 850°C for three hours produced a mixture which was found to contain large amounts of elemental silicon, whilst ten hours heating at this temperature yielded the silicide phases listed in Table 20. Reactions of $HfCl_4$ or $NbCl_5$ with magnesium silicide at 500°C for ten hours yielded products which contained $MgCl_2$ and no other crystalline material. These may have contained mixtures of elements and/ or amorphous silicides. Reaction of $ZrCl_4$ with Mg_2Si at 850°C for ten minutes produced Zr_2Si and unidentified phases. Four hours reaction time produced Zr_2Si and a considerable amount of $ZrSi_2$ with little

unidentified crystalline material. After twenty- four hours the major phase was $ZrSi_2$ with only a little Zr_2Si observed. These observations may be explained by the slow, nucleation led formation of $ZrSi_2$ as has been observed when this phase is formed from the elements.[140] Loss of zirconium to the ampoule wall would be required to explain the decreasing amount of metal in the sample.

Another important finding is that the filament initiated reaction of $MoCl_5$ with Mg_2Si gives a different product than the thermally initiated reaction, as was found in Chapter 3 for the reactions of Mg_3N_2 and Ca_3N_2. This will need to be investigated with any other reactions of this nature carried out in the future.

5.3 Mechanistic Discussion.

To occur effectively, reactions of Mg_2Si with metal chlorides needed to be carried out at 850°C. At this temperature the metal chlorides (except $NiCl_2$) will be molten, vapourised or decomposed. Thus the solid state diffusion barrier is not an influential factor when a reaction temperature of 850°C is used.

The products from these reactions strongly indicate that a reductive recombination type mechanism is more influential than an ionic metathesis one. The first piece of evidence is the observation of elemental silicon in the rare earth reactions when shortened reaction times were employed. Secondly, there is a tendency for most reactions to disproportionate to two product phases. In most cases the products do reflect the amount of metal and silicon in the reagents, however not the phase one would expect from an ionic mechanism. For example, the reaction with $HfCl_4$, Eqn. 96 and 97, would initially produce HfSi, which is stable according to the phase diagram.[139] This phase would then have to undergo a further process to yield the observed products. There appears to be little or no energetic advantage in $HfSi_2$ and Hf_2Si, the phases observed, over HfSi (although heats of formation vary between sources[139]).

$$HfCl_4 + Mg_2Si \rightarrow Hf^{4+} + Si^{4-} + 2MgCl_2 \qquad \text{-Eqn.96}$$

$$Hf^{4+} + Si^{4-} \rightarrow HfSi \rightarrow {}^1/_3Hf_2Si + {}^1/_3HfSi_2 \qquad \text{-Eqn.97}$$

The ionic process requires the use of the Si^{4-} ion, which is unlikely. No quantitative supporting evidence for this statement was found to be available. Electron affinities[140a] only appear to be measured for the reduction of neutral atoms or

molecules and standard potential tables[133a] make no reference to the Si^{4-} ion. However, the Pauling electronegativity (χ_p= 1.90[133a]) of the neutral atom is the same as that of copper, which gives an indication of silicon's low tendency to form negative ions. Presumably if this ion did form it would be extremely reducing and would be likely to reduce any metal ions and lead into an elemental process anyway. The elemental route can, however, explain all the observed products. The phases produced are then governed by the rate at which phases nucleate from the finely divided metal and silicon in the molten magnesium chloride flux.

5.4 Experimental.

Reagents, solvents and instrumentation have previously been described. Magnesium silicide was purchased from Aldrich Chemical Co.

Reactions of magnesium silicide.

Magnesium silicide (100 mg) and anhydrous metal chloride (1:2 ratio of magnesium to chloride) were ground together under a nitrogen atmosphere and placed into a quartz ampoule (Pyrex melts at around 650°C) which was sealed under vacuum. This was placed into a furnace and heated to 850°C for ten hours (or as stated in text), after which time the solid was fused into a grey/ dark grey lump and some material had sublimed onto the walls of the ampoule. When cool, the ampoule was broken open and the fused solid thoroughly ground in an agate pestle and mortar. This crude product was purified by washing with methanol or water and characterised using XRD, SEM and semiquantitative EDXA.

6. Reactions of Transition Metal Chlorides with Li_2O.

This chapter will discuss synthesis of d- block metal oxides using lithium oxide. Reactions of lithium oxide with lanthanide chlorides carried out simultaneously in our laboratory have also been reported.[141] In addition, reactions of sodium and Group 2 oxides with metal chlorides have been used to prepare a number of binary and ternary oxides.[142,143]

6.1 Properties of Oxides.

Oxides dominate traditional and advanced ceramic science and the technological importance is massive. Their application as superconductors, catalysts, engineering materials and semiconductors has resulted in a huge amount of interest from a variety of scientific sectors. Oxides form with molecular structures, as chains, as layers and with three dimensional networks. Transition metal oxides almost entirely adopt three dimensional structures. The feasability of variable valency leads frequently to variable composition and non- stoichiometric behaviour.

The main oxides of Group 4 are the dioxides.[8] TiO_2 is by far the most important of these. The rutile form is the most common in nature and also the most useful, being the most widely used of all white pigments.[8] It finds utility in paints, in the paper industry as a coating and in rubber and plastics as a filler. It has an exceptionally high refractive index and is chemically inert, so can be used to make long lasting opaque films. Thus, it displaced "White lead", $2PbCO_3 \cdot Pb(OH)_2$, for paints which used to blacken with formation of PbS in industrial atmospheres and presented a toxic hazard. Titanium forms several other oxides, these are semiconductors at room temperature except Ti_4O_7 which is metallic.[8] The dioxides are the only stoichiometric oxide phases which form with zirconium or hafnium. ZrO_2 is unreactive and has a high melting point (2710°C) and low coefficient of thermal expansion. It is a useful refractory and used as a solid solution with CaO or MgO for crucibles and furnace cores. Zirconium dioxide may also be produced as fibres suitable for weaving. It can be expected to find increasing utility as a non- toxic insulator and for the filtration of toxic liquids.[8] Ternary oxides of Group 4 are of exceptional interest in electronics. Barium titanate

and PZT are the most widely used dielectric and ferroelectric materials in compact capacitors and transducers such as microphones and pick- ups.[8]

The Group 5 metals form oxides of composition M_2O_5, MO_2, V_2O_3 and MO (M= V, Nb, Ta).[8] V_2O_5 is a versatile catalyst. Most importantly it catalyses the oxidation of SO_2 to SO_3 in the contact process to produce sulfuric acid, replacing platinum which is expensive and much more prone to poisoning. It also catalyses the oxidation of many organic compounds by air or hydrogen peroxide and the hydrogen reduction of alkenes and aromatic compounds. The ternary oxides of niobium and tantalum with lithium, $LiNbO_3$ and $LiTaO_3$, are of interest for their non- linear optical properties.

The major phases of Group 6 oxides are MO_3, MO_2 (M= Cr, Mo, W) and Cr_2O_3.[8] Several intermediate phases also occur. CrO_3, "Chromic acid", has wide utility in organic chemistry as a strong oxidant. Chromium dioxide is ferromagnetic and is used to produce magnetic tapes with better resolution and high frequency response than those made from iron oxide.

Manganese forms the heptoxide Mn_2O_7, a green oil which explosively oxidises organic materials. Manganese dioxide is used[145] in steel production, in zinc- carbon batteries to prevent hydrogen formation at the carbon electrode, in bricks as a pigment and in glass as a decolouriser, where traces left behind give glass it s characteristic green tint. MnO_2 is used as an oxidant in hydroquinone preparation. Large quantities are used in the production of manganese ferrite, $MnFe_2O_4$.[8]

Iron forms three oxides, FeO, Fe_3O_4 and Fe_2O_3, all of which are subject to non-stoichiometry.[146] Haematite, α- Fe_2O_3, is used as a pigment, as a reagent in preparation of ferrites and rare earth/ iron garnets and for polishing gemstones.[8] γ- Fe_2O_3 is metastable and is the most widely used magnetic recording medium. Ruthenium and osmium form only dioxides and tetraoxides.[8] The tetraoxides are yellow, volatile molecular compounds with tetrahedral MO_4 units. OsO_4 is used to oxidise alkenes to *cis*- diols and as a biological stain. The combination of extreme toxicity and volatility make both tetraoxides particularly dangerous. The ternary iron

oxide materials, ferrites and garnets, are technologically important.[86] Ferrites are widely used in magnetic applications. Yttrium iron garnet is used as a microwave filter in radar.

In Groups 9 and 10, the range of oxides which may be produced is diminished since fewer oxidation states are available.[8] The pure, well characterised phases which have been produced are limited to CoO, Co_3O_4, NiO, Rh_2O_3, RhO_2, PdO, IrO_2 and PtO_2.[8] CoO reacts with silica and alumina to produce pigments which are used in ceramics. NiO forms only with difficulty from heating the metal in oxygen and conversion is normally incomplete. It is produced by decomposition of the hydroxide, carbonate or nitrate. Rh_2O_3 and IrO_2 are the products from heating these metals in oxygen and are the most stable oxide phases formed by these elements. RhO_2 is formed by reaction of Rh_2O_3 in a high pressure of oxygen, whereas Ir_2O_3 forms by ignition of K_2IrCl_6 with Na_2CO_3 and readily oxidises to IrO_2.

Copper and silver form oxides of composition MO and M_2O,[8] with silver also forming the metallic conductor Ag_3O.[147] The only oxide of gold is Au_2O_3, which is produced by dehydration of a precipitate formed from Au (III) solutions with alkalis.[8] It is stable only to about 160°C.

Group 12 metals form monoxides. Zinc and cadmium also form peroxides. ZnO is the most important manufactured zinc compound and has been known for longer than the metal itself.[8] The normal method of production is by the burning of zinc vapour during smelting, as a finely divided white material. In rubber production ZnO shortens the time of vulcanisation. It has some application in paint but is limited by a lower refractive index and, therefore, opacity than TiO_2. It is used in special glasses, enamels and glazes to improve chemical durability. ZnO is a starting material in production of the zinc salts of fatty acids, such as zinc stearate or palmitate, which are used as paint dryers, plastics stabilisers and fungicides. On a smaller scale it is used in production of quaternary ferrites $Zn_xM_{1-x}Fe_2O_4$ (M= Mn or Ni) where the Curie temperature can be controlled by altering the value of x. Cadmium oxide, along with it's hydroxide, are used to colour decorative glasses and enamels. They are also used

in nickel- cadmium batteries. CdO catalyses several hydrogenation and dehydrogenation reactions. Hydrated zinc peroxide has antiseptic properties and finds widespread use in cosmetics.

Most of the main methods of ceramics synthesis have been applied to various oxide systems, including the traditional "Heat and beat" methods, precursor decomposition reactions, sol- gel,[25] thermite[58] and SHS[62] reactions. In addition, most of the various thin film producing methods have been applied to oxides.

6.2 Reactions with Lithium Oxide.

Mixtures of metal chlorides with lithium oxide were made up on a scale of 50mg Li_2O in an inert atmosphere with a 1:1 ratio of lithium to chlorine. These were sealed into Pyrex ampoules under vacuum and heated at 500°C for 2- 10 hours. Products were not found to change in composition with longer periods of heating, but did become more crystalline. The crude products, found as fused lumps of various colours, were ground and washed with methanol or water. Table 21 lists the phases observed by powder XRD. SEM showed smooth surfaces in crude materials and rough, sharp edged surfaces in the purified products. Metal and oxygen only were observed by EDXA in the purified products, whereas chlorine was also observed in the crude ones. Semiquantitative EDXA compositions closely matched those indicated by the phases observed by XRD. The only peak sometimes observed in the FT-IR spectra was a broad, weak band at around 500 cm^{-1}.

Many of the phases shown in Table 21 have the same metal oxidation state as that in the chloride reagent and can be explained by balanced equations, Eqn. 98- 102. These all form high stability oxide phases and could be attributed to ionic or elemental type mechanisms.

$$MCl_4 + 2Li_2O \rightarrow MO_2 + 4LiCl \qquad \text{-Eqn.98}$$

(M= Ti, Zr, Hf, V, W)

Table 21a. Products of reactions of Group 4- 7 chlorides with lithium oxide.

Reagent	Product	Colour	System, space group[81,103]
$TiCl_3$	TiO_2	Light grey	Tetragonal $I4_1/amd$
$TiCl_4$	TiO_2	White	Tetragonal $P4_2/mnm$
	(Li_2TiO_3)		Monoclinic C2/c
$ZrCl_4$	ZrO_2	Grey	Monoclinic $P2_1/c$
$HfCl_4$	HfO_2	Grey	Monoclinic $P2_1/c$
VCl_3	V_2O_3	Black	Hexagonal R3c
	$(LiVO_2)$		Hexagonal R3m
VCl_4	VO_2	Black	Tetragonal $P4_2/mnm$
	(Li_3VO_4)		Orthorhombic $Pmn2_1$
$NbCl_5$	$LiNbO_3$	Light grey	Hexagonal R3c
$TaCl_5$	$LiTaO_3$	Grey	Hexagonal R3c
$CrCl_3$	Cr_2O_3	Grey	Hexagonal R3c
$MoCl_3$	MoO_2	Black	Monoclinic $P2_1/c$
$MoCl_5$	MoO_2	Dark brown	Monoclinic $P2_1/c$
WCl_4	WO_2	Black	Monoclinic $P2_1/c$
$MnCl_2$	MnO	Brown	Cubic Fm3m
	(Mn_3O_4)		Tetragonal $I4_1/amd$
K_2ReCl_6	ReO_2	Dark grey	Orthorhombic Pbcn

Structural data are listed in Appendix 6.

$$MCl_3 + {}^3/_2Li_2O \rightarrow {}^1/_2M_2O_3 + 3LiCl \quad \text{-Eqn.99}$$
(M= V, Cr)

$$K_2ReCl_6 + 2Li_2O \rightarrow ReO_2 + 2KCl + 4LiCl \quad \text{-Eqn.100}$$

$$MCl_2 + Li_2O \rightarrow MO + 2LiCl \quad \text{-Eqn.101}$$
(M= Co, Ni, Zn, Cd, Hg)

$$CuCl + {}^1/_2Li_2O \rightarrow {}^1/_2Cu_2O + LiCl \quad \text{-Eqn.102}$$

The platinum metals are often used as inert materials at high temperature and are less susceptible to oxidation than most d- block metals. It is therefore of no surprise that

the metals are observed in addition to oxides in the products from the reactions described in Eqn. 103-106. Temperatures are not sufficiently high to cause decomposition of the oxides, so the presence of these phases is a strong indicator of an elemental mechanism. Incomplete recombination of metal and oxygen could yield the observed products and is likely even with finely divided metal due to the inertness of these elements. The excess metal could be removed from the oxides using aqua regia. The XRD pattern of the palladium product is shown in Fig. 30.

Table 21b. Products of reactions of Group 8- 12 chlorides with lithium oxide.

Reagent	Product	Colour	System, space group[81,103]
$FeCl_3$	Fe_3O_4	Dark brown	Cubic Fd3m
	(Fe_2O_3)		Hexagonal R-3c
K_2RuCl_6	RuO_2	Dark grey	Tetragonal $P4_2/mnm$
	Ru		Hexagonal $P6_3/mmc$
K_2OsCl_6	OsO_2	Dark grey	Tetragonal $P4_2/mnm$
	Os		Hexagonal $P6_3/mmc$
$CoCl_2$	CoO	Brown	Cubic Fm3m
$RhCl_3$	$LiRhO_2$	Black	Cubic
	Rh		Cubic Fm3m
Na_3IrCl_6	IrO_2	Black	Tetragonal $P4_2/mnm$
	(Ir)		Cubic Fm3m
$NiCl_2$	NiO	Light green	Cubic Fm3m
$PdCl_2$	PdO	Black	Tetragonal $P4_2/mmc$
	(Pd)		Cubic Fm3m
K_2PtCl_4	Pt_3O_4	Black	Cubic Pm3n
	(Pt)		Cubic Fm3m
CuCl	Cu_2O	Yellow	Cubic Pn3m
$ZnCl_2$	ZnO	White	Hexagonal $P6_3/mc$
$CdCl_2$	CdO	Grey	Cubic Fm3m
$HgCl_2$	HgO	Brown	Orthorhombic Pnma

Structural data are listed in Appendix 6.

$$K_2MCl_6 + 2Li_2O \rightarrow xMO_2 + (1\text{-}x)[M + O_2] + 2KCl + 4LiCl \qquad \text{-Eqn.103}$$

(M= Ru, Os)

$$Na_3IrCl_6 + {}^3/_2Li_2O \rightarrow {}^3/_4IrO_2 + {}^1/_4Ir + 3NaCl + 3LiCl \qquad \text{-Eqn.104}$$

$$PdCl_2 + Li_2O \rightarrow xPdO + (1\text{-}x)[Pd + {}^1/_2O_2] + 2LiCl \qquad \text{-Eqn.105}$$

$$K_2PtCl_4 + Li_2O \rightarrow {}^1/_4Pt_3O_4 + {}^1/_4Pt + 2KCl + 2LiCl \qquad \text{-Eqn.106}$$

Fig. 30. X-ray powder diffraction pattern of PdO/ Pd produced from $PdCl_2$ and Li_2O.

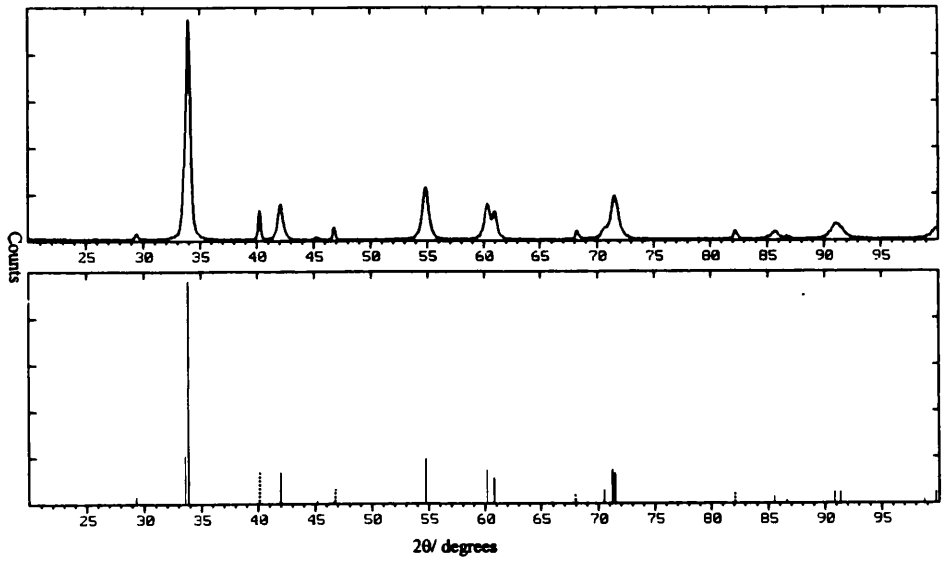

Pt_3O_4 is capable of trapping high levels of cations, forming platinum bronzes.[148] These are ternary oxides of platinum of general formula $M_xPt_3O_4$ where M is generally from Group 1 or 2 and $0 < x < 1$. Palladium also forms this type of compound. The Pt_3O_4/ Pt product synthesised in this study contained potassium below the EDXA detection threshold (~0.5%) and lithium at 0.01%. The bronzes form readily so it must be assumed that reaction conditions disallowed incorporation of cations due to the equal levels of alkali metal and chlorine. Even so, the cations could have had a role in causing Pt_3O_4 to form.

In contrast to the non- formation of platinum bronzes, in some cases ternary lithium metal oxides are the preferred products, Eqn. 107 and 108. These equations were

written to balance but reaction mixtures were made up with equal amounts of lithium and chlorine, so the thermodynamic favourability of the observed phases must be responsible. The $TaCl_5$ reaction was also performed with a two- fold excess of the chloride but the product, Ta_2O_5, was still found to contain significant amounts of $LiTaO_3$ and also Li_3TaO_4. $LiNbO_3$ and $LiTaO_3$ are useful for their non- linear optical properties. The XRD pattern of $LiTaO_3$ is shown in Fig. 31. With titanium and vanadium ternary lithium metal oxides were observed as by- products. Use of a two-fold excess of Li_2O with $TiCl_3$ or VCl_3 resulted in formation of the Li_3MO_3 phase, Eqn. 109. Performing the reaction of $ZrCl_4$ with a 1:1 ratio of lithium to chlorine in air resulted in Li_2ZrO_3.

$$MCl_5 + 3Li_2O \rightarrow LiMO_3 + 5LiCl \quad \text{-Eqn.107}$$
(M= Nb, Ta)

$$RhCl_3 + 2Li_2O \rightarrow LiRhO_2 + 3LiCl \quad \text{-Eqn.108}$$

$$MCl_3 + {}^5/_2Li_2O \rightarrow Li_2TiO_3 + 3LiCl + {}^1/_4O_2 \quad \text{-Eqn.109}$$
(M= Ti, V)

Some reactions involved a change in metal oxidation state with
no second phase observed by XRD. These are balanced in Eqn. 109- 112 by some oxygen, although ampoules were thoroughly evacuated and no oxygen was detected by GC after reactions. The phases which form are highly stable and this appears to be the factor which decides composition of the products.

$$TiCl_3 + {}^3/_2Li_2O + {}^1/_4O_2 \rightarrow TiO_2 + 3LiCl \quad \text{-Eqn.110}$$

$$MoCl_x + {}^x/_2Li_2O + (1-{}^x/_4)O_2 \rightarrow MoO_2 + xLiCl \quad \text{-Eqn.111}$$
(x= 3, 5)

$$FeCl_3 + {}^3/_2Li_2O \rightarrow {}^1/_3Fe_3O_4 + {}^1/_{12}O_2 + 3LiCl \quad \text{-Eqn.112}$$

Fig. 31. X-ray diffraction pattern of $LiTaO_3$ produced from $TaCl_5$ and Li_2O.

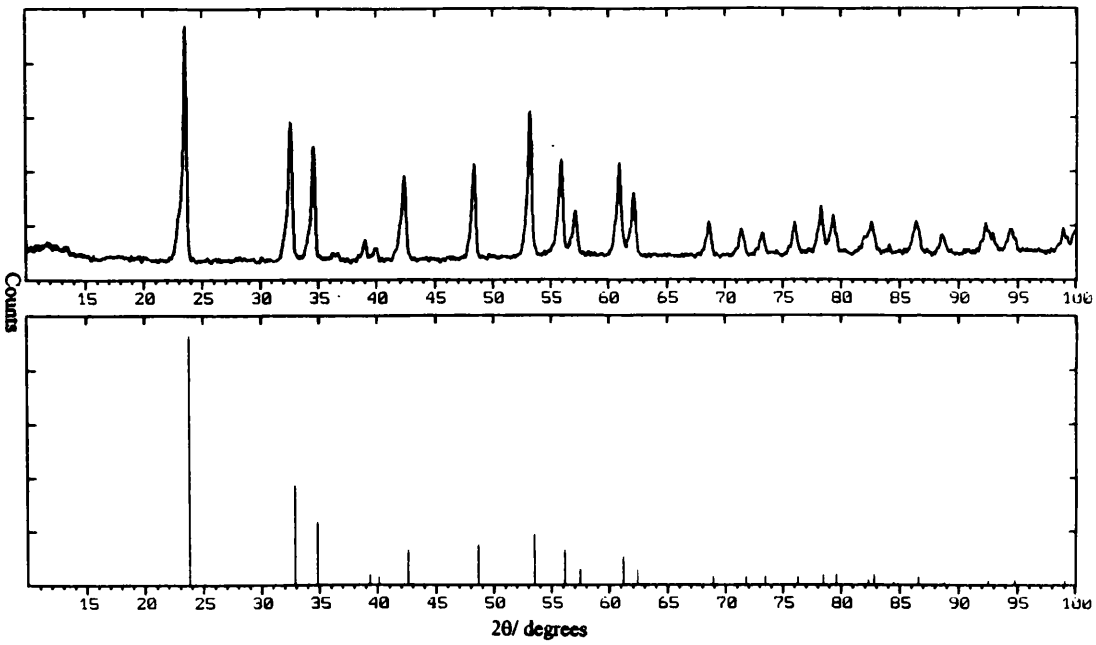

The reaction of $HfCl_4$ with Li_2O was studied by differential scanning calorimetry (DSC). A large exotherm was observed at 310- 325°C, Fig. 32, occurring over a time period of several minutes. Similar results were obtained with $NbCl_5$ and K_2PtCl_4. The energy of the exotherms was 120- 300 $kJmol^{-1}$. Blank runs of the chlorides and of Li_2O showed no major exothermic features in the temperature range studied. A sample of the $HfCl_4$/ Li_2O mixture heated to 295°C and held at this temperature yielded an exotherm occurring over a period of about 15 minutes. This was insufficient to yield crystalline products under normal conditions (larger scale and a tube furnace) so there is a possibility that reactions occurred under these mild conditions and the longer periods of heating were only required for complete reaction and to induce crystallinity. Heat transfer is easier in a metal DSC pan under argon than in an evacuated glass ampoule under vacuum. This could make a reaction under milder conditions possible.

The methods described in this chapter are a good way of producing a range of oxides simply and with a minimum of energy input. One specialist utility could be the incorporation of isotopically labelled oxygen in small scale reactions into an oxide lattice using initially labelled lithium oxide. Industrially useful materials such as

$LiNbO_3$, $LiTaO_3$, CoO, ZnO and CdO may be conveniently produced without the need for repeat grinding and heating cycles or high temperature annealling.

Fig. 32. Differential scanning calorimeter trace from a reaction of $HfCl_4$ with Li_2O.

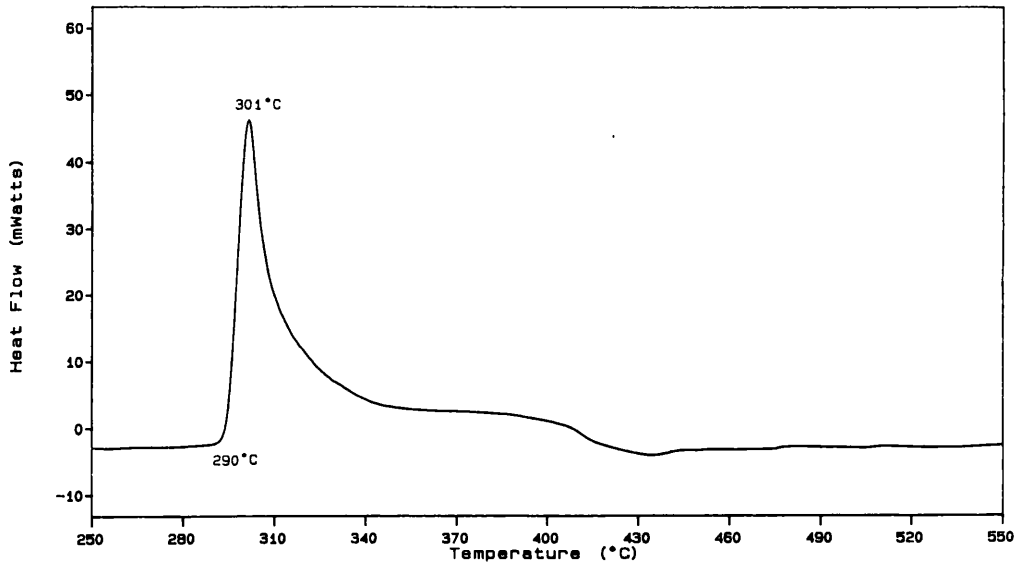

6.3 Experimental.

Most reagents, solvents and instrumentation have previously been described. In addition lithium oxide was purchased from Aldrich Chemical Co. and rhenium, platinum metal and cadmium salts were obtained as a loan from Johnson Matthey. Differential scanning calorimetry was carried out with a Polymer Laboratories instrument using open aluminium pans in an atmosphere of flowing argon with a heating rate of $10°Cmin^{-1}$.

Reactions of lithium oxide.

Lithium oxide (50mg) and anhydrous metal chloride (1:1 ratio of alkali metal, including any contained in metal chloride reagents, to chloride) were ground together under nitrogen, placed into a Pyrex ampoule and sealed under vacuum. The ampoule was placed into a furnace and heated at 500°C for 2- 10 hours. After cooling the

ampoule was opened and the contents ground and washed with methanol or water. The product was characterised using XRD, SEM, EDXA and lithium microanalysis. Yields were variable from 55% (VO_2) to 90% ($LiNbO_3$).

Lithium microanalysis:

ZnO %Li= 330 ppm.

Pt_3O_4/ Pt %Li= 130 ppm.

Appendix 1. Structural data for phosphides listed in Table 15.

Product	System, space group	Lattice parameters, (lit.[81,103] values) / Å a	b	c
YP	Cub. Fm3m	5.656		
LaP	Cub. Fm3m	6.024 (6.025)		
TiP	Hex. $P6_3/mmc$	3.498 (3.487)		11.697 (11.65)
ZrP	Cub. Fm3m	5.273 (5.242)		
HfP	Cub. Fm3m	5.214		
VP	Hex. $P6_3/mmc$	3.177 (3.176)		6.219 (6.22)
NbP	Tet. $I4_1md$	3.327 (3.334)		11.379 (11.378)
TaP	Tet. $I4_1md$	3.316 (3.319)		11.327 (11.314)
CrP	Orth. Pbnm	5.923 (6.108)	5.404 (5.362)	3.127 (3.113)
MoP ($MoCl_3$)	Hex. P6m2	3.225 (3.222)		3.196 (3.191)
MoP ($MoCl_5$)	Hex. P6m2	3.217 (3.222)		3.191 (3.191)
WP	Orth. Pbnm	6.279 (6.222)	5.716 (5.734)	3.250 (3.249)
FeP	Orth. Pbnm	5.856 (5.792)	5.179 (5.191)	3.128 (3.099)
CoP	Orth. Pbnm	5.574 (5.587)	5.112 (5.077)	3.309 (3.281)
Ni_2P	Hex. P62m	5.860 (5.864)		3.373 (3.385)
PtP_2	Cub. Pa3	5.675 (5.696)		
Zn_3P_2	Tet. $P4_2/nmc$	8.109 (8.097)		11.457 (11.44)

Appendix 2. Structural data for arsenides listed in Table 16.

Product	System, space group	Lattice parameters, (lit.[81,103] values) / Å a	b	c
YAs	Cub. Fm3m	5.808 (5.786)		
LaAs	Cub. Fm3m	6.165 (6.137)		
TiAs	Hex. $P6_3/mmc$	3.641 (3.642)		11.971 (12.064)
ZrAs	Hex. $P6_3/mmc$	3.862 (3.804)		12.877 (12.87))
HfAs	Hex. $P6_3/mmc$	3.752 (3.765)		12.555 (12.681)
$HfAs_2$	Orth. Pnam	6.766 (6.771)	8.910 (8.941)	3.656 (3.673)
VAs	Orth. Pnma	5.835 (5.879)	3.358 (3.334)	6.276 (6.317)
NbAs	Tet $I4_1md$	3.451 (3.452)		11.720 (11.679)
TaAs	Tet $I4_1md$	3.430 (3.435)		11.676 (11.641)
$TaAs_2$	Mono. C2/m	9.332 (9.385)	3.386 (3.304)	7.757 (7.757)
		β= 119.6 (119.7°)		
CrAs	Orth. Pnma	5.755 (5.742)	3.496 (3.504)	6.228 (6.223)
Mo_5As_4	Tet. I4/m	9.625 (9.601)		3.288 (3.278)
MoAs	Orth. Pnma	5.988 (5.989)	3.374 (3.360)	6.481 (6.415)
WAs_2	Mono. C2/m	9.067 (9.085)	3.316 (3.318)	7.698 (7.690)
		β= 119.7 (119.5°)		
MnAs	Hex. $P6_3/mmc$	3.717 (3.724)		5.686 (5.702)
$FeAs_2$	Orth. Pnnm	5.290 (5.300)	5.970 (5.983)	2.868 (2.882)
CoAs	Orth. Pmcn	3.458 (3.458)	5.850 (5.869)	5.280 (5.292)
Co_2As	Hex. P62m	11.970 (11.987)		3.590 (3.588)
$Ni_{11}As_8$	Tet. $P4_12_12$	6.866 (6.867)		21.785 (21.810)
Ni_5As_2	Hex. $P6_322$	6.822 (6.815)		12.446 (12.506)
Pt	Cub. Fm3m	3.902 (3.923)		
$PtAs_2$	Cub. Pa3	5.919 (5.967)		
Zn_3As_2	Tet. $I4_1/acd$	11.762 (11.783)		23.632 (23.652)

Appendix 3. Structural data for antimonides listed in Table 17.

Product	System, space group	Lattice parameters, (lit.[81,103] values) / Å a	b	c
YSb	Cub. Fm3m	6.152 (6.155)		
LaSb	Cub. Fm3m	6.551 (6.488)		
$TiSb_2$	Tet. I4/mcm	6.645 (6.666)		5.801 (5.817)
TiSb	Hex. $P6_3/mmc$	4.128 (4.115)		6.272 (6.264)
VSb_2	Tet. I4/mcm	6.544 (6.555)		5.628 (5.631)
$NbSb_2$	Mono. C2/m	10.190 (10.239)	3.618 (3.632)	8.306 (8.333)
		β= 119.96° (120.1°)		
$TaSb_2$	Mono. C2/m	10.262 (10.222)	3.653 (3.645)	8.299 (8.292)
		β= 120.48° (120.4°)		
Mo	Cub. Im3m	3.141 (3.147)		
Mo_3Sb_7	Cub. Im3m	9.552 (9.571)		
W	Cub Im3m	3.162 (3.165)		
Sb (WCl_4)	Hex R-3m	4.305 (4.307)		11.235 (11.273)
$FeSb_2$	Orth. Pnnm	5.819 (5.831)	6.523 (6.533)	3.196 (3.195)
CoSb	Hex. $P6_3/mmc$	3.895 (3.896)		5.182 (5.181)
NiSb	Hex. $P6_3/mmc$	3.923 (3.924)		5.156 (5.142)
$NiSb_2$	Orth. Pnnm	5.182 (5.180)	6.337 (6.314)	3.835 (3.838)
PtSb	Hex. $P6_3/mmc$	4.137 (4.138)		5.466 (5.483)
Pt_3Sb_2	Orth.	6.439 (6.446)	10.913 (10.939)	5.308 (5.319)
Zn_4Sb_3	Hex.	10.659 (10.7)		3.589 (3.54)
Sb ($ZnCl_2$)	Hex R-3m	4.309 (4.307)		11.214 (11.273)
Sb ($HgCl_2$)	Hex R-3m	4.306 (4.307)		11.310 (11.273)

Appendix 4. Structural data for compounds listed in Table 18.

Product	System, space group	Lattice parameters, (lit.[81,131] values) / Å a	b	c
TiP	Hex. $P6_3/mmc$	3.496 (3.487)		11.684 (11.65)
$Ti_{0.5}V_{0.5}P$	Hex. $P6_3/mmc$	3.376		10.516
VP	Hex. $P6_3/mmc$	3.250 (3.18)		6.035 (6.22)
TiAs	Hex. $P6_3/mmc$	3.636 (3.642)		12.014 (12.064)
$Ti_{0.75}V_{0.25}As$[a]	Hex. $P6_3/mmc$	3.603 (3.62)		6.116 (6.12)
$Ti_{0.5}V_{0.5}As$[a]	Hex. $P6_3/mmc$	3.588 (3.55)		6.146 (6.14)
$Ti_{0.25}V_{0.75}As$[a]	Orth. Pnma	5.858 (~5.93)	3.171 (~3.42)	6.480 (~6.32)
VAs	Orth. Pnma	5.846 (5.889)	3.361 (3.333)	6.291 (6.316)
$TiAs_{0.5}P_{0.5}$	Hex. $P6_3/mmc$	3.510 (3.556)		11.273 (11.84)
Sb ($TiCl_4$)	Hex. R-3m	4.311 (4.307)		11.277 (11.273)
$TiSb_2$	Tet. I4/mcm	6.678 (6.666)		5.802 (5.817)
Sb (VCl_4)	Hex. R-3m	4.305 (4.307)		11.282 (11.273)
VSb_2	Tet. I4/mcm	6.542 (6.555)		5.610 (5.631)
Bi ($TiCl_4$)	Hex. R-3m	4.549 (4.546)		11.897 (11.860)
Bi (VCl_4)	Hex. R-3m	4.548 (4.546)		11.895 (11.860)

a. Ref. 132

Appendix 5. Structural data for silicides listed in Table 20.

Product	System, space group	Lattice parameters, (lit.[81,103] values) / Å a	b	c
YSi_2	Hex. P6/mmm	3.822 (3.83)		4.124 (4.14)
$GdSi_2$	Orth. Imma	4.072 (4.09)	3.997 (4.01)	13.457 (13.44)
$DySi_2$	Tet. $I4_1/amd$	4.028 (4.03)		13.391 (13.38)
$HoSi_2$	Hex. P6/mmm	3.830 (3.816)		4.109 (4.107)
$TiSi_2$	Orth. Fddd	8.261 (8.253)	4.789 (4.783)	3.622 (3.605)
Ti_5Si_3	Hex. $P6_3/mcm$	7.439 (7.448)		5.111 (5.115)
$ZrSi_2$	Orth. Cmcm	3.717 (3.721)	14.669 (14.68)	3.672 (3.683)
Zr_2Si	Tet. I4/mcm	6.624 (6.612)		5.288 (5.294)
$HfSi_2$	Orth. Cmcm	3.631 (3.677)	14.564 (14.550)	3.657 (3.649)
Hf_2Si	Tet. I4/mcm	6.483 (6.48)		5.223 (5.21)
$NbSi_2$	Tet. $P6_222$	4.770 (4.797)		6.581 (6.592)
Nb_5Si_3	Tet. I4/mcm	6.553 (6.570)		11.897 (11.884)
Ta_5Si_3	Tet. I4/mcm	6.512 (6.517)		11.880 (11.873)
Mo_5Si_3	Tet. I4/mcm	9.607 (9.62)		4.883 (4.90)
$MoSi_2$	Tet. I4/mmm	3.191 (3.203)		7.848 (7.855)
W	Cub. Im3m	3.160 (3.165)		
WSi_2	Tet. I4/mmm	3.206 (3.212)		7.822 (7.835)
W_5Si_3	Tet. I4/mcm	9.579 (9.605)		4.982 (4.964)
FeSi	Cub. $P2_13$	4.537 (4.487)		
Ni_5Si_2	Hex. P321	6.653 (6.670)		12.217 (12.3)
Ni	Cub. Fm3m	3.509 (3.524)		
Si ($NiCl_2$)	Cub. Fd3m	5.436 (5.431)		
Pt	Cub. Fm3m	3.920 (3.924)		
Pt_2Si	Tet. I4/mmm	3.974 (3.933)		5.922 (5.910)
Pt_3Si	Mono. F2/m	7.712 (7.702)	7.767 (7.765)	7.758 (7.765)
		β= 88.72° (91.89°)		
Zn	Hex. $P6_3/mmc$	2.662 (2.665)		4.958 (4.947)
Si ($ZnCl_2$)	Cub. Fd3m	5.439 (5.431)		

Appendix 6. Structural data for oxides listed in Table 21.

Product	System, space group	Lattice parameters, (lit.[81,103] values) / Å a	b	c
TiO_2 ($TiCl_3$)	Tet. $I4_1/amd$	3.793 (3.785)		9.519 (9.514)
TiO_2 ($TiCl_4$)	Tet. $P4_2/mnm$	4.585 (4.593)		2.957 (2.959)
ZrO_2	Mono. $P2_1/c$	5.155 (5.142)	5.251 (5.206)	3.340 (3.313)
		β= 98.07° (99.31°)		
HfO_2	Mono. $P2_1/c$	5.124 (5.12)	5.201 (5.18)	5.255 (5.25)
		β= 97.62° (98.0°)		
V_2O_3	Hex. R-3c	4.948 (4.959)		13.941 (14.003)
VO_2	Tet. $P4_2/mnm$	4.534 (4.530)		2.881 (2.869)
$LiNbO_3$	Hex. R3c	5.155 (5.148)		13.851 (13.863)
$LiTaO_3$	Hex. R3c	5.159 (5.154)		13.727 (13.784)
Cr_2O_3	Hex. R-3c	4.962 (4.958)		13.586 (13.587)
MoO_2 ($MoCl_3$)	Mono. $P2_1/c$	5.646 (5.607)	4.872 (4.860)	5.656 (5.624)
		β= 118.99° (120.94°)		
MoO_2 ($MoCl_5$)	Mono. $P2_1/c$	5.611 (5.607)	4.872 (4.860)	5.622 (5.624)
		β= 120.73° (120.94°)		
WO_2	Mono. $P2_1/c$	5.559 (5.556)	4.889 (4.893)	5.656 (5.658)
		β= 120.31° (120.42°)		
MnO	Cub. Fm3m	4.440 (4.445)		
ReO_2	Orth. Pbcn	4.824 (4.809)	5.622 (5.643)	4.486 (4.601)
Fe_3O_4	Cub. Fd3m	8.399 (8.394)		
RuO_2	Tet. $P4_2/mnm$	4.502 (4.491)		3.111 (3.106)
Ru	Hex. $P6_3/mmc$	2.703 (2.706)		4.282 (4.281)
OsO_2	Tet. $P4_2/mnm$	4.496 (4.500)		3.167 (3.184)
Os	Hex. $P6_3/mmc$	2.723 (2.735)		4.310 (4.319)
CoO	Cub. Fm3m	3.929 (3.933)		
$LiRhO_2$	Cub.	4.274 (4.258)		
Rh	Cub. Fm3m	8.409 (8.413)		
IrO_2	Tet. $P4_2/mnm$	4.506 (4.498)		3.162 (3.154)
NiO	Cub. Fm3m	4.277 (4.195)		
PdO	Tet. $P4_2/mmc$	3.042 (3.043)		5.330 (5.336)
Pt_3O_4	Cub. Pm3n	5.608 (5.585)		
Cu_2O	Cub. Pn3m	4.267 (4.268)		
ZnO	Hex. $P6_3/mc$	3.258 (3.250)		5.164 (5.207)
CdO	Cub. Fm3m	4.670 (4.695)		
HgO	Ortho. Pnma	6.637 (6.613)	5.556 (5.521)	3.540 (3.522)

References

1. R. T. Paine in *Inorganometallic Chemistry*, T. P. Fehlner (Ed.), *Modern Inorganic Chemistry* series, J. P. Fackler Jr. (Ser. Ed.), Plenum, New York, 1992.

2. L. L. Hench and D. R. Ulrich (Eds.), *Ultrastructure Processing of Ceramics, Glasses and Composites*, Wiley, New York, 1984.

3. R. W. Rice in *Design of New Materials*, D. L. Cocke and A. Clearfield (Eds.), Plenum, New York, 1978.

4. D. Segal, *Chemical Synthesis of Advanced Ceramic Materials*, Cambridge, Cambridge, 1989.

5. A. Bauger, J. C. Moutin and J. C. Niepce, *J. Mater. Sci.*, 1983, **18**, 3041.

6. C. D. Chandler, Q. Powell, M. J. Hampden- Smith and T. T. Kodas, *J. Mater. Chem.*, 1993, **3**, 775.

7. L. E. Toth, *Transition Metal Carbides and Nitrides*, Plenum, New York, 1971.

8. N. N. Greenwood and A. Earnshaw, *Chemistry of the Elements*, Pergamon, London, 1984.

9. D. M. P. Mingos and D. R. Baghurst, *Chem. Soc. Rev.*, 1991, **20**, 1.

10. P. K. Bachmann, *Adv. Mater.*, 1990, **2**, 195.

11. R. N. Gedye, F. E. Smith and K. G. Westaway, *Can. J. Chem.*, 1988, **66**, 17.

12. S. L. McGill and J. W. Walkiewiez, *J. Microwave Power Electromag. Energy Symp. Summ.*, 1987, 175.

13. K. Chatakondu, M. L. H. Green, D. M. P. Mingos and S. M. Reynolds, *J. Chem. Soc., Chem. Commun.*, 1989, 1515.

14. D. R. Baghurst, A. M. Chippindale and D. M. P. Mingos, *Nature*, 1988, **332**, 311.

15. D. R. Baghurst and D. M. P. Mingos, *J. Chem. Soc., Chem. Commun.*, 1988, 829.

16. A. G. Whittacker and D. M. P. Mingos, *J. Chem. Soc., Dalton Trans.*, 1992, 2751.

17. C. C. Landry and A. R. Barron, *Science*, 1993, **260**, 1653.

18. R. Dagani, *Chem. Eng. News*, 1988, **66**, 7.

19. M. Ebelman, *Ann. Chimie. Phys.*, 1846, **16**, 129.

20. M. Ebelman, *C. R. Acad. Sci.*, 1847, **25**, 85.

21. L. L. Hench and J. K. West, *Chem. Rev.*, 1990, **90**, 33.

22. L. L. Hench and D. R. Ulrich (Eds.), *Science of Ceramic Chemical Processing*, Wiley, New York, 1984.

23. S. H. Wang, C. Campbell and L. L. Hench, in *Ultrastructure Processing of Advanced Ceramics*, J. D. Mackensie and D. R. Ulrich (Eds.), Wiley, New York, 1988.

24. B. E. Yoldas, *Bull. Am. Ceram. Soc.*, 1975, **54**, 286.

25. C. J. Brinker and G. W. Scherer, *Sol- Gel Science: The Physics and Chemistry of Sol- Gel Processing*, Academic Press Ltd, London, 1990.

26. E. Matijevic, M. Bundnick and L. J. Meites, *J. Colloid Interface Sci.*, 1977, **61**, 302.

27. E. Matijevic, in *Science of Ceramic Chemical Processing*, L. L. Hench and D. R. Ulrich (Eds.), Wiley, New York, 1986.

28. E. Matijevic in *Ultrastructure Processing of Advanced Ceramics*, J. D. Mackensie and D. R. Ulrich (Eds.), Wiley, New York, 1988.

29. A. Szweda, A. Hendry and K. H. Jack, *Proc. Brit. Ceram. Soc.*, 1981, **31**, 107.

30. A. H. Cowley, R. A. Jones, C. M. Nunn and D. L. Westmoreland, *Chem. Mater.*, 1990, **2**, 221.

31. Q. Li, C. M. Sorensen, K. J. Klabunde and G. C. Hadjipanayis, *Aerosol Sci. Tech.*, 1993, **19**, 453.

32. S. Lee, O. A. Shlyaktin, M. O. Mun, M. K. Bae and S. I. Lee, *Superconductor Sci. Tech.*, 1995, **8**, 60.

33. E. Uzunova, D. Klissurski and S. Kassabov, *J. Mater. Chem.*, 1994, **4**, 153.

34. G. A. M. Hussein, *Thermochim. Acta*, 1994, **244**, 139.

35. H. W. Wang, D. A. Hall and F. R. Sale, *J. Therm. Anal.*, 1994, **41**, 605.

36. E. Matijevic, *Ann. Rev. Mater. Sci.*, 1985, **15**, 483.

37. T. Trindade, J. D. Pedrosa de Jesus and P. O'Brien, *J. Mater. Chem.*, 1994, **4**, 1611.

38. S. M. Stczynski, J. G. Brennan and M. L. Steigerwald, *Inorg. Chem.*, 1989, **28**, 4431.

39. T. A. Guiton, C. I. Czkaj, M. S. Rau, G. L. Geoffroy and C. G. Pantano, *Mater. Res. Soc. Symp. Proc.*, 1988, **121**, 503.

40. M. L. Steigerwald, *Chem. Mater.*, 1989, **1**, 52.

41. J. G. Brennan, T. Siegrist, S. M. Stuczynski and M. L. Steigerwald, *J. Am. Chem. Soc.*, 1989, **111**, 9240.

42. D. V. Baxter, M. H. Chisholm, V. F. Distasi, G. J. Gama, A. L. Hector and I. P. Parkin, *Chem. Mater.*, submitted for publication.

43. R. M. Laine and A. S. Hirschon in *Transformation of Organometallics into Common and Exotic Materials: Design and Activation*, R. M. Laine (Ed.), M. Nijhoff, Dordrecht, 1988.

44. G. L. Brown and L. Maya, *J. Am. Ceram. Soc.*, 1988, **71**, 78.

45. S. Yajima, K. Okamura, J. Hayashi and M. Omori, *J. Am. Ceram. Soc.*, 1976, **59**, 324.

46. K. Okamura, *Composites*, 1987, **18**, 107.

47. S. Yajima, T. Iwai, T, Yamamura, K. Okamura and Y. Hasegawa, *J. Mater. Sci.*, 1981, **16**, 1349.

48. K. Okamura, M. Sato, Y. Hasegawa and T. Amano, *Chem. Lett.*, 1984, 2059.

49. S. T. Oyama, *Catal. Today*, 1992, **15**, 179.

50. L. Leclercq, K. Imura, S. Yoshida, T. Barbee and M. Boudart, *Preparation of Catalysts II*, B. Delmon, P. Grange, P. A. Jacobs and G. Poncelet (Eds.), Elsevier, Amsterdam, 1979.

51. S. Iwana, K. Hayakawa and T. Arizumi, *J. Crystal Growth*, 1982, **56**, 265; *ibid.*, 1984, **66**, 189.

52. P. Ronsheim, A. Mazza and A. N. Christensen, *Plasma Chem. Plasma Process.*, 1981, **1**, 135.

53. A. Brenner and R. L. Burwell Jr., *J. Am. Chem. Soc.*, 1975, **97**, 2566.

54. D. E. Willis, *J. Catal.*, 1983, **84**, 344.

55. M. J. Ledoux, C. Pham- Huu, S. Marin, M. Weibel and J. Guille, *C. R. Acad. Sci. Paris*, t. 310, Serie II, 707, 1990.

56. J. S. Lee, S. T. Oyama and M. Boudart, *J. Catal.*, 1987, **106**, 125.

57. L. Volpe and M. Boudart, *J. Sol. St. Chem.*, 1985, **59**, 332.

58. L. L. Wang, Z. A. Munir and Y. M. Maximov, *J. Mater. Sci.*, 1993, **28**, 3693.

59. D. Belitkus, *J. Metals*, January 1972, 30.

60. A. G. Mershanov and I. P. Borovinskaya, *Comb. Sci. Tech.*, 1975, **10**, 195.

61. L. M. Sheppard, *Adv. Mater. Proc.*, 1986, **2**, 25.

62. H. C. Yi and J. J. Moore, *J. Mater. Sci.*, 1990, **25**, 1159.

63. B. Manley, J. B. Holt and Z. A. Munir, *Mater. Sci. Res.*, 1984, **16**, 303.

64. O. R. Bermann and J. Barrington, *J. Amer. Ceram. Soc.*, 1966, **49**, 502.

65. M. Ouabdesselam and Z. A. Munir, *J. Mater. Sci.*, 1987, **22**, 1799.

66. K. Hirao, Y. Miyamoto and M. Koizumi, *Materials (Jpn.)*, 1987, **36** (400), 12.

67. M. Ohyanagi, M. Koizumi, K. Tanihata, Y. Miyamoto, O. Yamada, I. Matsubara and Y. Yamashita, *J. Mater. Sci. Lett.*, 1993, **12**, 500.

68. K. Sato, K. Terase and H. Kijimuta, *U. S. Patent*, 4,399,115 (1983).

69. R. R. Chianelli and M. B. Dines, *Inorg. Chem.*, 1978, **17**, 2758.

70. A. D. F. Toy in *Comprehensive Inorganic Chemistry*, J. C. Bailar, H. J. Emeléus, R. Nyholm and A. F, Trotman- Dickenson (Eds.), Vol. 2, Pergamon, Oxford, 1973.

71. S. Hilpert and A. Wille, *Z. Phys. Chem.*, 1932, **18B**, 291.

72. D. E. Corridge, *Phosphorus and an Outline of it's Chemistry , Biochemistry and Technology*, Elsevier, Oxford, 1978.

73. P. R. Bonneau, R. K. Shibao and R. B. Kaner, *Inorg. Chem.*, 1990, **29**, 2511.

74. P. R. Bonneau, R. F. Jarvis Jr. and R. B. Kaner, *Nature*, 1991, **349**, 510.

75. J. B. Wiley, P. R. Bonneau, R. E. Treece, R. F. Jarvis Jr., E. G. Gillan, L. Rao and R. B. Kaner, *A. C. S. Symp. Ser.*, 1992, **499**, 369 (Chap. 26).

76. P. R. Bonneau, R. F. Jarvis Jr. and R. B. Kaner, *Inorg. Chem.*, 1992, **31**, 2127.

77. J. B. Wiley and R. B. Kaner, *Science*, 1992, **255**, 1093.

78. R. E. Treece, G. S. Macala and R. B. Kaner, *Chem. Mater.*, 1992, **4**, 9.

79. I. P. Parkin and A. T. Rowley, *Adv. Mater.*, 1994, **6**, 780.

80. I. P. Parkin and A. T. Rowley, *J. Mater. Chem.*, 1995, **5**, 909.

81. *PDF-2* database, International Centre for Diffraction Data, Swarthmore, PA 19081, USA, 1990.

82. K. Jones in *Comprehensive Inorganic Chemistry*, J. C. Bailar, H. J. Emeléus, R. Nyholm and A. F, Trotman- Dickenson (Eds.), Vol. 2, Pergamon, Oxford, 1973.

83. B. R. Brown in *Mellor's Comprehensive Treatise on Inorganic and Theoretical Chemistry*, Vol. 8, Suppl. 1, *Nitrogen*, Part I, Section III, Longman, London, 1964.

84. J. Flahaut and P. Laruelle, *Progress in the Science and Technology of the Rare Earths*, Vol. 13, Pergamon Press, UK, 1968.

85. C. K. Jorgenson, *Oxidation Numbers and Oxidation States*, Spriger- Verlag, New York, 1969.

86. A. F. Wells, *Structural Inorganic Chemistry*, 5th Ed., Oxford, London, 1984.

87. *Handbook of Chemistry and Physics*, CRC Press, 55th Ed., 1974.

88. A. Münster, *Angew. Chem.*, 1957, **69**, 281.

89. H. H. Hausner and M. G. Bowman (Eds.), *Fundamentals of Refractory Compounds*, Plenum, New York, 1968.

90. H. A. Johansen, in *Survey of Progress in Chemistry 8*, A. Scott (Ed.), Academic Press, New York, 1977, p.57.

91. E. G. Kendall, in *Ceramics for Advanced Technologies*, J. E. Hove and W. C. Riley (Eds.), Wiley, New York, 1965.

92. E. A. Almond in *Transformation of Organometallics into Common and Exotic Materials: Design and Activation*, R. M. Laine (Ed.), M. Nijhoff, Dordrecht, 1988.

93. S. R. Kurtz and R. G. Gordon, *Thin Solid Films*, 1986, **140**, 277.

94. A. R. Williams, *Mat. Res. Soc. Symp. Proc.*, 1983, **19**, 17.

95. M. Boudart, S. T. Oyama and L. Leclecq, *Proc. 7th Int. Cong. Catal.*, Tokyo, 1980, T. Seiyama and K. Tanabe (Eds.), Vol. 1, p. 587, Kodansha, 1980.

96. S. T. Oyama, *J. Catal.*, 1992, **133**, 358.

97. C. B. Murchison and D. A. Murdick, *Hydrocarbon Processing*, 1981, **60**, 159.

98. G. S. Ranhotra, A. T. Bell and J. A. Reimer, *J. Catal.*, 1987, **108**, 40.

99. D. J. Sajkowski and S. T. Oyama, *Symposium on The Chemistry of W/ Mo Catalysts*, 199th A. C. S. National Meeting, Petroleum Chemistry Division, Boston, Massachusetts, April 22- 27, 1990.

100. M. L. Cohen, *Phys. Rev. B*, 1985, **32**, 7988.

101. K. Naito and N. Kagegashira, *Adv. Nucl. Sci. Tech.*, 1976, **9**, 99.

102. I. P. Parkin and J. D. Woolins, *Phosphorus, Sulfur and Silicon*, 1990, **47**, 141.

103. P. Eckerlin and P. H. Kandler, *Structure Data of Elements and Intermetallic Phases*, Vol. 6, and W. Pies and A. Weiss, *Crystal Structure Data of Inorganic Compounds*, Vol. 7, in *Landolt- Börnstein Numerical Data and Functional Relationships in Science and Technology, New Series*, K. -H. Hellwege and A. M. Hellwege (Eds.), Springer- Verlag, Berlin, 1971.

104. H. P. Klug and L. E. Alexander, *X- ray Diffraction Procedure for Polycrystalline and Amorphous Materials*, 2nd Ed., Wiley, New York, 1974.

105. K. Nakamoto, *Infrared and Raman Spectra of Inorganic and Coordination Compounds*, 3rd Ed., Wiley, Chichester, 1978.

106. R. L. LaDuca and P. T. Wolczanski, *Inorg. Chem.*, 1992, **31**, 1311.

107. D. V. Baxter, M. H. Chisholm, G. J. Gama, A. L. Hector and I. P. Parkin, *Chem. Vap. Deposition*, 1995, **1**, 49.

108. O. Kubaschewski, C. B. Alcock and P. J. Spencer, *Materials Thermochemistry*, 6th Ed., Pergamon, Oxford, 1993.

109. Equations solved using *Mathematica* program, Version 1.0, T. Gray, Wolfram Research Inc., Champaign, Il 61820.

110. *1983 Complete Temperature Measurement Handbook*, Table VI, Omega Engineering Inc., Stanford, CT 06907.

110a. *Practical Surface Analysis. Volume 1- Auger and X-ray Photoelectron Spectroscopy*, D. Briggs and M. P. Seah (Eds.), 2nd Ed., Wiley, Chichester, 1990.

111. E. G. Gillan and R. B. Kaner, *Inorg. Chem.*, 1994, **33**, 5693.

112. *Optimised Boron Analysis with the Kevex Microanalysis System*, Microanalysis Tech. Bull. No. 11, Kevex Corporation, 1105 Chest Drive, Foster City, CA 94404.

113. D. A. Vennos, M. E. Badding and F. J. DiSalvo, *Inorg. Chem.*, 1990, **29**, 4059.

114. D. A. Vennos and F. J. DiSalvo, *J. Sol. State Chem.*, 1992, **98**, 318.

115. L. Rao, E. G. Gillan and R. B. Kaner, *J. Mater. Res.*, 1995, **10**, 353.

116. A. Wilson in *Mellor's Comprehensive Treatise on Inorganic and Theoretical Chemistry*, Vol. VIII, Suppl. III, *Phosphorus*, Section VII, Longman, London, 1971.

117. J. D. Smith in *Comprehensive Inorganic Chemistry*, J. C. Bailar, H. J. Emeléus, R. Nyholm and A. F, Trotman- Dickenson (Eds.), Vol. 2, Pergamon, Oxford, 1973.

118. A. T. Rowley and I. P. Parkin, *J. Mater. Chem.*, 1993, **3**, 689.

119. J. C. Fitzmaurice, I. P. Parkin and A. T. Rowley, *J. Mater. Chem.*, 1994, **4**, 285.

120. R. E. Treece, G. S. Macala, L, Rao, D. Franke, H. Eckert and R. B. Kaner, *Inorg. Chem.*, 1993, **32**, 2745.

121. R. E. Treece, J. A. Conklin and R. B. Kaner, *Inorg. Chem.*, 1994, **33**, 5701.

122. N. N. Greenwood and E. A. Earnshaw, *The Chemistry of the Elements*, Pergamon, London, 1990.

123. D. E. C. Corbridge, *Topics in Phosphorus Chemistry*, 1966, **3**, 57.

124. J. H. Krieger, *Agr. Chemicals*, 1952, **7**, 46 and 135.

125. R. E. Treece, E. G. Gillan and R. B. Kaner, *Comment Inorg. Chem.*, 1995, **16**, 313.

126. R. V. Parish, *NMR, NQR, EPR and Mössbauer Spectroscopy in Inorganic Chemistry*, Ellis Horwood, Chichester, 1990.

127. K. S. Irani and K. A. Gingerich, *J. Phys. Chem. Solids*, 1963, **24**, 1153.

128. Values of T_{ad} were calculated as described in section 2.3 using published data.[108] Heat capacity data for HfP were estimated by the methods of Kelly and Kellogg with Ünal's revised data tables (assumes a predominantly ionic compound).[108]

129. F. Hulliger, *Struct. Bonding*, 1968, **4**, 83.

130. *Magnetic Properties*, J. S. Kouvel, *Intermetallic Compounds*, J. H. Westbrook (Ed.), Wiley, 1967.

131. W. B. Pearson, *A Handbook of Lattice Spacings and Structures of Metals and Alloys- 2*, G. V. Raynor (Ed.), *International Series of Monographs in Metal Physics and Physical Metallurgy*, Pergamon, Oxford, 1967.

132. H. Fjellvåg and A. Kjekshus, *Acta Chem. Scand.*, 1986, **A40**, 17.

133. M. Okada, R. A. Guidotti and J. D. Corbett, *Inorg. Chem.*, 1968, **7**, 2118.

133a. *Inorganic Chemistry*, D. F. Shriver, P. W. Atkins and C. H. Langford, Oxford University Press, Oxford, 1992.

134. E. G. Rochow in *Comprehensive Inorganic Chemistry,* J. C. Bailar, H. J. Emeléus, R. Nyholm and A. F, Trotman- Dickenson (Eds.), Vol. 2, Pergamon, Oxford, 1973.

135. For more recent discussions on silicide bonding: J. H. Weaver, A. Franciosi and V. L. Moruzzi, *Phys. Rev. B*, 1984, 1984, **29**, 3293; G. Rossi, *Surf. Sci. Rep.*, 1987, **7**, 1; C. Calandra, O. Bisi and G. Ottaviani, *Surf. Sci. Rep.*, 1985, **4**, 271.

136. L. Topor and O. J. Kleppa, *Met. Trans. A*, 1986, **17**, 1217.

137. A. Franciosi, J. H. Weaver and D. G. O'Neill, *Phys. Rev. B*, 1983, **28**, 4889.

138. M. S. Chandrasekharaiah, J. L. Margrave and P. A. G. O'Hare, *J. Phys. Chem. Ref. Data*, 1993, **22**, 1459.

139. M. E. Schlesinger, *Chem. Rev.*, 1990, **90**, 607.

140. F. M. d'Heurle, *J. Mater. Res.*, 1988, **3**, 167.

140a. *Gas Phase Ion and Neutral Thermochemistry*, S. G. Lias, J. E. Bartmess, J. F. Liebman, J. L. Holmes, R. D. Levin and W. G. Mallard, *J. Phys. Chem. Ref. Data*, 1988, **17**, suppl. 1.

141. A. T. Rowley and I. P. Parkin, *Inorg. Chim. Acta*, 1993, **211**, 77.

142. G. Combe, A. L. Hector, A. V. Komarov, M. Lavender and I. P. Parkin, manuscripts in preparation.

143. A. V. Komarov and I. P. Parkin, *Polyhedron*, in press; A. V. Komarov and I. P. Parkin, *J. Mater. Sci. Lett.*, in press.

144. A. M. Prokhorov and Y. S. Kuz'minov, *Physics and Chemistry of Crystalline Lithium Niobate*, IOP Publishing Ltd, Bristol, 1990.

145. S. A. Weiss, *Manganese, the Other Uses*, Metal Bulletin Books, London, 1977.

146. N. N. Greenwood, *Inorganic Crystals, Lattice Defects and Nonstoichiometry*, Chap. 6, Butterworths, London, 1968.

147. W. Beesk, P. G. Jones, H. Rumpel, E. Schwarzmann and G. M. Sheldrick, *J. Chem. Soc., Chem. Commun.*, 1981, 664.

148. D. Cahen, J. A. Ibers and M. H. Mueller, *Inorg. Chem.*, 1974, **13**, 10 and references therein.

Publications

The following papers have been published during the course of this work:

1) "Rapid synthesis of TiN, HfN and ZrN from solid state precursors." J. C. Fitzmaurice, A. Hector and I. P. Parkin. *Polyhedron*, 1993, **12**, 1295.

2) "Convenient, low energy, solid- liquid metathesis reactions: synthesis of TiN, TiO_2, VN, VO_2 and Ti_xV_yN (x+y=1)." A. Hector and I. P. Parkin. *J. Chem. Soc., Chem. Commun.*, 1993, 1095.

3) "Low temperature solid state routes to transition metal oxides *via* metathesis reactions involving lithium oxide." A. Hector and I. P. Parkin. *Polyhedron*, 1993, **12**, 1855.

4) "Low temperature routes to early transition metal nitrides." J. C. Fitzmaurice, A. L. Hector and I. P. Parkin. *J. Chem. Soc., Dalton Trans.*, 1993, 2435.

5) "A convenient, rapid, low energy route to crystalline TiN, VN and Ti_xV_yN (x+y=1)." I. P. Parkin and A. L. Hector. *J. Mater. Sci. Lett.*, 1993, **12**, 1856.

6) "Rapid, low energy synthesis of lanthanide nitrides." J. C. Fitzmaurice, A. Hector, A. T. Rowley and I. P. Parkin. *Polyhedron*, 1994, **13**, 235.

7) "Low energy initiated routes to crystalline metal phosphides and arsenides." J. C. Fitzmaurice, A. Hector and I. P. Parkin. *J. Mater. Sci. Lett.*, 1994, **13**, 1.

8) "Solid state metathesis preparations of group VIII metal oxide powders." A. L. Hector and I. P. Parkin. *J. Mater. Sci. Lett.*, 1994, **13**, 219.

9) "Self- propagating routes to transition metal phosphides." A. L. Hector and I. P. Parkin. *J. Mater. Chem.*, 1994, **4**, 279.

10) "Room temperature initiated routes to titanium and vanadium pnictides." A. L. Hector and I. P. Parkin. *Inorg. Chem.*, 1994, **33**, 1727.

11) "Metal pnictide synthesis; Self- propagating reactions involving sodium arsenide, antimonide and bismuthide." A. L. Hector and I. P. Parkin. *Z. Naturforsch. B*, 1994, **49b**, 477.

12) "Solid state routes to crystalline group IIB chalcogenides. Applications of metathesis reactions." J. C. Fitzmaurice, A. Hector and I. P. Parkin. *Main Group Met. Chem.*, 1994, **17**, 537.

13) "A synthesis of bismuth (III) phosphide: the first binary phosphide of bismuth." C. J. Carmalt, A. H. Cowley, A. L. Hector, N. C. Norman and I. P. Parkin. *J. Chem. Soc., Chem. Commun.*, 1994, 1987.

14) "Synthesis of metal silicide powders by thermolysis of metal chlorides with magnesium silicide." J. C. Fitzmaurice, A. L. Hector, I. P. Parkin and A. T. Rowley. *Phosphorus, Sulfur and Silicon*, 1995, **101**, 47.

15) "Sodium azide as a reagent for solid state metathesis preparations of refractory metal nitrides." A. L. Hector and I. P. Parkin. *Polyhedron*, 1995, **14**, 913.

16) "Low pressure chemical vapour deposition of metallic films of iron, manganese, cobalt, copper, germanium and tin employing Bis(trimethyl) silylamide complexes $M(N(SiMe_3)_2)_n$." D. V. Baxter, M. H. Chisholm, G. J. Gama, A. L. Hector and I. P. Parkin. *Chem. Vap. Deposition*, 1995, **1**, 49.

17) "Magnesium and calcium nitrides as nitrogen sources in metathetical reactions to produce metal nitrides." A. L. Hector, I. P. Parkin and A. T. Rowley. *Chem. Mater.*, 1995, **7**, 1728.

18) "Room temperature synthesis in liquid ammonia of zinc, cadmium and mercury sulfides." A. L. Hector, G. Henshaw, I. P. Parkin and G. A. Shaw. *Main Group Chem.*, in press.

19) "Molecular routes to metal carbides, nitrides and oxides; Studies of the ammonolysis of metal dialkylamides and silylamides." D. V. Baxter, M. H. Chisholm, V. F. Distasi, G. J. Gama, A. L. Hector and I. P. Parkin. *Chem. Mater.*, submitted for publication.